RHEOLOGICAL CHARACTERIZATION AND EXTRUSION OF ALUMINA BASED PASTES FOR THE PREPARATION OF TUBULAR CERAMIC MEMBRANE SUPPORTS

A Thesis Submitted to
the Graduate School of Engineering and Sciences of
İzmir Institute of Technology
in Partial Fulfillment of the Requirements for the Degree of

MASTER OF SCIENCE

in Materials Science and Engineering

by
Kenan YILMAZ

March 2016
İZMİR

We approve the thesis of **Kenan YILMAZ**

Examining Committee Members

_____

Prof. Dr. Muhsin ÇİFTÇİOĞLU
Department of Chemical Engineering, İzmir Institute of Technology

_____

Asst. Prof.Dr. Ufuk ŞENTÜRK
Department of Chemical Engineering, İzmir Institute of Technology

_____

Asst.Prof.Dr.Mücahit SÜTÇÜ
Department of Materials Science and Engineering, Katip Çelebi University

3 March 2016

_____

Prof. Dr. Muhsin ÇİFTÇİOĞLU
Supervisor, Department of Chemical Engineering, İzmir Institute of Technology

_____ _____

Prof. Dr. Mustafa Muammer Demir
Head of the Department of Materials Science and Engineering

Prof. Dr. Bilge KARAÇALI
Dean of the Graduate School of Engineering and Sciences

ACKNOWLEDGEMENTS

I would like to express my profound appreciation and gratitude to my advisor Prof. Dr. Muhsin ÇİFTÇİOĞLU for his valuable guidance, ideas and encouragement in the preparation of this manuscript.

I ought to thank my co-advisor, Dr. Burcu ALP for her precious help, valuable comments and contributions for my entire MSc time. I would like to thank to Rukiye ÇİFTÇİOĞLU for her interest, support, and great help in difficult times.

My absolute thanks to my colleagues Hüsnü Arda YURTSEVER, Öncel KIRKBAŞ, Kaan YALTRIK, Safiye YALDIZ and İklima ODABAŞI for their interest, valuable contributions, sincere friendship, and endless understanding for all times. Thank you for everything. I am very grateful to my lab mates for their friendship and support.

I would also thank to my girlfriend Cansu KIVRAK for her spiritual support during my MSc. Her presence and love gave me the determination to work throughout this study.

I would like to express my gratitude to my father, my mother and my sister, for their deepest love, invaluable patience, understanding, support and encouragements all throughout my life.

This study was supported by The Scientific and Technological Research Council of Turkey (TUBITAK) within the context of ÇAYDAG 113Y344 project.

ABSTRACT

RHEOLOGICAL CHARACTERIZATION AND EXTRUSION OF ALUMINA BASED PASTES FOR THE PREPARATION OF TUBULAR CERAMIC MEMBRANE SUPPORTS

Membrane applications in the industry currentlyis dominated by polymeric membranes, however, in recent years the development of ceramic membranes gained significant attention because of their superior chemical/thermal stability and corrosion resistance. The separation capacities of ceramic membranes basically depend on the nature of the selective oxide layers formed on the inner surfaces of tubular ceramic supports.

Ceramic tubular membrane supports were prepared from alumina pastes, with solid loadings as high as 55 vol. % and water was used as the major liquid phase. Boehmite along with hydroxypropyl cellulose ethers with different molecular weightswere used as binder materials. Glycerol was used as a lubricant in the paste formulations. Extrusion of alumina paste was conductedwith a ram extruder using capillary dies with a series of L/D ratios at different extrusion velocities and the data was analyzed by using Benbow and Bridgwater model. The rheological properties of various pastes were determined according to the 4 and 6-parameter models.The six parameter model was concluded to better represent the experimental data. The viscosities of the paste batches were also determined by using the model parameters σ_o, β_1, and exponent n. The pastes were determined to have a shear thinning behaviour

Piston extruder was used for shaping of tubular ceramic supports and the pressure varied in the 20-90 bar range with paste composition and rheology. The tubular extruded supports were dried, debinded to burn out organic binders and sintered at 1525ºC for the formation of about 40% porous mechanically strong membrane supports.

ÖZET

TÜBÜLER SERAMİK MEMBRAN DESTEKLERİNİN HAZIRLANMASINA YÖNELİK ALÜMİNA BAZLI HAMURLARIN REOLOJİK KARAKTERİZASYONU VE EKSTRÜZYONU

Membranlar biyokimyasal ayırma süreçleri, tekstil, kağıt ve metal endüstrisi gibi farklı endüstrilerde saflaştırma ve ayrıştırma işlemleri için kullanılmaktadır. Seramik membranlar genel olarak seçici oksit katmanlarının tübüler seramik destekler üzerine konulmasıyla oluşturulur.

Katı madde oranları yüzde 55 seviyesine kadar olan ve ana ortam sıvısı su olacak şekilde hazırlanan alumina hamurlarından, seramik tübüler membranlar hazırlanmıştır. Bağlayıcı malzeme olarak böhmit ile birlikte farklı molekül ağırlıklarınıa sahip hidroksi selülöz eterler kullanılmıştır. Hamur hazırlanışında gliserin yağlayıcı olarak kullanılmıştır. Ön çalışmalar için orifice tipi kalıpta ram extrüzyon kullanılmış ve veriler mekanik mukavemet test cihazıyla alınmıştır. Alümina hamur ekstrüzyonu farklı L/D oranlarına sahip kapileri kalıplar kullanılarak farklı ekstrüzyon hızlarında ram ekstrüderi ile gerçekleştirilmiş ve alınan veriler aynı test cihazıyla Benbow Bridgwater modeli kullanılarak analiz edilmiştir. Çeşitli hamurların reolojik özellikleri 4 ve 6 parametreli modellere bağlı olarak belirlenmiştir. 6 parametreli modelin alumina hamurlarıyla daha yakın ekstrüztyon grafiklerine sahip olduğu belirlenmiştir. Hazırlanan seramik hamurlarının viskoziteleri model parametreleri σ_o, β_1, ve n kullanılarak hesaplanmıştır.

Tübüler seramik hamurlarının şekillendirilmesi piston ekstrüder kullanılarak yapılmış ve hamurunun reolejisi ve kompozisyonuna bağlı olarak piston ekstrüder basıncı 20-90 bar arasında değişiklik göstermiştir. Ekstrüde edilmiş tübüler destekler kurutulup organik bağlayıcılarından arındırılmış ve %40 poroziteye sahip mekanik olarak güçlü membran destekleri elde etmek amacıyla 1525ºC'de ısıl işlem uygulanmıştır.

TABLE OF CONTENTS

LIST OF FIGURES viii

LIST OF TABLES xii

CHAPTER 1. INTRODUCTION 1

CHAPTER 2. MEMBRANES 5

2.1 History of Membranes 5

2.2 Classification of Membranes 6

2.3 Materials for Membranes 9

2.4 Ceramic Membranes 12

2.4.1 Advantages and disadvantages of Ceramic Membranes 13

2.4.2 Applications of Ceramic Membranes 14

2.5 Ceramic Membrane Supports 15

2.5.1 Processing of Ceramic Membrane supports 15

2.5.2 Manufacturing Methods of Ceramic Membrane Supports 16

2.5.3 Selective Layer Formation on The Support Surfaces 21

CHAPTER 3. RHEOLOGY OF PASTES 23

3.1 Rheology 23

3.2 Paste Flow in Extrusion 26

CHAPTER 4. CERAMIC EXTRUSION 27

4.1 History of the Extruder in Ceramics 27

4.2 Types of Extruders 28

4.2.1 Auger (screw) extruder 28

4.2.2 Piston extruder 29

4.3 Additives for Ceramic Extrusion 30

4.3.1 Dispersant 31

4.3.2 Binder 31

4.3.3 Plasticizer 33
4.3.4 Lubricants 33
4.4 Benbow and Bridgwater Model 33
4.5 Viscosity of Ceramic Paste 36

CHAPTER 5: EXPERIMENTAL 38
5.1. Materials 38
5.2. Preliminary Experiments with Orifice Die 39
5.3. Preparation of Tubular Alumina Ceramic Supports 41
5.3.1 Dry Mixing and Kneading of Pastes 43
5.3.2 Rheological Characterization of the Pastes 45
5.3.3 Piston Extrusion 46
5.3.4 Drying and Heat Treatment of Tubes 47
5.4. Characterization of Tubular Alumina Ceramic Membrane Supports 48

CHAPTER 6: RESULTS & DISCUSSION 50
6.1. Powder characterization 50
6.2. Characterization of preliminary experiments 57
6.3. Rheological Characterization of Alumina Pastes 59
6.4. Characterization of Tubular Alumina Ceramic Membrane Supports 73

CHAPTER 7: CONCLUSIONS 83

REFERENCES 84

APPENDİX A. BENBOW AND BIRIDGWATER MODEL 4 AND 6 PARAMETER PLOTS 87

LIST OF FIGURES

Figure **Page**

Figure 2.1. Schematic illustration of membrane structures. 6
Figure 2.2. SEM image of a polymeric asymmetric membrane structure. 7
Figure 2.3. Pressure driven membrane separation processes characteristics.....8
Figure 2.4. Ceramic membrane development in history. 12
Figure 2.5. Ceramic membrane layers gradation according to pore size. 13
Figure 2.6. Generalized flow chart of ceramic membrane processing……16
Figure 2.7. Schematic illustration of slip casting process. 17
Figure 2.8. Schematic illustration of tape casting process.....18
Figure 2.9. Schematic illustration of pressing. 19
Figure 2.10. Some different tubular ceramic membrane shapes. 20
Figure 3.1. Types of rheological behavior exhibited by colloidal dispersions: (a) Newtonian flow; (b) shear thinning (pseudoplastic); (c) shear thickening; (d) Bingham plastic; and (e) pseudoplastic with a yield stres. 24
Figure 3.2. Schematic illustration of ceramic paste flow in piston extruder 26
Figure 4.1. Schematic illustration of Auger extruder. 28
Figure 4.2. Auger (screw) extruder with different designs. 29
Figure 4.3. Ram Extruder 34
Figure 5.1. Extrusion of ceramic pastes in the mechanical test device (Testometric SN 500-526) with orifice die. 41
Figure 5.2. Flowchart of experimental work. 42
Figure 5.3. The screw extruder 45
Figure 5.4. Processing of paste sausages 45
Figure 5.5. Piston extruder.....46
Figure 5.6. Extrusion of tubes from the piston extruder.....47
Figure 5.7. Tubular alumina ceramic membrane supports 49
Figure 6.1. SEM image of CT 3000 SG-0.5 µm alumina powder.....51
Figure 6.2. SEM image of CT 1200 SG-1.3 µm alumina powder 51
Figure 6.3. SEM image of CT 3000 SG-5.2 µm alumina powder 52

Figure 6.4. 0.5 μm Alumina powder 52
Figure 6.5. 1.3 μm Alumina powder 53
Figure 6.6. 4 μm Alumina powder 53
Figure 6.7. 5.2 μm Alumina powder 53
Figure 6.8. XRD patterns of alumina powders. *:α-alumina..... 54
Figure 6.9. SEM image of boehmite powder..... 54
Figure 6.10. XRD pattern of boehmite powder 55
Figure 6.11. TGA curve of methocel F4M 56
Figure 6.12. TGA curve of methocel A4M 56
Figure 6.13. Extrusion graphics of HEMS binder used alumina ceramic pastes and conventional industrial ceramic paste 57
Figure 6.14. Extrusion graphics of HPMS binder used alumina ceramic pastes and conventional industrial ceramic paste. 58
Figure 6.15. Extrusion graphics of HPMS binder and boehmite used alumina ceramic pastes and conventional industrial ceramic paste 58
Figure 6.16. Extrusion forces of batches 14, 15, 16 and 18 at velocity 0.0002 m/s..... 59
Figure 6.17. Extrusion forces of batches 14, 15 and 16 at velocity 0.0011 m/s..... 60
Figure 6.18. Extrusion forces of batches 14, 15, 16 and 18 at velocity 0.0021 m/s..... 60
Figure 6.19. Extrusion forces of batches 14, 15, 16 and 18 at velocity 0.0053 m/s..... 61
Figure 6.20. Extrusion forces of batches 14, 15, 16 and 18 at velocity 0.0106 m/s..... 61
Figure 6.21. Extrusion forces of batches 14, 15 and 16 at velocity 0.0213 m/s..... 62
Figure 6.22. P vs. L/D plots of Batch 14 63
Figure 6.23. P_1 vs.V plot of Batch 14..... 63
Figure 6.24. lnV vs $\ln[P_1/2\ln(D_0/D)]-\sigma_0$ plot of batch 14..... 64
Figure 6.25. P_2 vs L/D plots of Batch 14 65
Figure 6.26. $\ln[P_2/4L/D]-\tau_0$ vs lnV plots of Batch 14 65

Figure 6.27. [$P_1/2\ln(D_0/D)$]- σ_0 vs V plot of batch 14 66
Figure 6.28. [$P_2/4L/D$]- τ_0 vs V plot of batch 14 67
Figure 6.29. Experimental, 6 parameter and 4 parameter model
comparison of batch 14.....68
Figure 6.30. Experimental, 6 parameter and 4 parameter model
comparison of batch 15.....69
Figure 6.31. Experimental, 6 parameter and 4 parameter model
comparison of batch 16.....69
Figure 6.32. Experimental, 6 parameter and 4 parameter model
comparison of batch 18.....70
Figure 6.33. Viscosity versus shear rate plots of batches 14, 15, 16 and 18.....71
Figure 6.34. Shear stress versus shear rate plots of batches 14, 15, 16 and 18.....72
Figure 6.35. SEM image of Batch 5; A. Fracture surface at 2500 X, B. Tube inner
Surface 2500 X, C Fracture surface at
higher magnification at 10 kX 74
Figure 6.36. SEM image of Batch 8; A. Fracture surface at 1000 X, B. Tube inner
Surface 5000 X, C. Fracture surfaceat
higher magnification at 10 kX.....75
Figure 6.37. SEM image of Batch 15; A. Fracture surface at 1500 X, B. Tube inner
Surface 2500 X, C Fracture surface
at higher magnification at 10 kX.....76
Figure 6.38. SEM image of Batch 16; A. Fracture surface at 1000 X, B. Tube inner
Surface 2500 X, C Fracture surface
at higher magnification at 10 kX.....77
Figure 6.39. SEM image of Batch 17; A. Fracture surface at 2500 X, B. Tube inner
Surface 2500 X, C Fracture surface at higher magnification at 10 kX 78
Figure 6.40. SEM image of Batch 18; A. Fracture surface at 2500 X, B. Tube inner
Surface 2500 X, C Fracture surface at higher magnification at 10 kX 79
Figure 6.41. Mercury porosimetry plots of Batch 12a. Cumulative Pore Area versus
Pore size and b. Log Differential Intrusion vs Pore size 80
Figure 6.42. Mercury porosimetry plots of Batch 14 a. Cumulative Pore Area versus
Pore size and b. Log Differential Intrusion vs Pore size 80

Figure 6.43. Mercury porosimetry plots of Batch 15 a. Cumulative Pore Area versus Pore size and b. Log Differential Intrusion vs Pore size. 81

LIST OF TABLES

Table		Page
Table 1.1.	Chronologically milestone developmentsof membrane science	1
Table 1.2.	Asymmetric ceramic membrane properties.	2
Table 1.3.	Ceramic membrane manufacturers and membranes properties	3
Table 2.1.	Membrane separation characteristics	8
Table 2.2.	Membrane materials for different separation process.	10
Table 2.3.	Some chemical reactions in CVD process.	22
Table 4.1.	List of additives commonly used in ceramic extrusion pastes.	31
Table 5.1.	Specifications of α-Alumina from Sigma Aldrich Co.	38
Table 5.2.	Specifications of Boehmite from Sasol Co.	38
Table 5.3.	Specifications of HPMS (hydroxy propyl methyl cellulose) received from DOW Chemical Co	39
Table 5.4	Sources of other important additives	39
Table 5.5.	Sample codes and compositions of the prepared ceramic pastes for preliminaryexperiments.	40
Table 5.6.	Volumetric % contents of extruded pastes	44
Table 6.1.	Particle size of alumina powders (d90, d50 and d10)	50
Table 6.2.	Results of six parameter model	68
Table 6.3.	Results of four parameter model	68
Table 6.4.	Apperant viscosity values of batches 14, 15, 16 and 18	71
Table 6.5.	Archimedesdensity analysis and mechanical strength test results for different batches	73

CHAPTER 1

INTRODUCTION

Membrane separation process is a developing and expanding technology in various industries. Membrane technology can be traced back to the middle 1700s, although real breakthrough for industrial applications of membranes started in the 1960s. Milestone developments of membrane technology are listed in chronological order in Table 1.

In 1960s, discovery of asymmetric inorganic membranes is a milestone for membrane technology. In industrial applications, harsh environments is a challenge for organic membranes. Asymmetric inorganic membranes attracted significant R&D interest by researchers due to their advantages. Inorganic membranes can be made by various materials however it is mainly dominated by ceramic membranes. Advantages of ceramic membranes like high thermal /chemical stability, corrosion resistance and biocompatibility make them the bestmaterials of choice among the various types of inorganic membranes.

Table 1.1. Chronologically milestone developments of membrane science. (Source: Fane et al., 2008)

Year	Devolopment/discovery	Scientist(s)
1748	Discovery of osmosis phenomenon	A. Nollet
1833	The law of gaseous diffusion	T. Graham
1855	Phenomenological laws of diffussion	A. Fick
1860s-1880s	Semipermeable membranes: osmotic pressure	M. Traube, W. Pfeffer, J.W. Gibbs, J.H. van'tHoff
1907-1920	Porous membrane filters	R. Zsigmondy
1920s	Research on reverse osmosis	L. Michaelis, E. Manegod, J.W. McBain
1930s	Electrodialysis membranes	T. Teorell, K.H. Meyer, J.F. Sievers
1950s	Electrodialysis, micro- and ultra-filtration, hemodialysis and ion-exchange membranes	Many
1963	Defect-free, high flux, asymmetric reverse osmosis membranes	S. Loeb, S. Sourirajan
1970-1980	Membrane and process improvements	Many
1980s	Industrial membrane gas separation processes	J.M.S Henis, M. Tripodi
1990s	Hybrid and novel membrane processes	Many

Asymmetric ceramic membranes are composed of different layers. Top layer has the smallest pore size and it is the selective layer. The interlayers supply a smooth surface with narrow pore size to enable the formation of the relatively thinner selective top layer. The support have bigger pores and provides the necessary mechanical strength to the asymmetric ceramic membrane. All layers have different thicknesses and pore diameters. An example of asymmetric membrane layer properties can be seen in Table 1.2.

Table 1.2. Asymmetric ceramic membrane properties.
(Sorce: de Vos and Verweij, 1998)

Layer	Top (selective)	Intermediate	Support
Material	SiO_2	γ-Al_2O_3	α-Al_2O_3
Thickness	30-200 nm	10^3-$4*10^3$ nm	$2*10^6$nm
Pore Diameter	0.3-0.8 nm	2-5 nm	80-120 nm

Ceramic membrane supports can be prepared by different methods, such as slip casting, pressing, tape casting and extrusion (Li, 2007, Drioli and Giorno, 2010). In wastewater treatment alumina is one of the mostwidelyused material for ceramic membrane support preparation. Industrially used ceramic membrane materials, properties, shapes and leading companies are listed in Table 1.3 (Benko et al. 2011).

Table 1.3.Ceramic membrane manufacturers and membranes properties.
(Source: Benko et al. 2011)

Product Line(s)	Filtration Range	Support Materials		Membrane Materials	Channel Configuration
Pall	Membralox®Schumasiv®	5nm to 0.2 μm	Al_2O_3	Al2O3 (MF) ZrO2 and TiO2 (UF)	Hexagonal and round
Corning	CerCor®	5nm to 0.2 μm	Mullite ($3Al_2O_3$•$2SiO_2$)	ZrO2 (MF) TiO2 (UF)	Square and round
TAMI	Ceram Inside®	0.02 μm to 1.4μm	ATZ	ZrO2 (MF) TiO2 (UF)	Flower shaped
Atech	Atech	0.01 μm to 1.2 μm	Al2O3	Al2O3 (MF) ZrO2 and TiO2 (UF)	Single or multiple round
Orelis	Kerasep™	5 kDa to 0.8 μm	Al2O3	ZrO2 and TiO2	Single or multiple round

Extrusion is the most efficient method to produce tubular ceramic membranesupports and it provides higher cross sectional separation area. Extrusion of ceramic paste can be accomplished by using different type of extruders. One type of extruder is auger extruder which works with a screw like an auger shaft. Auger extruders are continuous machines; therefore, they are generally used in industrial applications. Another extruder type is piston extruder. Advanced ceramic membrane extrusion is a complicated process where purityis crucial and higher pressures are required compared to the traditional ceramic extrusion. The use of a piston extruder is commonly more favorable for advanced ceramic extrusion due to these reasons (Handle 2007, de Jong 2009).

Evaluation of the rheological parameters of ceramic pastes is a key factor for successful extrusion. Rheological behaviour of ceramic pastes can be analysed by using different models such as Bingham plastic, Herschel-Bulkley or Benbow and Bridgwater model. Past resarch on advanced ceramic extrusion indicated thatBenbow and Bridgwater model represents the data better than the other models.

Tubular alumina ceramic membrane supports were prepared by extrusion in this thesis. The effect of different polymeric and inorganic additives on paste rheology and

extrusion were investigated. The experimental work on the rheological characterization of alumina pastes wereconducted with a capillary die extruder and the data were analyzed by using Benbow and Bridgwater model. The effect of polymeric binder molecular weight and inorganic binder boehmite on paste characteristics were determined.

CHAPTER 2

MEMBRANES

2.1. History of Membranes

Membrane separation was first introduced in 1748. Abbe Nolet conducted experiments on semi-permeable membrane for water separation and introduced the term "osmosis". In 1866 Sir Thomas Graham had found the hydrogen absorption ability of palladium and he used this material as a gas separation membrane (Sammells and Mundschau 2006, Howell et al 1993).

In 1855 first synthetic membrane was produced by Fick and the material was nitrocellulose. In this developing area, Bechold found a way to control the pore size and measure the pore diameter, in addition to that, he was the first scientist who used the term ultrafiltration (Tamime 2013).

In 1927 first commercial membrane was produced in Germany by Sartariuscompany. Until 1940s membranes were used for separation of microorganisms and particles from liquids and gases. The term reverse osmosis appeared in membrane technology in 1931 which is a separation technique used for desalination of seawater.

Souriarjan and Loeb had found a process which allows the production of defect free membranes with high fluxes for desalination of sea water in the earlier years of the 1960s. The reduction of the membrane thickness was believed to be the best choice of researchers for increasing the flux in thoseyears. Souriarjan and Loeb while using annealing method on cellulose acetate membranes for reducing the membrane thickness made a new unexpected discovery. At high temperatures pores of the membrane was reduced but the rejection of the salt and also the flux was increased. Souriarjan and Loeb discovered the asymmetric membraneduring their succeeding research efforts. This was a great breakthrough in membrane technology (Tamime 2013).

In the middle of the 1980s nanofiltration and reverse osmosis membranes have been produced for industrial applications. In the same years, inorganic ceramic membranes have attracted an increasing attention because of their superior advantages.

Zirconium and titanium oxide membranes became available commercially and they were used in microfiltration, ultrafiltration and nanofiltration separation processes (Tamime 2013).

2.2. Classification of Membranes

Membranes can be natural or synthetic with various thicknesses, can be homogeneous or heterogeneous depending on the strucuture and can be classified based on different criteria. The first classification is by nature, biological or synthetic membranes. Synthetic membranes can be subdivided into organic (polymeric or liquid) and inorganic (e.g. ceramic, metal) membranes(Mulder 1997).

Another classification whch is based on structure or morphology also is very descriptivebecause membrane structure determines the separation mechanism. Synthetic membrane structure can be subdivided into two classes as symmetric and asymmetric. In Figure 2.1.shows the structural classification of membranes. (Mulder 1997)

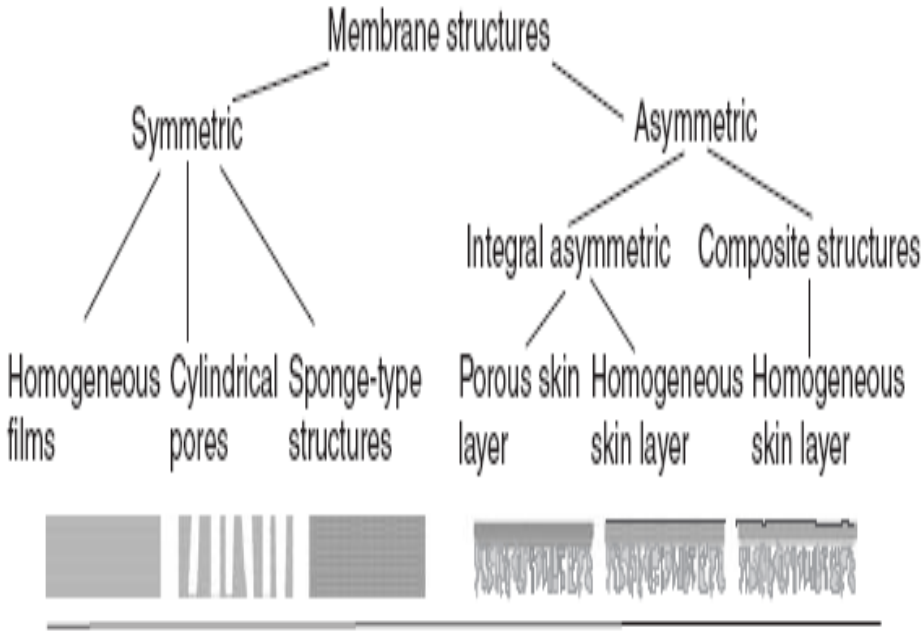

Figure 2.1. Schematic illustration of membrane structures
(Source:Drioli and Giorno, 2010)

The structure and the transport properties are identical over the entire cross section of symmetric membranes and the thickness of the entire membrane determines the flux. Symmetric membranes are mainly used in dialysis and electrodialysiscurrently (Drioli and Giorno, 2010).

Asymmetric membranes are the milestone for membrane technology. The Asymmetric membrane may consist of several layers where the top layer is the selective layer. Selective layer determines the selectivity and the thickness of the selective layer determines the flux of the membrane. Porous sublayer acts as a support for membrane and has little effect on separation. Asymmetric membranes are commonly used for pressure-driven membrane processes such as microfiltration, ultrafiltration, nanofiltration and reverse osmosis. They are used for gas and vapor separation because of their satisfactory properties such as high fluxes and mechanical stability. Asymmetric membrane structure can be seen in Figure 2.2. (Nath 2008, Drioli and Giorno 2010).

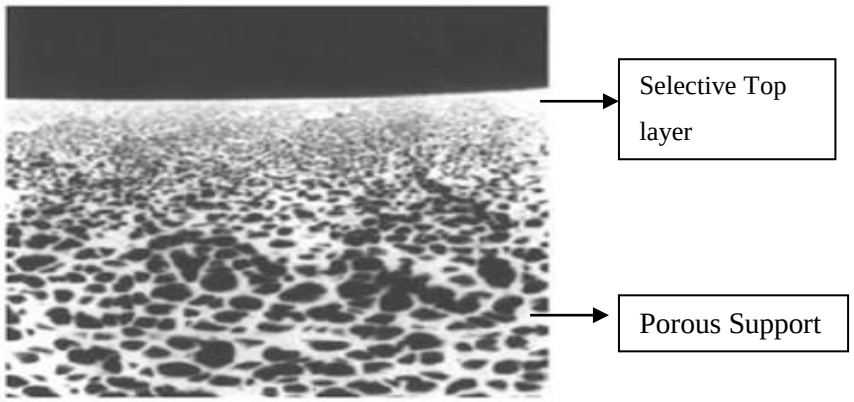

Figure 2.2. SEM image of asymmetric membrane structure
(Source: Drioli and Giorno 2010)

Separation process is another important classification method. According to the separation process, membranes can be divided into seven main groups; microfiltration, ultrafiltration, nanofiltration, dialysis, electrodialysis, and reverse osmosis membranes. Table 2.1 shows the membrane separation process characteristics for different processes. However, more common separation processes are pressure driven process

(micro, ultra, nano, reverse osmosis filtrations). Pressure driven membrane separation process characteristics can be seen Figure 2.3 (Cheryan 1998).

Table 2.1. Membrane separation characteristics.
(Source: Cheryan 1998)

Process	Driving Force	Retentate	Permeate
Osmosis	Chemical potential	Solutes,water	Water
Dialysis	Concentration difference	Large molecules, water	Small molecules, water
Microfiltration	Pressure	Suspended particles, water	Dissolved solutes, water
Ultrafiltration	Pressure	Large molecules, water	Small molecules, water
Nanofiltration	Pressure	Small molecules, divalent salts, dissociated acids, water	Monovalent ions, undissociated acids, water
Reverse osmosis	Pressure	All solutes, water	Water
Electrodialysis	Voltage/current	Nonionic solutes, water	Ionized solutes, water
Pervaporation	Pressure	Nonvolatile molecules, water	Volatile small molecules, water

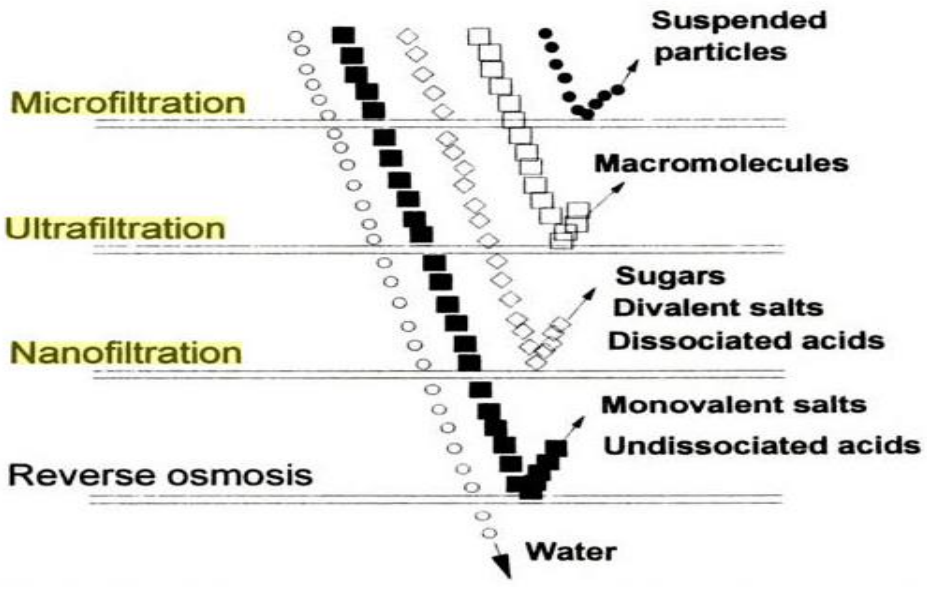

Figure 2.3. Pressure driven membrane separation processes characteristics. (Source: Cheryan, 1998.)

Microfiltration is used for the filtration of solid particles with diameters in the 0.1-0.5 µm range. (bigger particles can be separated easily with conventional cake filtration) (Cheryan 1998). This separation process works under low pressures (1-4 bars). Most known microfiltration applications are liquid clarification and sterile filtration (Hutten 2007).

Ultrafiltration can be described as a transition separation process in the filtration of colloidal particles and molecular species. Particles in the 0.004-0.1µm size range can be separated in ultrafiltration. Viruses and molecules with molecular weights higher than 10 kDa can also be rejected in ultrafiltration. Working pressure for this filtration is between 5-10 bar. Separation of macromolecular solutions can be achieved with ultrafiltration (Hutten 2007).

Nanofiltrationisgenerally used for the separation of multivalent ions from solutions. It can be considered as a form of reverse osmosis filtration. Particles and molecules can be separated with sizes range in the 1.2-12 nm size range and working pressure is between 20-40 bar (Hutten 2007).

Reverse osmosis is different from other pressure driven processes because in this process ions will be separated water. Most of the molecular species (in water or solvent) are impermeable for this process. Applied pressure must be overcome than natural osmotic pressure with that high pressure water will flow from higher concentration site to lower concentration site. Therefore, working pressure will be in the range of 30-60 bar. Most of the molecular species (in water or solvent) are impermeable for this process. Most known application of reverse osmosis filtration is desalinization. (Hutten 2007, Cheryan 1998, Mulder 1997)

2.3. Materials for Membranes

The materials used for membrane manufacturing can be both organic (polymeric) and inorganic, and/or combination of these materials, which is called composite membranes. Commonly used materials for membrane manufacturing can be seen in Table 2.2.

Table 2.2. Membrane materials for different separation process. (Source: Cheryan 1998)

Material	**Application(s)**
Cellulose acetates	RO, UF, MF
Aromatic polyamides	RO, UF
Fluorocarbon polymers	RO, UF, MF
Polyamides	RO, UF
Polysulfone	UF, MF
Nylons	UF, MF
Polycarbonate	UF, MF
Polyvinyl chloride PVDF Polyphosphazene	UF
Alumina (gama)	UF
Alumina (alfa)	MF
Glass	RO, UF
Zirconia	UF, MF
Zirconia (hydrous)	DM(RO, UF)
Silver	MF
Stainless stell	MF

Polymeric Membranes

Polymeric membranes have the largest market share in separation industry since they have been introduced in the 1960s because they are very economical and perform satisfactorily in most industrial applications. Chain rigidity, interactions of chains, stereoregularity, and polarity of their functional groups are important parameters in the production of suitable polymeric membranes. Cellulose acetate is the most widely used polymeric membrane material due to its hydrophilic nature which avoids fouling. They

are also low cost and relatively easy handling materials (Erdem 2002).Other common polymers for preparation of polymeric membranes are polyether sulfone, polysulfone, polyamide, polyacrylonitrile, and polyvinylidene fluoride. Polymeric membranes can be prepared with different techniques such as track etching, coating, interfacial polymerization and phase inversion depending on the type of the polymer. Phase inversion (immersion precipitation) is the most popular technique for the preparation of polymeric membranes (Richardson et al. 1997).

Inorganic Membranes

The interest in inorganic membranes have been increasing in recent years and rapid developments in their synthesis and applications was reported due to their superior advantages over organic membranes (Mulder 1997, Hsieh 1996). Inorganic membranes can be classified in three main groups as ceramic, glass and metallic membranes (Mulder 1997). They can be operated at higher temperatures, in a wider pH range and inert to common chemicals and can be cleaned by backwashing. Backwashing is accomplished by applying high pressures in opposite direction of the normal permeate flow. Ceramic inorganic membranes have long operational life which is a very important advantage in industrial application. Their brittle nature and high capital cost are their major disadvantags. The high capital cost can be compensated by significantly longer operational lifetime of inorganic ceramic membranes. They can be used for many years where the ceramic membranes used in nuclear fuel enrichment can be a good example (Erdem 2002).

Inorganic membranes can also be classified in two groups according to their structure as porous and dense membranes (Hsieh 1996). Porous membranes are generally made of ceramic materials. Porous ceramic membranes commonly have been use in harsh conditions in terms of high temperature or chemically corrosive environments.The polymeric membranes on the other hand can be deformed or loose their separative capacities under these conditions. Porous ceramic membranes generally are made from metal oxides like alumina (Al_2O_3), zirconia (ZrO_2), titania (TiO_2) and silica (SiO_2) and their composites can be used in the preparation of porous ceramic membranes.

Dense membranes are mainly produced by using metals and most known materials are palladium and its alloys. Thomas Graham discovered that hydrogen permeates through palladium in 1866 which started extensive investigations on dense metallic membranes (Hsieh 1996).

2.4. Ceramic Membranes

Membrane industry ismainly dominated by polymeric membranes. However in recent years demand for inorganic membranes have increased due to their superior advantages. Ceramic membranes are the most widely used inorganic membranes. Ceramic membranes have been used in various industries like food, biotechnological, pharmaceutical, petrochemical, and electronic industry (Laitinen 2002). Ceramic membranes are mainly used for water treatment applications currently and their application areas are still under development. Gas separation membranes and catalytic membrane reactors are currently important R&D areas on ceramic membranes (Pabby 2015). Ceramic membrane development timeline can be seen in Figure 2.4.

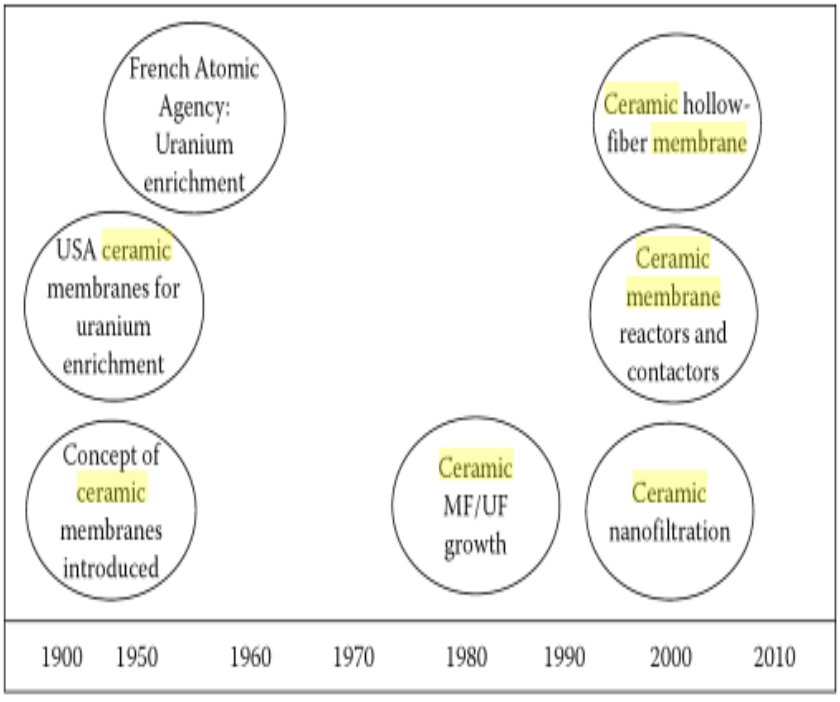

Figure 2.4. Ceramic membrane development in history. (Source: Kingsbury 2010)

Ceramic membranes commonly have asymmetric structure which have been discussed in earlier sections. Asymmetric membrane structure description can also be based on pore sizes of the various layers. The support has a macroporous structure, the interlayers have a mesoporous structure and the selective layers have a microporous structure (Li 2007). Figure 2.5. shows the pore size characteristics of the layers.

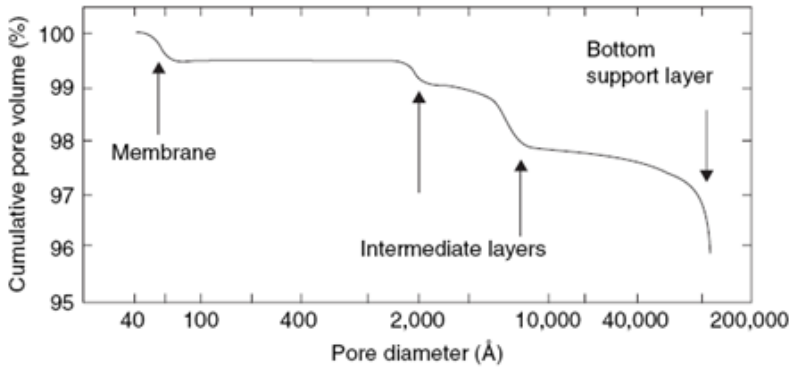

Figure 2.5. Ceramic membrane layers gradation according to pore size. (Source: Hsieh 1988)

Ceramic membranes can be produced in different shapes like a disc, flat sheet or tube. The surface area to volume ratio of the membrane should be high for efficient separation with high fluxes. Tubular ceramic membranes have higher surface area to volume ratios and the tubes are assembled in a module for much higher values (Li 2007). Hsieh conducted research on alumina membranes and reported that the surface area to volume ratios are around 30–250 m^2 m^{-3} for tubes, 130–400 m^2 m^{-3} for multichannel and up to 800 m^2 m^{-3} for honeycomb multichannel monolithic structures (Hsieh 1996).

2.4.1. Advantages and Disadvantages of Ceramic Membranes

The major advantage of ceramic membranes over their polymeric counterparts is their high thermal stability. Organic membranes can not operate at high temperatures whereascommercial ceramic membranes can be operated in the range of 200 to 1000 °C (Wade et al. 2007). For example fuel cell ceramic membranes can be operated at 1000 °C (Ehsani et al. 2005).

Mechanical stability of ceramic membranes is higher than their polymeric counterparts and they can be operated at high pressures. They are also chemically stable in a wide pH range(1-14). Ceramic membranes are also biocompatible, long life operational, able to backwash, easy to shape and in some cases they can show electrocatalytic activity (Burggraaf and Cot 1996, Laitinen 2002, Yelken, 2000, Hsieh 1996).

Ceramic membranes have a brittle character which makes them weak in pressure driven separation processes. Their use in pressure driven separation processes necessitate some special configurations and supporting systems which increases the capital installation cost. Sealing technology at high temperature applications can also be complicated.

2.4.2. Applications of Ceramic Membranes

Ceramic membranes have been used for many applications in industry. Their high performance and superior advantages (thermal stability, mechanical strength, chemical stability etc.) makes them the only choice for harsh environment applications where polymeric membranes can not operate. Ceramic membranes are generally developed for wastewater treatment applications but they are used successfully in a large number of separation processes in the industry.

These aplications are :

- *Chemical industry:*

- Separation of alkaline suspensions

- Catalyst separation

- Separation of paints

- Desalination.

- *Metal industry / Surface engineering:*

- Enhancementof oil /water emulsion properties.

- Extraction of heavy metals.

- Wastewater recovery from after metal process.

- *Textiles / Pulp and paper industry:*

-Wastewater recovery

- *Biochemical industry*

- Concentration fractionation, isolation and sterilization for antibiotics, enzymes, proteins, amino acids and vitamins.

- Separation, concentration and dewatering of biomass and algae.

- Disposal of fat emulsions.

- Separation of yeast.

- Desalination.

- *Food and beverages:*

- Purification of juice and beer.

- Sterilization of milk and whey.

- Desalination of whey.

- Dewatering of the products.

2.5. Ceramic Membrane Supports

2.5.1. Processing of Ceramic Membrane supports

Processing of ceramic membrane supports involves a series of steps like suspending the particles in the desired formation, shaping the particle suspension (slurry or paste) as a flat sheet, monolith or tube, and sintering the shaped membrane support at high temperatures. Commonly used flowsheet for the preparation of ceramic membrane supports can be seen in Figure 2.6 where some of the different shaping techniques such as pressing, extrusion, slip casting and tape casting are also indicated. The use of a high temperature heat treatment (partial sintering) step is a must (similar to ceramic processing in general) in the processing although the consolidation technique mayvary

during processing. Multi-layer membranes (asymmetric membranes) can be produced on these membrane supports by different coating techniques such as sol-gel dip coating, CVD or PVD.

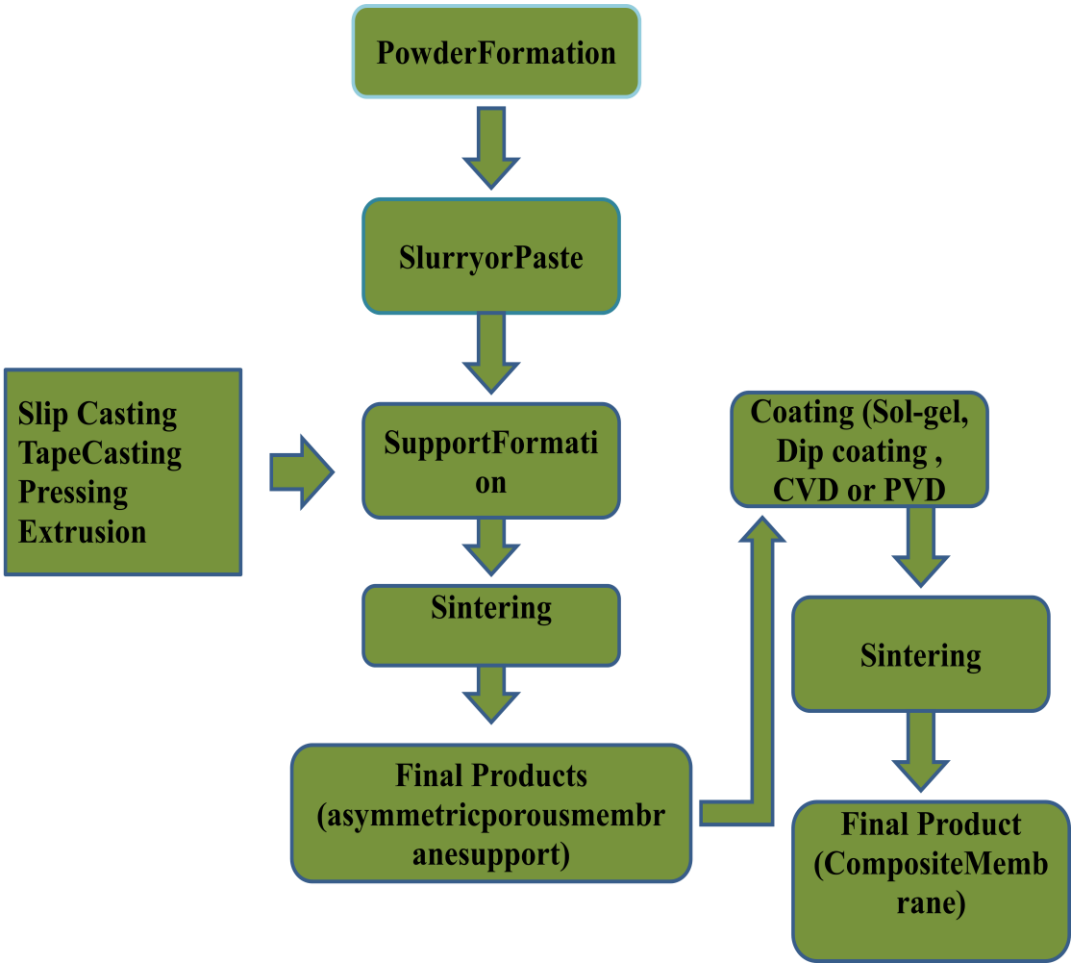

Figure 2.6. Generalized flow chart of ceramic membrane processing.

2.5.2. Manufacturing Methods of Ceramic Membrane Supports

Slip Casting

Slip casting is probably the most commonly used technique in ceramic membrane and ceramic membrane support preparation. This technique is really easy to

apply however there are some drawbacks such as controlling the wall thickness which is usually thick and the casting time is generally long. As shown in Figure 2.7a well mixed slurry is poured into a porous mould where the liquid component of the slurry will be absorbed into the poresdue to capillary forces. The particles are packed on the surface of the mould and form a thin green ceramic layer (Li 2007). Therelatively fast formation of the thin layer is important for the unwanted transport of the particles present in the suspension through the inner pores of the mould. Important slip casting processing parameters are the viscosity and solids content of the slurry and the suspended powder particle size distribution. The suspended powder particle size distribution determines the pore size distribution in the ceramic supports during slip casting process (Li 2007).

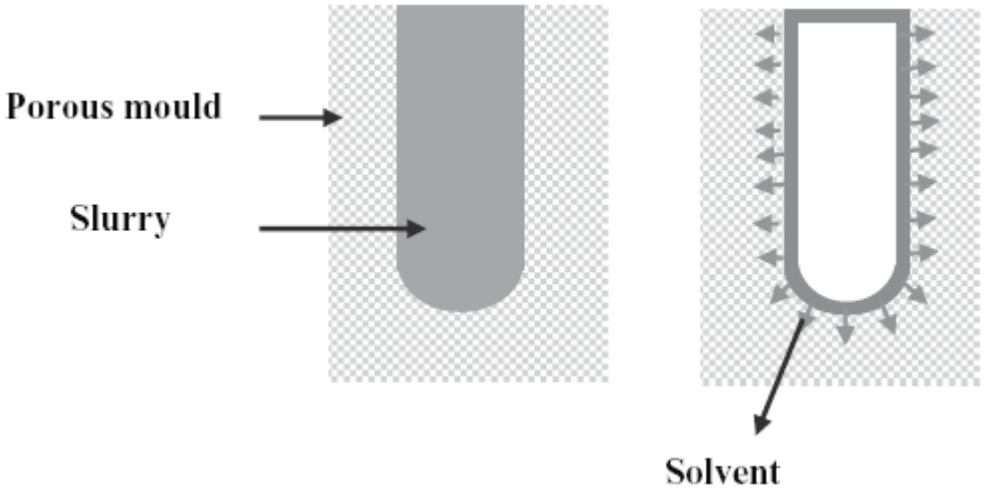

Figure 2.7. Schematic illustration of slip casting process.
(Source: Li 2007)

Tape Casting

Tape casting is a method generally used for the preparation of flat sheet ceramic membrane supports. Figure 2.8 shows the working principle of the tape casting process. The process consists of a fixed casting knife, a bunker for powder suspensions (slurry), a moving carrier and a drying zone. Well dispersed and degassed slurry is poured into the moving bunker and the slurry is casted on the drying zone with the movement. The

thickness of the cast layer can be varied by changing the gap between the casting knife and the casting tape. The viscosity of the slurry, the speed of the carrier and bunker depth are other important variables (Li 2007). The tape cast cake is tranferredto a drying chamber and the liquid component of the cast tape is removed. The dried green body of the ceramic membrane support is usually strong enough for slicing (Bengisu 2001). Tape casting method is used as a continuous process in the industry (Li 2007).

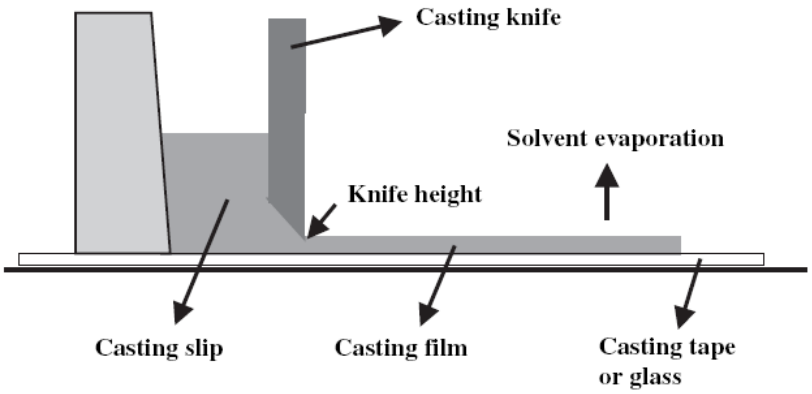

Figure 2.8. Schematic illustration of tape casting process.
(Source: Li 2007)

Dry Pressing

Dry pressing is a simple low cost industrially important process which is used for the preparation of disc and flat sheet inorganic membrane supports. The consolidation of the powders occur by the application of a force on a die creating significant levels of pressure as shown in Figure 2.9 (Li 2007). Applied pressure is dictated by the powder and green structure properties but can vary from a few to hundreds of MPa. High pressures form strong and dense green bodies decreasing the shrinkage level during sintering step. Pressing of ceramic powders can be improved by adding some additives. A low level of water decreases the dry pressing pressure and organic binders can reduce the friction forces between powder particles and die surfaces while increasing the green body strength (Drioli and Giorno 2010).

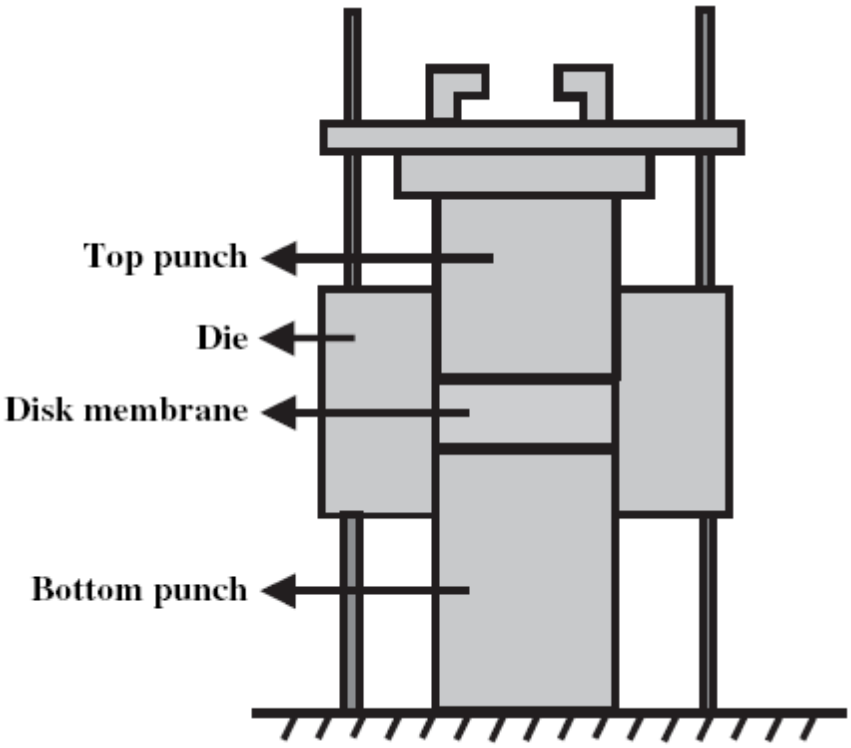

Figure 2.9. Schematic illustration of pressing.
(Source: Drioli and Giorno 2010)

Extrusion

Extrusion is a very appropriate green-forming technique for both industrial and laboratory products. Inorganic and polymeric materials can be shaped with this technique (Li 2007, Drioli and Giorno 2010). Traditional ceramics such as tile and brick have been shaped by extrusion for a very long time. Advanced ceramics can also be shaped by extrusion such as porcelain electrical insulators, thermocouple protection tubes, furnace tubes, magnets and electronic substrates, catalyst supports and tubular membrane supports (Li 2007). A wide varietyof tubular ceramics in various geometries such as monolithic honeycomb tubes and single or multichannel tubes can be formed by extrusion. Tubular extruded ceramic membranes with various geometries are shown in Figure 2.10 (Drioli and Giorno 2010). A ceramic paste which exhibits plastic behaviour is forced under high pressuresto pass through a desired geometrydie in extrusion. The paste should be stiff enough so that the extruded ceramic maintains its physical integrity during the subsequent drying stage. Alumina is commonly used as a tubular ceramic

membrane support material but rarely mullite and cordierite can also be used (Drioli and Giorno 2010).

Figure 2.10. Some different tubular ceramic membrane shapes.
(Source: Drioli and Giorno 2010)

Centrifugal casting

Centrifugal casting is a new technique for ceramic tube shaping. In this method powder suspension ispoured into acylindrical mold and rotated rapidly around its axis. The powder suspension will form a cake layer on the walls of the mold during this rotation which is the green body of the ceramic membrane support. (Harabi and Bouzerara 2011).

2.5.3. Selective Layer Formation on The Support Surfaces

Membrane selective layer determines the separation capacity of the membrane which was discussed in previous chapters and the formation of theselctive layer on support surfaces is a very important issue which determines the membrane performance. Sol-geldip-coating and chemical vapour deposition methods are the most commonly used techniques for the selective layer formation.

Sol-Gel Process

The use of sol-gel method in membrane processing started with Leenaars et al. (1985)'s research on the preparation of ceramic ultrafiltration membranes. The biggest advantage of the sol-gel method is that the pore size of the selective layer can be closely controlled even for nanoscale pores. Preparation of ceramic selective membrane layers by sol-gel method is achieved mainly through two basic routes.

1- The colloidal route: Metaloxide powders (commonly used materials are Al_2O_3, ZrO_2, TiO_2, SiO_2 and Boehmite AlO(OH)) are dispersed in water to form a sol which is further used for coating the membrane support surface. It forms a colloidal gel film on the support surface which becomes the selective layer after drying and heat treatment.
2- The polymeric route: Metalorganic precursors are mixed with alcohols and a low level of water for the formation of a polymeric sol which results in the formation of a polymeric gel on the membrane support surface (Li 2007).

The use of the sol-gel method in ceramic membrane processing has been reported in a large number of research papersin the scientific literature (Larbotet al. 1989), Andersonet al. 1988, Moosemiller et al.1989, Yelken 2000, Akbarnezhad et al. 2010).

Dip-Coating method

Dip coating method has been widely used for the preparation of ceramic membranes. A membrane support is slowly immersed intoa particle suspension and withdrawn from the suspension with a coated surface after a previously set time which is critical for the nature and thickness of the coating in this method. In dip coating

method different parameters like the viscosity/solids content of the powder suspension, dipping time/speed and the removing speed of the coated article from the dip suspension are important on determining the coating properties. Drying stage starts simultaneously at atmospheric conditions and after the ceramic is totally dried, a heat treatment stage is applied for mechanical/thermalstability (Buonomenna and Golemme 2012).

Chemical Vapour Deposition (CVD)

Chemical Vapour Deposition can be described as the condensation of a desired material (in the gas phase) on the surface of the membrane through chemical reactions. In CVD method coating material is diluted in a gas carrier and heated at high temperatures in a reaction chamber with membrane support. The gas phase/surface reactions occurring between a number of added reactants with the coating phase precursors in the reaction chamberforms the desired selective membrane layer on the surface of the membrane support.Some typical examples to these CVD reactions are given in Table 2.3.

Table 2.3. Some chemical reactions in CVD process.
(Source: Li 2007)

Reaction	Equation
Thermal decompositon	$2Al(OC_3H_7)_2 \rightarrow Al_2O_3 + 6C_3H_6 + 3H_2O$
Oxidation	$SiH_4 + O_2 \rightarrow SiO_2 + 2H_2$
Hydrolysis	$2AlCl_3 + 3H_2O \rightarrow Al_2O_3 + 6HCl$
Coreduction	$TiCl_4 + 2BCl_3 + 5H_2 \rightarrow TiB_2 + 10HCl$

CHAPTER 3

RHEOLOGY OF PASTES

3.1 Rheology

Rheology is the study of the deformation and flow of matter under an applied force. Rheological behavior and characteristics of a paste also gives valuable information on the shape forming of a material by extrusion. Rheological behavior of a materialis mainly determined through the relations between shear stress, shear strain, viscosity and yield stress.

Fluids can be classified according to their rheological behavior as Newtonian or non-Newtonian. The viscosity of a Newtonian fluid/suspension is independent of shear rate and shear stress mainly due to the very low solids content and the rheological behavior is commonly similar to that of the liquid component. In non-Newtonian pastes, the solid content is high enough for the formation of relatively strong interactions between powder particles which causes resistance to flow. Ceramic rheological behavior was first introduced by Bingham while conducting research on deformation behaviour of clay and paint suspensions/pastes in the early 1920's (Duvarcı 2009). Ideal systems can be described with linear equations like Hooke's law for ideal solids or Newton's law for ideal liquids (Figure 3.1.a) but for a better understanding of the rheology of complex systems (such as pastes, suspensions or foams) a combination of different equations is necessary.

The viscosity of Newtonian fluids which can be related toshear rate and shear stress by the following equation is a constant which is a function of temperature and pressure:

$$\tau = \eta\gamma \tag{3.1}$$

where$\tau$is the shear stress, $\eta$is the viscosity and γ is the shear rate.

Non-newtonian materials can be classified in different groups because viscosity is a function of shear rate and shear stress. Increasing shear rate can make structural changes in the material causing an easier flow and a decrease in the viscosity. These materials are **shear-thinning** or **pseudoplastic** materials (Figure3.1.b).In **shear-thickening** or **dilatant** materials viscosity increases with increasing shear rate (Figure3.1.c). Material stays rigid when the shear stress is lower than yield stress value but flow like newtonian materials if shear stress exceeds the yield stress in **Bingham plastic**non-newtonian materials(Figure 3.1.d).The flow of material starts beyond a specific shear stress (yield stress) and the viscosity decreases with further increase in shear stress for another class of materials(Figure3.1.e).

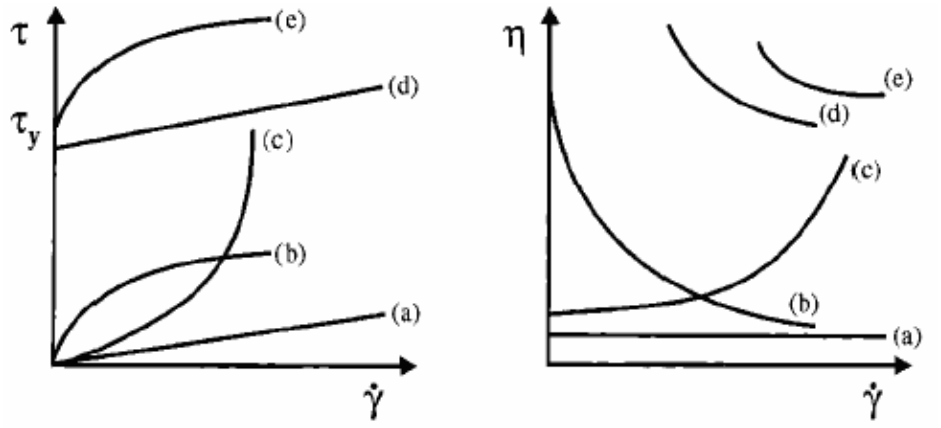

Figure 3.1. Types of rheological behavior exhibited by colloidal dispersions: (a) Newtonian flow; (b) shear thinning (pseudoplastic); (c) shear thickening; (d) Bingham plastic; and (e) pseudoplastic with a yield stres. (Source: Lewis 2000)

Description of the non-Newtonian rheological behavior can be accomplished by using different equations. Bingham plastic behaviour is basically very similar to newtonian fluids except that the material starts to flow at higher shear stresses (Figure 3.1.d). Bingham plastic behaviour can be expressed by the following equation (Bingham 1916):

$$\tau = \tau_0 + \eta\gamma \tag{3.2}$$

In this equation, τ is the shear stress, τ_0 is the yield stress, η is the viscosity and γ is the shear rate. This equation was reported to satisfactorily describe the rheological behaviour of mineral-water suspensions, slurries/sludges and electro-magneto rheological fluids (Radhakrishnan 2002, Bernadou 1999).

The following equation called the Power Law is another commonly used relation between shear stress and shear rate:

$$\tau = k\gamma^n \tag{3.3}$$

where*k* is the flow consistency, γ is shear rate and *n* is the flow index. The material exhibits shear thinning behaviour (*n* is between 0 and 1) or shear thickening behaviour (*n*>1) based on the value of the flow index.The substitution of equation 3.3 in 3.1 gives the following equation for the viscosity of the material (Johnson 2012) :

$$\eta = k\gamma^{(n-1)} \tag{3.4}$$

Herschel-Bulkley model is the simplest model which accounts for the non-linear relationship between shear rate and shear stress at high yield stress value. It is similar to the Bingham plastic model. This model can be expressed by the following equation which reduces to Bingham Plastic behaviour model for an *n* value of 1:

$$\tau = \tau_0 + \eta\gamma^n \tag{3.5}$$

This model is used for the description of the physical behaviours of three dimensional structures and their resistance to flow. The shear stress/shear rate relation is nonlinear unlike the linear dependence observed in bingham plastic model at high shear rates.

3.2. Paste Flow in Extrusion

Flow of a paste in extrusion occurs by the application of pressure on the the ram and can be divided into two stages. These are the flow through the die and the flow from barrel to the die as shown in a piston extruder in Figure 3.2. Paste flow in the extruder die is assumed to move as a plug and plug flow dominates the paste flow. Slippage occurs in the liquid layer at the die wall (Zheng and Carlson 1992). In extruder near to the walls shear region increases but not all of the paste is subjected to shear stress. Friction at the walls can not stop the flow of paste because yield stress usually exceeds the friction force. The applied pressure and the velocity of the ram/piston are important variables and the relationship between them is a key issue for a better understanding of paste rheology. This relation can be better understood by using Benbow and Bridgwater model which will be discussed in the next chapter (Powell Et al., 2013; Blackburn and Biihm, 1996; Horrobin and Nedderman, 1998).

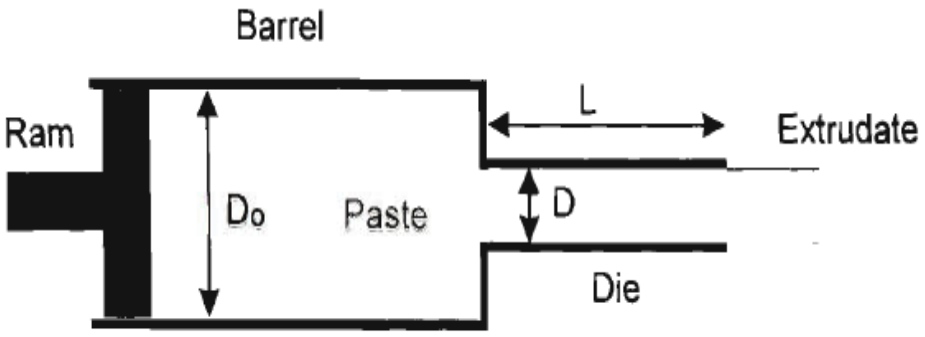

Figure 3.2. Schematic illustration of ceramic paste flow in piston extruder. (Source: Das et al. 2002)

CHAPTER 4

CERAMIC EXTRUSION

Extrusion is a plastic shaping method. It has been used in industry fora wide range of applicationssuch as the production of bricks, catalyst supports, tubular ceramic membranes, pipes, heat exchanger tubes etc.

4.1. History of the Extruder in Ceramics

Extrusion processwas originally developed for structural ceramic industry however it was later used in a large number of applications in variousindustries such as food, plastics, chemical industry etc.

Extrusion of ceramics has been investigated for many years and its first large scale industrial application was for the production of bricks in the earlier years of 17^{th} century. Research on ceramic extrusion was conducted for traditional ceramics processing until 1970s. Advanced ceramics attracted significant interest after 1950s due to their high application potentials and with that attention extruders have found applications in shaping of advanced ceramics. The very first test was conducted in Germany in 1960 for the production of ceramic honeycomb catalyst convertersbut the test was not successful at the time. The first successful test was conducted by Japanese researchers in 1970 which then started the very first large scale production in 1975 (Handle 2007).

4.2. Types of Extruders

4.2.1. Auger (Screw) Extruder

Auger (screw) extruder is a complicated equipment. Figure4.1 shows schematic illustration of an auger (screw) extruder. The pug mill is the main part of auger extruder which contains the auger shaft with mounted blades (shaped like a screw).

Kneading is the main step for the preparation of a ceramic paste. For an effective kneading process, paste should show low adhesion and high cohesion properties. Deagglomeration and homogeneity must be achieved by the kneading processsimilar to the commonly utilized mixing process (Guire et al. 2004).The paste is then fed into the pug mill.Kneading of the paste in the pug mill further improves the homogeneity and the plasticity with the removal of air from the paste. The kneaded paste is finally forced to flow through the dies. Ball milling of the powder components is essential in breaking down the present agglomerates improving the mixture homogeneity prior to the kneading process (Nagaoka et al. 2007). Reduction in the size of the agglomerates will prevent the future cacks and improve the strength of the alumina tubes (Alford et al. 1987).

Auger (or screw) configuration can vary in a pug mill and could be formed from one, two or more screws where the rotation of screws can be in similar or in opposite directions(Richerson 2005, Handle 2007, Terpstra et al. 1995).Schematic illustrations of different screw designs are shown in Figure 4.2.

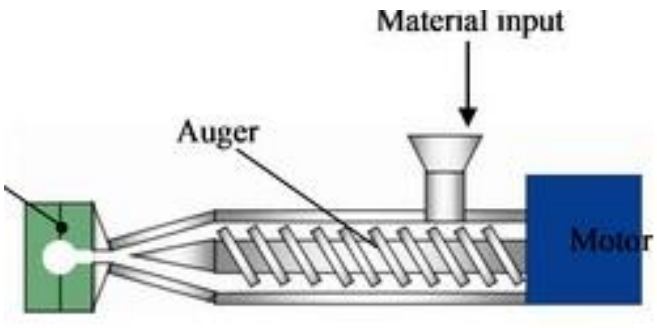

Figure 4.1. Schematic illustration of Auger extruder.
(Source: Leo et al. 2014)

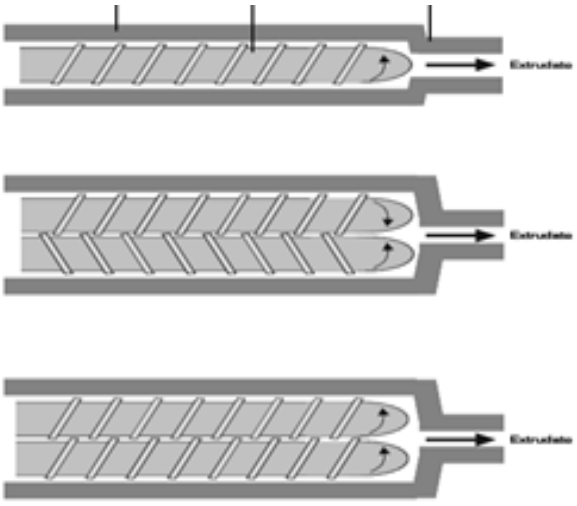

Figure 4.2. Auger (screw) extruder with different designs.
(Source: Handle 2007).

Some auger extruders are additionally equipped with deairing chamber which applies vacuum to the paste for removing the air and than forces the paste through the die(Richerson, 2005).Auger extrusion is a continuous process and it can process large quantities of materials which can be as high as 1000 tonnes per hour (Terpstraet al. 1995).

There are some disadvantages of auger extrusion processing. Technical ceramics are generally very hard materials which can wear the metallic surfaces of the auger extruder which may cause significant iron contaminationin the paste. The formation of laminated layers during extrusion is another important disadvantage which may cause crack formation in the green body making the rejoining of the pasteharder (Handle 2007,Terpstraet al. 1995).

4.2.2 Piston Extruder

Piston extruder is the first extruder type that had been patentedin 1623. It was used for shaping traditional ceramic material “brick” (Handle 2007). Piston extruder is not solely used for ceramic materials but also for some other applications like shaping plastics, metals (aluminum profiles, wrought copper alloys etc.) and even food industry (production of pasta) (Handle 2007).

Piston extruder has a simple design and the main parts are barrel, piston and the die (Terpstraet al., 1995;Kong et al. 2015). Piston extruder is a batch operational

machine mostly used for lab scale applications. The paste is fed into the barrel and forced through the die by a piston with pressure. Vacuum can be applied for deairing the paste.

The major advantagesof a piston extruder over the auger (screw) extruder can be listed asfollows:

- It enables extrusion with high pressures,
- Contamination (caused by abrasion) will be low compared to a screw extruder,
- Easy to clean and a minimum amount of waste material,
- Laminations will be less compared to an auger extruder,
- Abrasive pastes can be produced with relatively low wear rates (Handle 2007, de Jong 2009).

4.3 Additives for Ceramic Extrusion

Additives with various functions/chemistries are used in ceramic extrusion pastes for different purposes. Plasticity of the ceramic paste is important for preventing tearing and bending of the tube green bodies (Nagaoka et al., 2007, Bayer et al., 2012, Liu et al., 2000). The positive effects of hydroxy propyl methyl cellulose (HPMC) and hydroxy ethyl methyl cellulose (HEMC) addition on ceramic paste extrusion and rheology was reported by Roland Bayer (Bayer et al., 2012). The use of boehmite as an inorganic binder for the reduction ofcarbon dioxide emissions and the minimization of the binder burn out problems encountered during heat treatment was also investigatedbesides the above polymeric plasticizers (Kumar et al., 1997). Commonly used ceramic paste additives are listed in Table 4.1.

Table 4.1. List of additives commonly used in ceramic extrusion pastes. (Source: Boch et al., 2007)

Dispersant	Ammonium acetate, ammonium polyacrylate
Binders	Polyethylene glycol with high molecular weight, cellulosederivatives (methyl cellulose, ethyl cellulose, hydroxyethyl cellulose), polyvinyl alcohol
Plasticizer	Glycols with low molar weight, polyethylene oxide, traditional pastes: water
Lubricants	Polyelectrolytes, sodium carbonate, sodium silicate, stearates,

4.3.1 Dispersant

The presence of well dispersed powder particlesin a plastic paste is important in the properties of extruded green bodies. Dispersants are used in paste formulations for the prevention of agglomeration in extrusion pastes which also decreases the viscosity (Boch and Nièpce,2007).

4.3.2 Binder

Binders are one of the most important additives for ceramic extrusion. Extruded green body should have enough strength for handling and it should not collapse before sintering. Binder materials for extrusion paste can be divided into two major groups as organic and inorganic binders (Ananthakumar et al., 2007).

Clay is the most commonly used inorganic binder in the traditional ceramic industrybut their use in advanced ceramics poses serious problems due to the presence of high levels of impurities in clay. In preparation of advanced ceramics,clay would not be the proper choice because purity plays an important role for advanced ceramics (Ananthakumar et al., 2007). Aluminum silicate and sodium silicate have been reported as an inorganic binder material in earlier studies (Miller and Haber, 1991).

Alumina is widely used for producing tubular ceramic membranes by extrusion method. Alumina behaves as a non-plastic ceramic material. Alumina paste should present plastic behaviour for extrusion and after sintering tubular membrane should be faultless. The use of traditional inorganic binders can generate microstructural problems during heat treatment and deteriorate chemical and thermal properties of the ceramic supports (Ananthakumar et al. 2007). Boehmite has been used in alumina ceramic pastes as a binder in many studies (Ananthakumar et al., 2007; Kumar et al., 1997; Nagaoka et al. 2007). Boehmite transforms to γ-alumina at higher than 350-400 ^{o}C and at temperatures above 1200 ^{o}C it transforms to α-alumina in the membranesupport matrix. This phase also forms fine alumina grains during heat treatment which may also contribute significantly to the mechanical strength of the alumina tubes (Ananthakumar et al., 2007).

The presence of water and inorganic binders in the paste formulations can not always provide the necessary paste properties for successful extrusion. Inorganic binders more likely show shear thickening or shear thinning rheological behaviour. For successful extrusion, pastes should show visco-elastic behaviour, therefore addition of organic binder isessential. The presence of the organic binder contributes significantly to the green strength of the bodies after the removal of the water during the drying stage. Major disadvantage of the organic binders is the burnout problem which can cause cracks or damage on the membrane surface during the binder removal step. The organic binder content of the pastes should therefore be optimized and selected to be as low as possible in the ceramic paste.

The use of different organic binders and their effects on the ceramic paste extrusion was investigated in a series of research articles. The effects of hydroxy propyl methyl cellulose (HPMC) (Ananthakumar et al.2007), hydroxy ethyl cellulose (HEC)(Khan et al.), and both methylcellulose (MC) and polyvinyl alcohol (PVA) (Das et al.) as a binderon ceramic paste properties and extrusion was reported.

4.3.3 Plasticizer

Plasticizer is used for modifying the rheology of the binder for better plastic behaviour of ceramic pastes (Carter and Norton, 2013). Organic plasticizers decrease the glass transition temperature of the organic binder and make it more ductile for easy shaping on the die of extruder.

4.3.4 Lubricants

Lubricants are used for minimizing the friction between barrel and the paste (Handle, 2007;Boch and Nièpce, 2007). Lubricants also have a small effect on decreasing the working pressure.

4.4 Benbow and Bridgwater Model

Extrusion paste rheology depends on various processing parameters. Benbow and Bridgwater developed a method for analysing paste rheology in a ram extruder (Benbow and Bridgwater, 1993). Properties of material flow, extrusion velocity and die geometry all are taken into consideration in this model.It is a commonly used very useful technique for the determination of the properties of ceramic pastes. It can also be used to model both industrial and laboratory scale extrusion applications.

Benbow and Bridgwater had examined the paste rheology for different die shapes. Figure 4.3 shows an example of capillary extrusion. First they had examined behaviour of a paste which is shaped by square entry die.The established equation representsthe paste rheology based on the pressure *P g*eneratedwhen paste flow through a barrel of diameter $D_0$and a cylindrical die-land of length *L* and diameter *D*. *P* canbe expressed as:

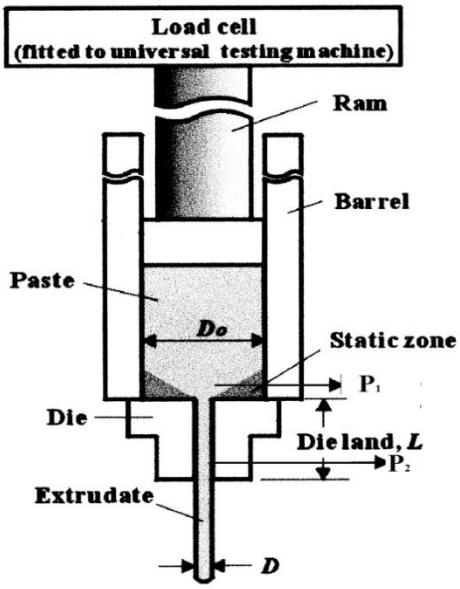

Figure 4.3 Ram extruder.
(Source: Li et al. 2000)

$$P=P_1+P_2 \tag{4.1}$$

$$P=2(\sigma_0+\alpha V)\ln D_0/D +4(\tau_0+\beta V)(L/D) \tag{4.2}$$

where σ_0 is an initial yield stress, α is a characteristic factor which effects velocity of the paste in die entry, V is the extrudate velocity, D_0 is the barrel diameter, D is the die diameter. Equation 4.2 is also known as four parameter model (Horrobin and Nedderman, 1998).

The first part of this equation gives the die entry pressure drop,

$$P_1= 2(\sigma_0+\alpha V)\ln D_0/D \tag{4.3}$$

Plug flow (which is discussed in earlier sections) occurs in the die land and the bulk paste is likely to be separated from the wall by the surrounding lubricating liquid layer. Wall shear stress thus becomes a function of the velocity of the bulk paste. Die

land pressure drop (P_2) therefore is represented by the second part of the equation as follows;

$$P_2=4(\tau_0+\beta V)(L/D) \quad (4.4)$$

where τ_0 is the initial wall stress, L is the die length, β is the characteristic factor which effects velocity of the paste in die land. The die wall shear stress is equivalent to $\tau_0+\beta V$ at a given velocity. Paste flow in the barrel was assumed to be zero by Benbow and Bridgwater.

Benbow and Bridgwater observed that the actual die entry pressure and die land pressure was greater than the predicted value by Equation 4.4 during their experimental studies. They formulated a better description for the non-linear behaviour of the paste flow [Benbow and Bridgwater, 1993, Martin et al., 2001) which is known as the six parameter model:

$$P=2(\sigma_0+\alpha_1 V^m)\ln D_0/D +4(\tau_0+\beta_1 V^n)(L/D) \quad (4.5)$$

where α_1 is the characteristic velocity factor in the die entry ($m\neq1$), m is the bulk velocity exponent, β_1 is the characteristic velocity factor in the die land ($n\neq1$), n is the wall velocity exponent. In this equation α_1, m, β_1 and n are assumed independent from die geometry.

Many researchers have used Benbow and Bridgwater model to understand the rheological behaviour of different pastes. Ribeiro et al.(2006) used Benbow and Bridgwater model for predicting the rheological behaviour of alumina and cordierite pastes. Khan et al.(2001) investigated the effect of hydroxy ethyl cellulose (HEC) binder on alumina paste rheology. They used piston type extruder and capillary dies with different die length and diameter (L/D=1, L/D=2, L/D=4, L/D=8) to determine six parameters of paste rheology. Sample pastes were extruded with Testometric mechanical test device with mounted various load cells at different velocities. The applied pressure (P) was recorded during these tests.

The extrapolation of theP – L/D plots to zero L/D yields P_1accordingto Equation 4.5. Die land pressure P_2becomes zero when L/D is equal to zero and Equation 4.5 can be rewritten as:

$$\frac{P_1}{\left[2ln\left(\frac{D_0}{D}\right)\right]} - \sigma_0 = \alpha_1 V^m \tag{4.6}$$

The $\log\left(\frac{P_1}{\left[2\ln\left(\frac{D_0}{D}\right)\right]} - \sigma_0\right)$ versus log V plot gives a straight line and its slope is α_1 and its intercept is m. The σ_0 parameter is obtained from a plot of $P/2\ln(D_o/D)$ versus V. The subtraction of P_1 from P yields P_2 (Equation 4.3) which is further used for the determination ofτ_0, β_1 and nwith a similar approach.

4.5 Viscosity of Ceramic Paste

The apparent viscosity of ceramic pastes which are considered to be non-Newtonian fluids is given by the ratio between the true shear stress and the apparent shear strain at the die wall (Azzolini et al., 2014, Sharmin K., 2014):

$$\eta_a = \frac{\tau_w}{\dot{\gamma}_a} \tag{4.7}$$

where$\eta_a$is the apparent viscosity, τ_w is the shear stress at the die wall and $\dot{\gamma}_a$is the apparent shear rate. Azzolini et al. (2014) have proven that the calculation of the apparent viscosity of non-Newtonian fluids (such as ceramic pastes) by Equation 4.7 matches very well with the Krieger–Dougherty model viscosity calculation.

Capillary flow analysis were conducted by Mooney for non-Newtonion fluids (Mooney, M., 1931) and was used for the measurement of the pressure-drop/flowrate relationship which was further used for the determination of the true wall-shear rate and the corresponding shear-rate-dependent viscosity. Definition of shear rate by Mooney

was used by different resarchers (Adams et al. 1995, Khan et al. 2001, Ochoa et al. 2005). According to Mooney analysis, shear rate can be written as:

$$\dot{\gamma}_a = \frac{4Q}{\pi R^3} \tag{4.8}$$

where Q is the volumetric flow rate given by the extrudate velocity times the cross sectional area of the die and R is the radius of the die.

Determination of the shear stress at the die wall (τ_w) for extrusion processcan be conducted by using Benbow and Bridgwater model.The apparent viscosity of the ceramic paste can be calculated by using Equation 4.7. In extrusion process shear stress usually acts on the paste at die walls therefore shear stress at the die wall (τ_w) should be known for calculating the viscosity of the pastes. τ_w is simply related to the extrudate velocity in the die land. Second part of Equation 4.5 corresponds to the pressure drop in the die land in which τ_o is the initial wall shear stress and $\beta$is the characteristic velocity factor in the die land. The apparent viscosity of the ceramic paste can be determined after the determination ofτ_w and $\dot{\gamma}_a$.

CHAPTER 5

EXPERIMENTAL

5.1. Materials

Alumina ceramic tubes were prepared by using α-alumina, boehmite, methocel, glycerol and water. The pastes used for preliminary experiments were prepared by using α-alumina, boehmite, methocel, glycerol, prejel, Al-stearate and water. Specifications and sources of these materials are given in Tables 5.1-5.4

α-Alumina powders were characterized with FEI QUANTA 250 FEG Scanning Electron Microscope(SEM) in order to determine particle size and morphology and their particle size distributionswere determined by using Micromeritics Sedigraph 5100. Phase characterization of the α-Alumina, boehmite and methocelpowders was conducted with Philips X'Pert Pro XRD. Thermal behaviourof the methocel powders weredetermined bySchimadzu TGA51 up to 1000^{o}C in dry air with a heating rate of 10^{o}C/min.

Table 5.1. Specifications of α-Alumina powdersreceived from Almatis Co.

	CL 4400 FG	**CL 3000 SG**	**CT 1200 SG**	**CT 3000 SG**
Particle size / d_{50} [μm]	5.2	4.0	1.3	0.5
BET Surface Area [m^2/g]	0.6	1.0	3.1	7.5

Table 5.2. Specifications of Boehmite powders received from Sasol Co.

Particle size / d_{50} [μm]	25
BET Surface Area [m^2/g]	180
Dispersed Particle Size [nm]	80
CrystalliteSize[nm]	10

Table 5.3. Specifications of HPMS (hydroxy propyl methyl cellulose) received from DOW Chemical Co.

Commercial Code	Degree of substitution of Methoxyl	Molar substitution of Hydroxypropyl	Viscosity (mPa.s) (%2 solution)	Gelation temperature (°C)	The average degree of polymerization	Average molecular weight (Mn)
Methocel F50	1.8	0.13	50	63	110	20.000
Methocel F4M	1.8	0.13	4000	67	460	86.000
Methocel A4M	1.8	-	3000-5500	43	460	86.000

Table 5.4 Sources of other important additives.

HEMS (Hydroxy ethyl methyl cellulose)	DOW Co.
Glycerol	Dalan Kimya
Al-Stearate	Pendik Nişasta
Prejel	Acar Kimya Tekstil Ltd. Şti.

5.2. Preliminary Experiments with Orifice Die

Powders (Alumina, boehmite, HPMS/HEMS, Prejel, Al-Stearate) were dry mixed in an agate mortarand the liquid components (water and glycerol) were then added to the powder mixture. The paste like mixture was kneaded in the mortar with a pestle for about 15 minutes. The prepared paste batches were about 40-100 grams in weight.

A 3 mm diameterorifice die (L/D ~zero)was used in the preliminary experiments. The barrel internal diameter and length were 16 mm and 60 mm, respectively during the experiments. Prepared ceramic paste compositions and their

codes are given in Table 5.5. The experimentally determined extrusion forces are also given in the same table. Barrel was lubricated with stearic acid and ~10 grams of paste were fed into the barrel. Tests were carried out in mechanical test device (Testometric SN 500-526) with mounted 100 kN load cell with acrosshead velocity of 5 mm/min. A picture of the extrusion process can be seen in Figure 5.1.

Table 5.5. Sample codes and compositions of the prepared ceramic pastes for preliminaryexperiments.

Batch No	**HEMS**	**HPMS (Methocel F50)**	**Al-Stearate**	**Prejel**	**Glycerol**	**Boehmite**	**Volumetric solid percentage (%)**	**Force (N)**
P1	Industrial Ceramic Paste							150-250
P2	+	-	+	+	+	-	58	346
P3	+	-	+	+	+	-	55.6	266
P4	+	-	+	+	+	-	55	202
P5	-	+	+	+	+	-	55	192
P6	-	+	+	+	+	-	57.9	233
P7	-	+	+	+	+	-	61.5	272
P8	-	+	-	-	+	+	56.6	208
P 9	-	+	+	+	+	+	56.8	195
P10	-	+	+	+	+	+	56.5	160

Figure 5.1. Extrusion of ceramic pastes in the mechanical test device (Testometric SN 500-526) with orifice die.

5.3. Preparation of Tubular Alumina Ceramic Supports

Tubular alumina ceramic supports were prepared by extrusion. Processing flowchart is given in Figure 5.2. Thetubular alumina ceramic support processing steps can be listed as dry mixing, kneading, extrusion, drying, debinding and sintering. The preparedpaste batches were about 4500-5000 grams in weight.

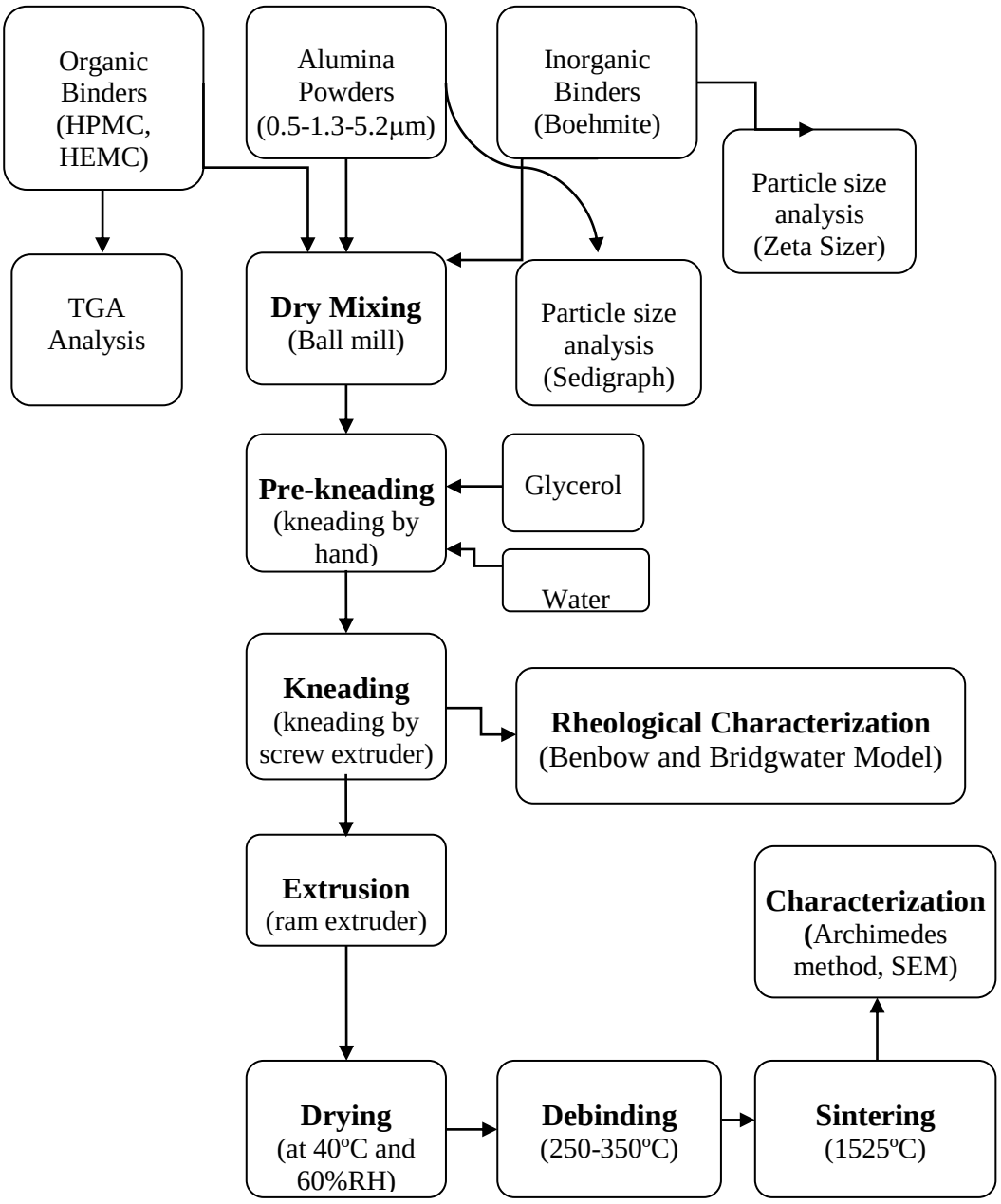

Figure 5.2. Flowchart of experimental work.

5.3.1 Dry Mixing and Kneading of Pastes

Alumina powders, polymeric and inorganic binders were dry mixed using a ball mill in a plastic container with alumina balls at 35 rpm for 2 hr. Table 5.6 shows the composition of the extruded pastes. The piston extrusion pressures of the samples are also given in the same table.Liquid phase of the pasteswas prepared separately from dry powders. Predetermined amounts of glycerol and water were mixed with a metal spoon until the blurry solution became a homogeneous transparent solution.

Pre-kneading of the ball milled powders and the liquid solution wereconducted in a plastic container by the incremental addition of the liquid mixture to the ball milled powders in a plastic container and kneaded by hand. The pre-kneaded pastelike mixture was further kneaded in a screw extruder and a picture of this screw extruder can be seen in Figure 5.3. The pastewas extruded under vacuum (to prevent air bubble entrapment in the final paste) with the same extruder in order to produce sausage like tubes with a 56 mm diameter die after passing the paste through the extruder 6 times. Paste sausage preparation with screw extruder can be seen in Figure 5.4. Die diameter was set at 56 mm which is close to the diameter of the piston extruder barrel in order to minimize the bubble entrapment in the paste during tube extrusion.

Table 5.6. Volumetric % contents of extruded pastes.

Batch No	Volume %									Piston Extruder Pressure bar
	Alumina [µm]			Inorganic Additive	Polymeric Additive			Glycerol	Water	
	5,2	1,3	0,5	Boehmite	F4M	F 50	A4M			
1	35.02	7.00		7.15	5.31			1.85	43.66	50
2	44.31	5.27		3.79	4.96			2.19	39.46	90
3	42.69	5.08		3.65	4.78			3.82	39.96	45
4	41.97	4.99		3.59	4.70			5.45	39.28	42
5	41.20	4.90		3.55	4.61			5.35	40.39	41
6	41.59	4.95		3.56		4.66		5.40	39.82	30
7	42.84	5.09	2.40		4.80			3.84	41.02	20
8	43.47	5.17	2.43		4.87			3.90	40.14	23
9	42.23	5.02	2.36	1.81	4.73			3.89	39.95	25
10	43.35	5.15	2.43	1.76		4.61		3.78	38.91	26
11	43.35	5.15	2.43	1.76	4.61			3.78	38.91	33
12	44.41	5.27	2.50	1.80	4.72			3.87	37.41	34
13	44.84	5.32	2.51	1.82	4.77			3.91	36.81	38
14	43.90	5.22	2.03	1.88	4.92			4.04	37.99	38
15	40.53	4.81	1.88	1.73			4.54	3.72	42.76	25
16	43.91	5.22	2.03	5.08	1.70			4.04	38.00	40
17	43.90	5.22	2.03	3.40	3.40			4.04	37.99	29
18	42.55	4.95	4.03	---	6.21			3.83	39.31	25

Figure 5.3. The screw extruder.

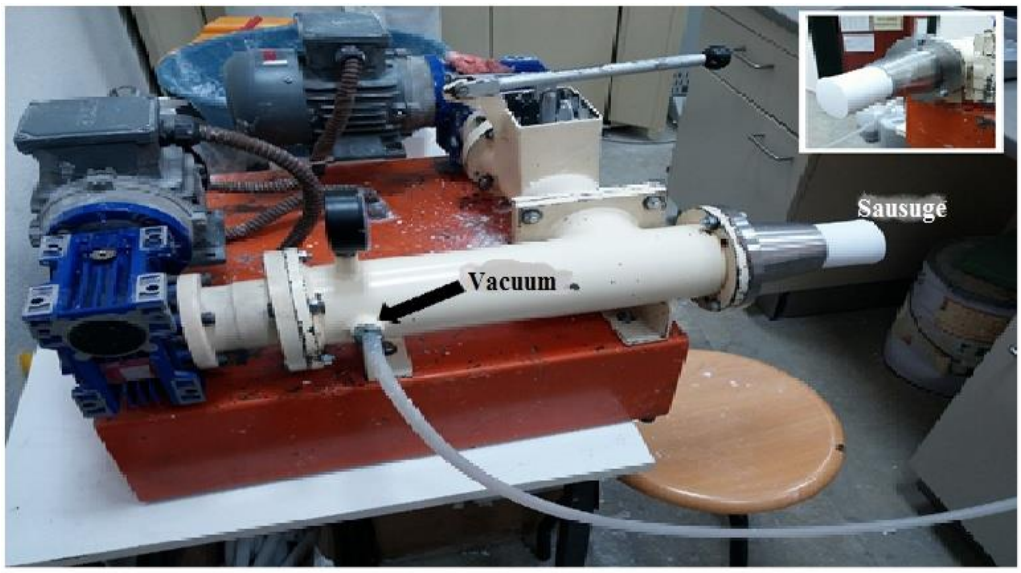

Figure 5.4. Processing of paste sausages.

5.3.2 Rheological Characterization of the Pastes

Piston type extruder with different capillary dies in different die length and diameter (L/D=1, L/D=2, L/D=4, L/D=8) was used for the experimental part of the characterization studies. Sample pastes were extruded by using a mechanical test device (Testometric SN 500-526) with mounted 100 kN load cell at different extrudate

velocities (0.0011, 0.0021, 0.0053, 0.0106, 0.0213, 0.0436 all with m/sunits). Benbow and Bridgwater model (Equation 4.2 and equation 4.5) was used for the modelling and the determination of the rheological propertie of alumina ceramic pastes. Properties of the 14, 15, 16 and 18 coded pastes were analysed with Benbow and Bridgwater model.

5.3.3 PistonExtrusion

After rheological characterization, proper pastes were selected for tube extrusion. Piston extruder was selected for tube extrusion. Prepared sausage like pastes were placed in the barrel and pressure was applied by a piston under vacuum. Piston extruder used in the experiments can be seen in Figure 5.5. Extruded tubes were 16/25 mm in ID/OD and 200 mm in length. Tube extrusion process can be seen Figure 5.6.

Figure 5.5. The piston extruder.

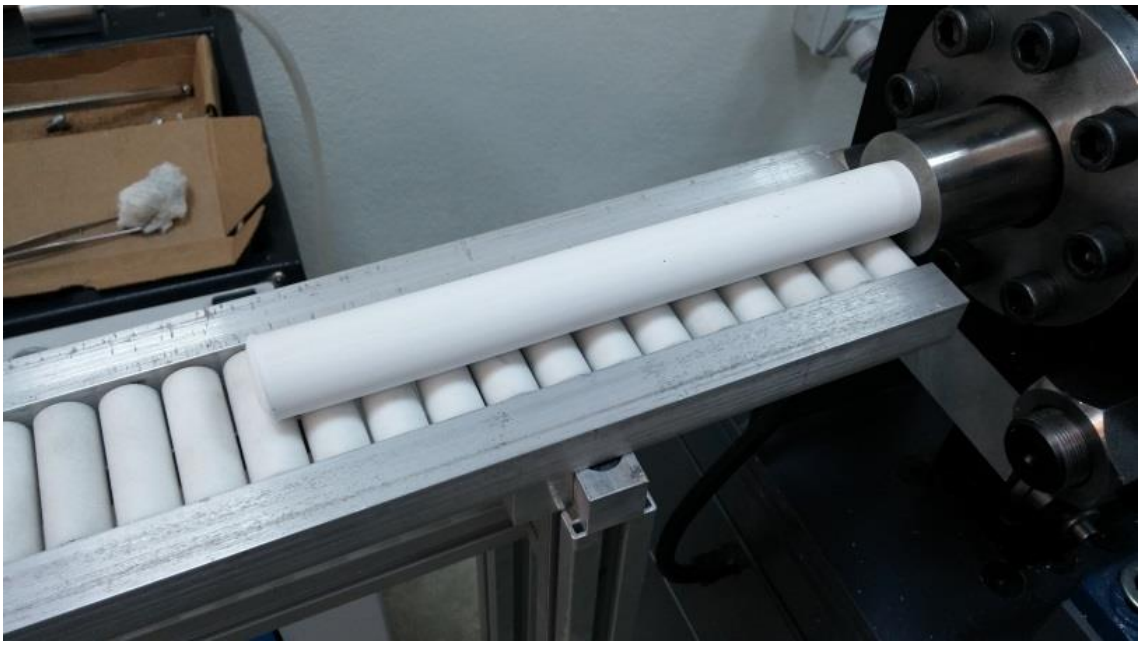

Figure 5.6. Extrusion of tubes from the piston extruder.

5.3.4. Drying and Heat Treatment of Tubes

Drying is a critical process because bending or the formation of cracks can occur on the surfaces of the tubes if the drying conditions/temperature schedules are improperly set.The deformation/bending of the tube surfaces mostly would cause the defective selective coating layers in later stages of membrane processing. Extruded tubes were dried at room temperature for one day and further dried inan oven at 45º-50º C(Memmert100-800) for one more day.

The dried tubes were gradually heat treated with a selected schedule and this selection was based on the thermal degradation behaviour of the organic binders present in the paste formulations. Rapid increase of temperature can damage the ceramic bodies due to the burn out problem of organic binders (Ananthakumar et al., 2001, Nagaoka et al., 2007). Therefore, before sintering process debinding process was applied to ceramic tubes according to the TGA analysis of organic binders.The debinding process of ceramic tubes with Methocel F4M binder/plasticizerwas conducted by the following outlined schedule. The temperature of the furnace was increased to 250ºC with 2ºC/min heating rate followed by one hour hold at that temperature. The temperature was then

increased to 275ºC (2ºC/min) with one hour hold followed by a third step where the temperature was increased to 340ºC (2ºC/min) with one hourhold at this temperature. In the final step of the heat treatment schedule the furnace temperature was increased to 1250ºC with no dwelling time with a heating rate of 5ºC/min. Ceramic tubes with methocel A4M in their compositions were subjected to a slightly different debinding process with different peak temperatures (260ºC, 285ºC, 350ºC and 1250ºC applied,respectively) with similar heating rates and hold times at all the peak temperatures. The ceramic tubes were further heat treated in a Carbolite RHF 1600 high temperature furnace at 1525ºC (with 5ºC/min) with 2 hour hold after debinding heat treatment.

5.4 Characterization of Tubular Alumina Ceramic Membrane Supports

Archimedes method was used for the determination of the pore contents of the tubular ceramic membrane supports.Mercury porosimetry (AutoPore IV 9500 V1.09) was used for the determination of the pore size distribution of the tubular alumina ceramic membrane supports. Grain size and morphologywere characterized with scanning electron microscope (SEM-FEI QUANTA 250 FEG). Mechanicalstrength tests werecarried out in the filtration set-up. The supports were placed in the membrane modules. The TMP (Trans membrane pressure: Pressure difference between the retentate and permeatesides) in the filtrationset-upwas gradually increased up to the collapse level of the support where the TMP suddenly decreases to zero. This TMP level(in bars) was recorded as the mechanical strength of the tubes which is mostly reported by commercial membrane suppliers.

Some of the tubular alumina ceramic membrane supportsafter the final processing step (Length = 200 mm, inner and outer diameters = 16and 25mm, respectively) can be seen in Figure 5.7.

Figure 5.7. Tubular alumina ceramic membrane supports.

CHAPTER 6

RESULTS AND DISCUSSION

6.1. Powder Characterization

Particle size and morphology of alumina powders (0.5 µm, 1.3µm and 5.2 µm) were characterized by SEM pictures. Mainly coaxial rounded alumina particles indicative of extensive ball milling were determined to be dominant morphology in the powders. SEM images of the powders can be seen in Figures 6.1-6.2-6.3.The SEDIGRAGH particle size distributions of the alumina powders are given in Figures 6.4-6.5-6.6-6.7. The average particle size reported by the manufacturer (Table 5.1) was about similar to the determined d50 particle size.The particle sizes (d10, d50 and d90) of the powders are further tabulated in Table 6.1. The XRD patterns of the alumina powders are given in Figure 6.8. Phase structure characterization by XRD indicated that all alumina powders have a pure α-alumina phase structure.

Table 6.1 Particle size of alumina powders (d90, d50 and d10)

	Alumina Powders			
	0.5 µm	**1.3 µm**	**4 µm**	**5 µm**
d90	15	3.25	9	15
d50	0.7	1.8	4.5	6
d10	0.25	0.85	2.6	4

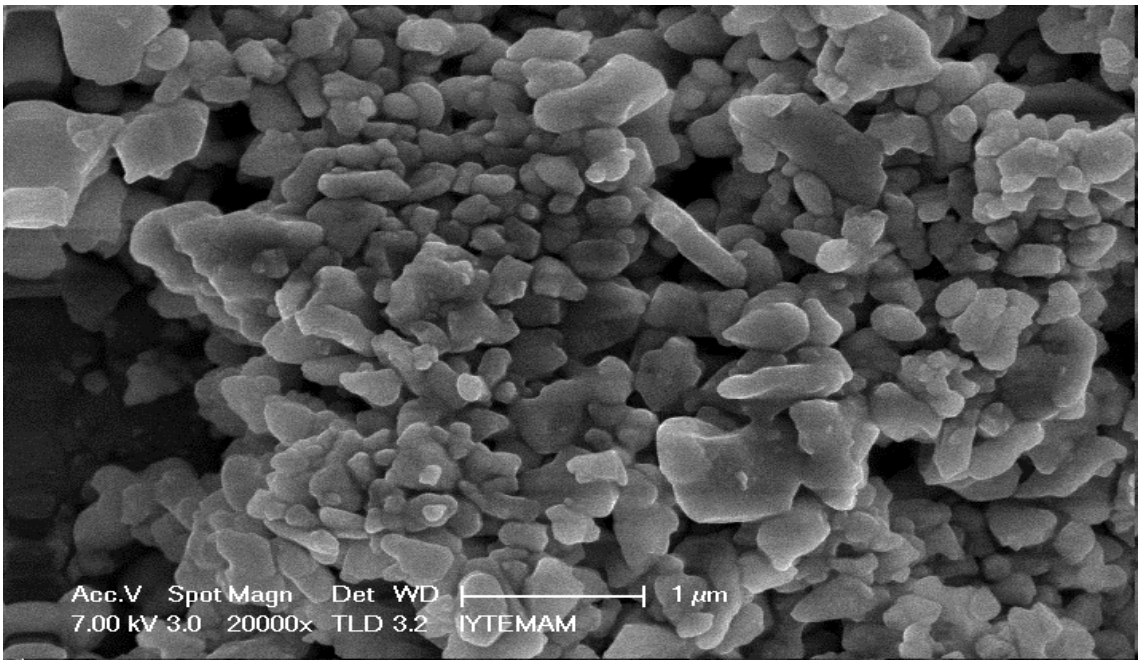

Figure 6.1. SEM image of CT 3000 SG-0.5 μm alumina powder.

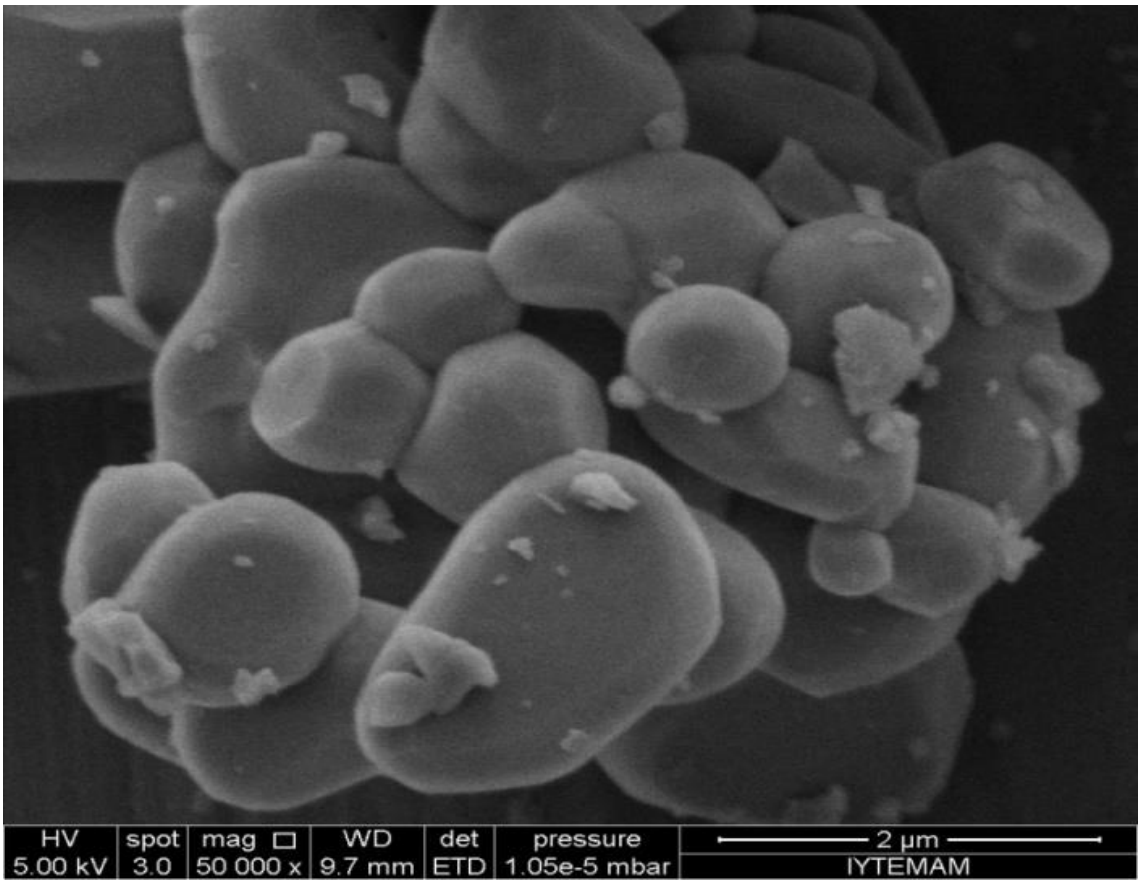

Figure 6.2. SEM image of CT 1200 SG- 1.3 μm alumina powder.

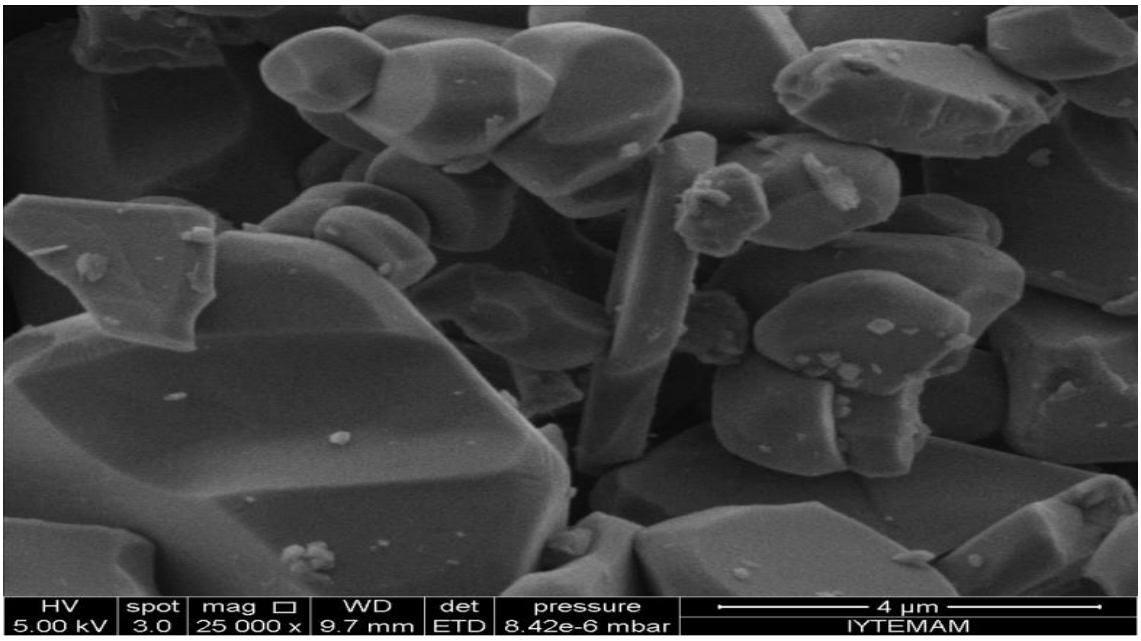

Figure 6.3. SEM image of CL 4400FG-5.2 µm alumina powder.

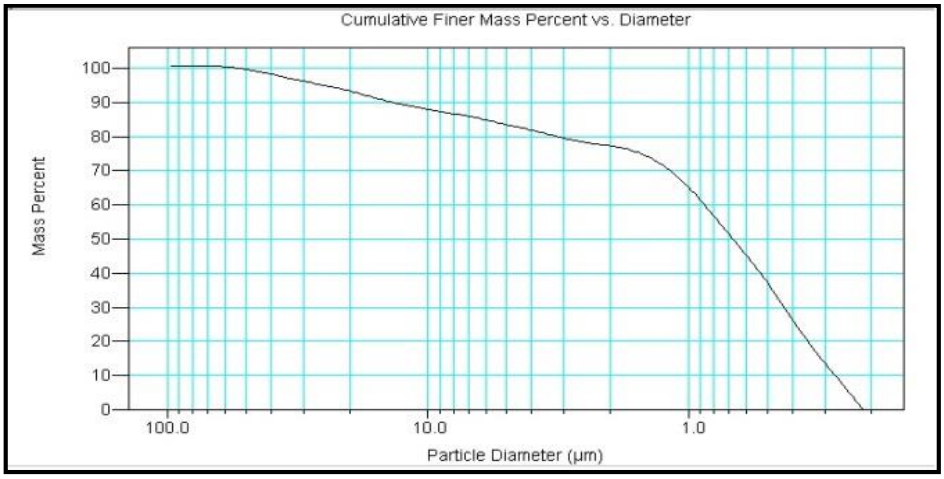

Figure 6.4. 0.5 µm Alumina powder.

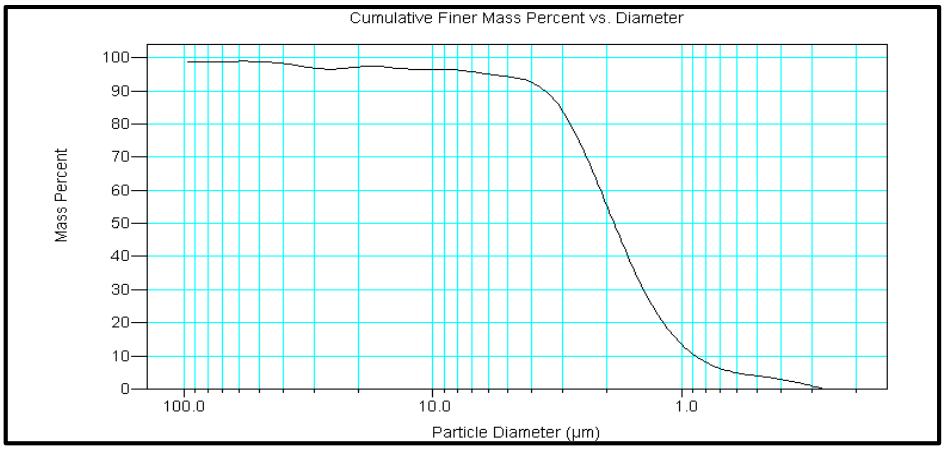

Figure 6.5. 1.3 µm Alumina powder.

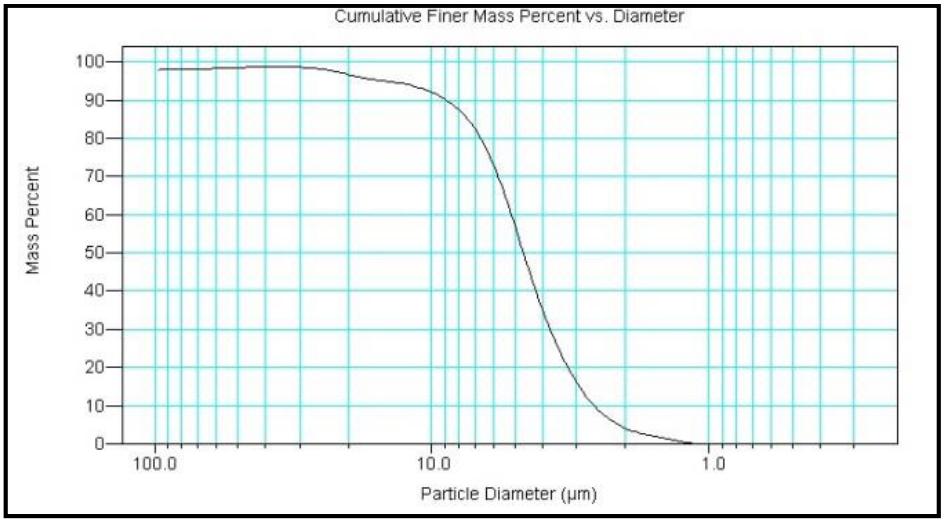

Figure 6.6. 4 µm Alumina powder.

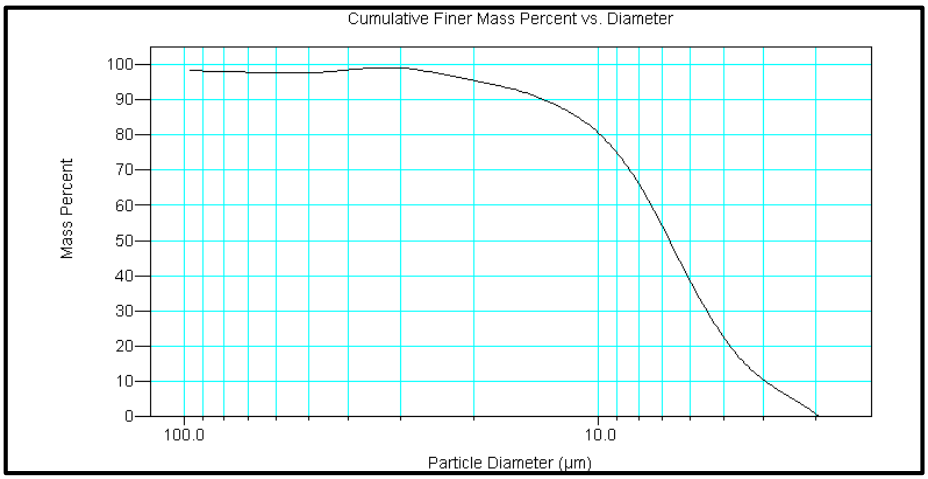

Figure 6.7. 5.2 µm Alumina powder.

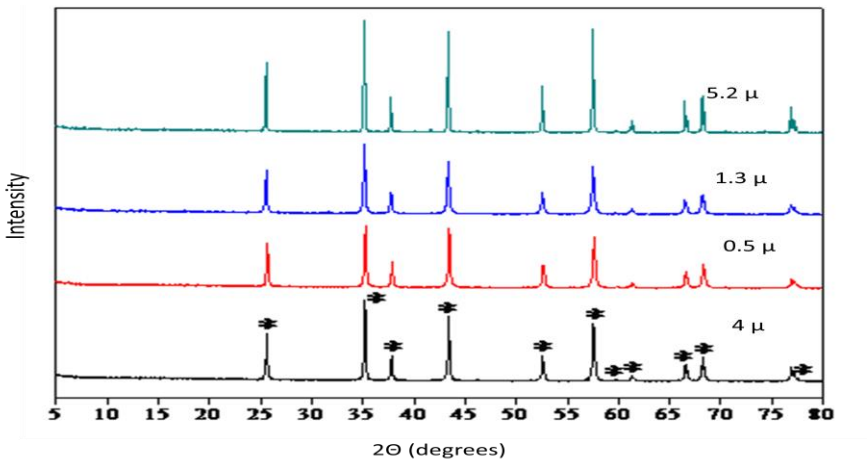

Figure 6.8. XRD patterns of alumina powders. *:α-alumina

Figure 6.9. shows the SEM image of boehmite powder. SEM images of boehmite powder shows that boehmite particles are in the nanosize range and they have a platelikemorphology. XRD pattern of boehmite powder is given in Figure 6.10. which indicated that the powder structure is phase pure boehmite.

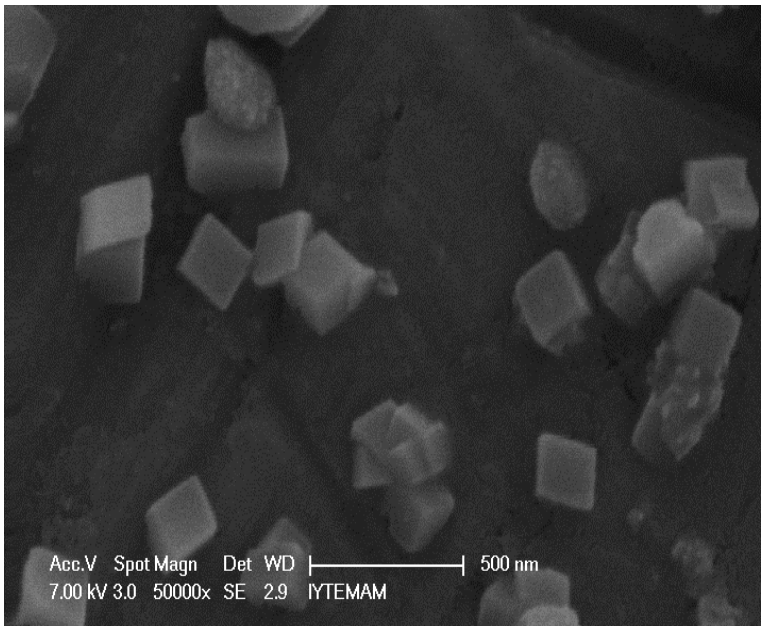

Figure 6.9. SEM image of boehmite powder.

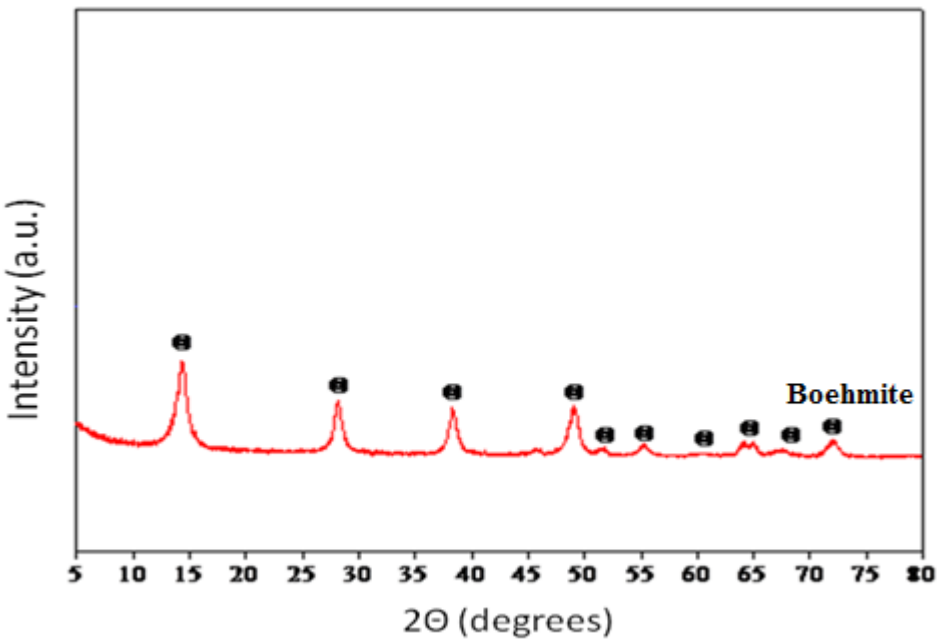

Figure 6.10. XRD pattern of boehmite powder.

TGA analysis was used for the determinationofthe thermal behaviour of HPMS polymeric binders(methocel F4M and A4M). Figure 6.11 and 6.12 shows TGA curves of methocel F4M and A4M, respectively. TGA analysis indicated that the weight loss of methocel F4M starts at approximately 265ºC and %80 of the polymer was degraded at 367ºC. The weight loss of methocel A4M started at 275ºC and %80 of the polymer was degraded at 375ºC. The binder/plasticizer TGA behaviour in dry air was essentially used to form the heat treatment schedule during the debinding process.

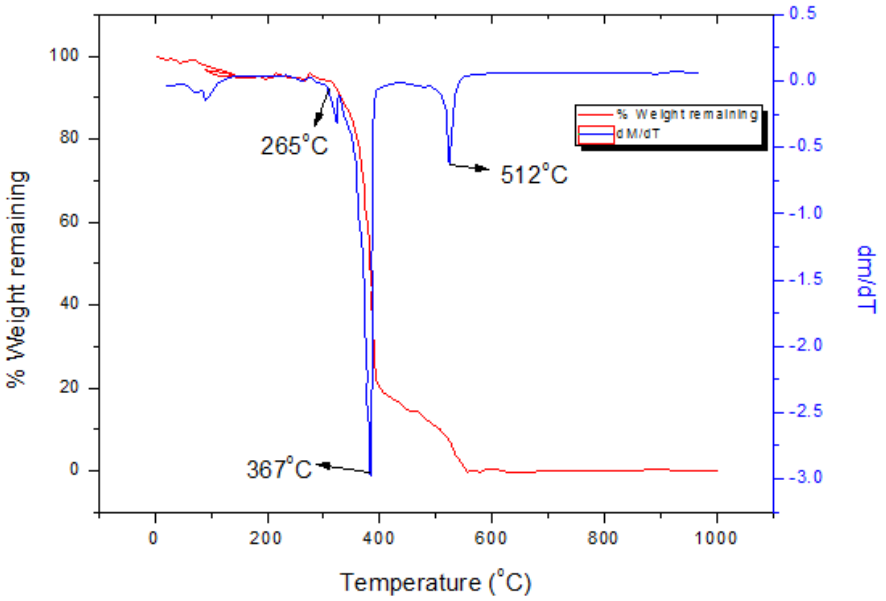

Figure 6.11. TGA curve of methocel F4M.

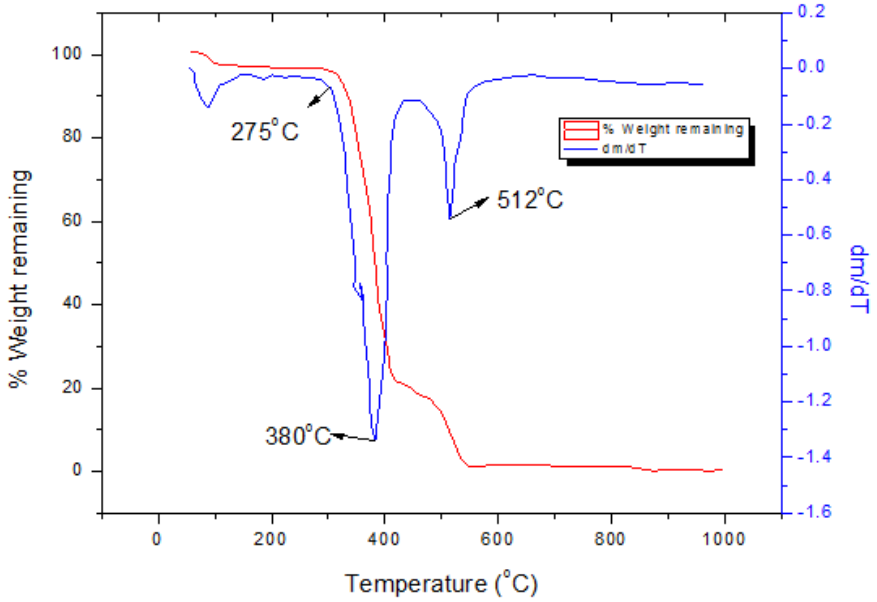

Figure 6.12. TGA curve of methocel A4M.

6.2. Characterization of preliminary experiments

An industrial conventional ceramic paste was obtained from a ceramic company in Söğüt-Bilecik as a reference paste in the preliminary orifice die extrusion experiments. Industrial conventional ceramic paste was characterizedsimilarly with prepared alumina pastes. The compositionand the codes of the characterized pastes are given in Table 5.5. The percentage of solids by volume in the experiments was fixed as 55% but pastes prepared with HPMS was liquid like and had a tendency to stick to the walls of the barrel of the extruder. The solids content of alumina was therefore increased HPMS containing pastes. Extrusion graphics of alumina pastes are given in Figures 6.13, 6.14 and 6.15. Extrusion force increased with solids content for HEMS added ceramic pasteswhich is shown in Figure 6.13. HPMS binder added ceramic pastes without boehmite addition were extruded atrelatively higher extrusion forces than the industrial ceramic paste which can be seen in Figure 6.14. The HPMS and Boehmite added alumina ceramic pastes with %56-57 solids content both have shown similar extrusion behaviour with the conventional industrial ceramic paste which can be seen in Figure 6.15.

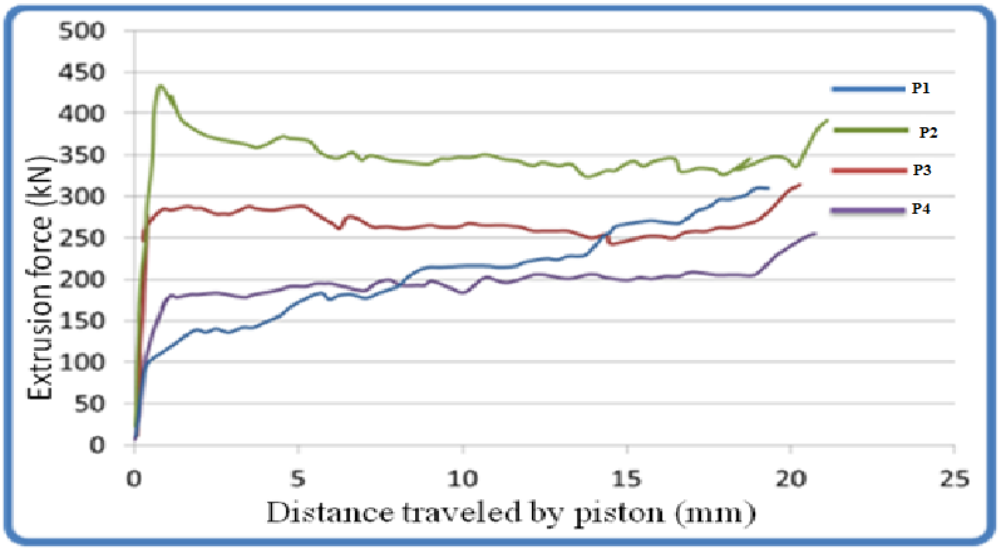

Figure 6.13. Extrusion graphics of HEMS binder used alumina ceramic pastes and conventional industrial ceramic paste.

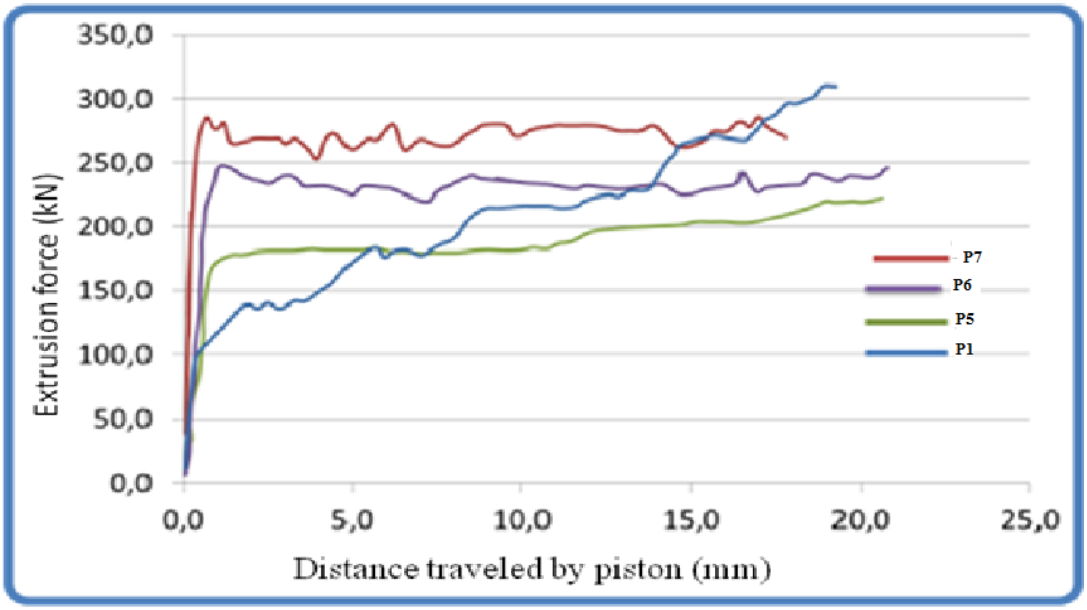

Figure 6.14. Extrusion graphics of HPMS binder used alumina ceramic pastes andconventional industrial ceramic paste.

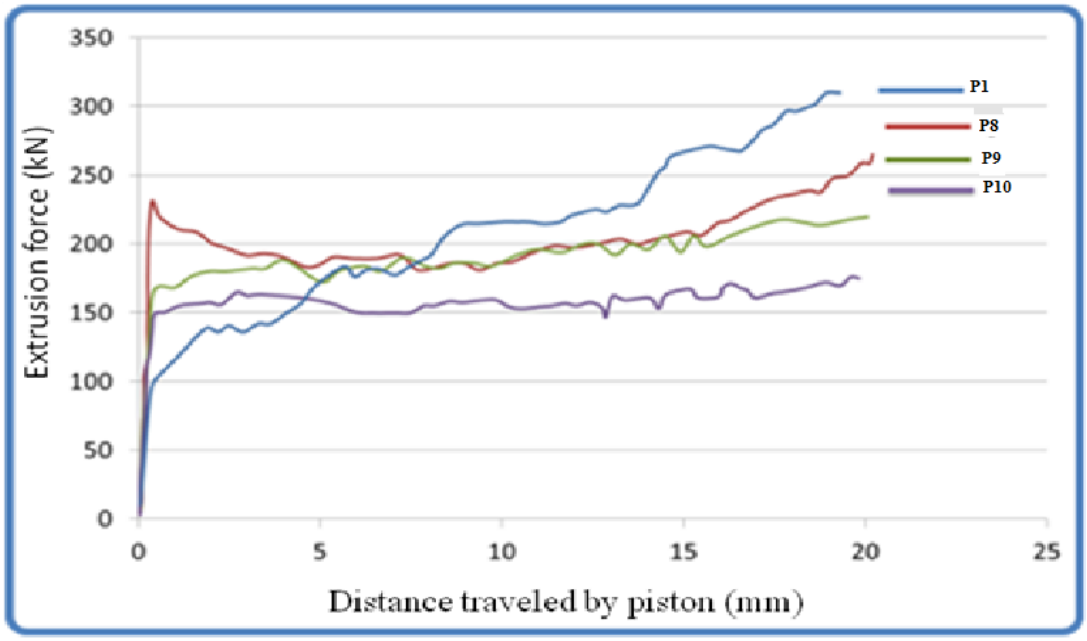

Figure 6.15. Extrusion graphics of HPMS binder and boehmite used alumina ceramic pastes and conventional industrial ceramic paste.

.

6.3. Rheological Characterization of Alumina Pastes

Benbow and Bridgwater model was used for modelling the rheological behaviour of alumina ceramic pastes. The six important rheological parameters in equation 4.5 was determined for each of the pastes.

The force vs. distance traveled by piston curves/data were obtained by using mechanical test devicefor Benbow and Bridgwater's six parameter model analysis. Extrusion force raw data at diffeent velocities (0.0002, 0.0011,0.0021, 0.0053, 0.0106 and 0.0213 m/s) and L/D ratios (1,2,4 and 8) can be seen in Figures 6.16 to 6.21 (Batches 14, 15, 16 and 18). The Benbow and Bridgwater model solution method for Batch 14 is presented in detail representing all other batches along with the results for all batches.

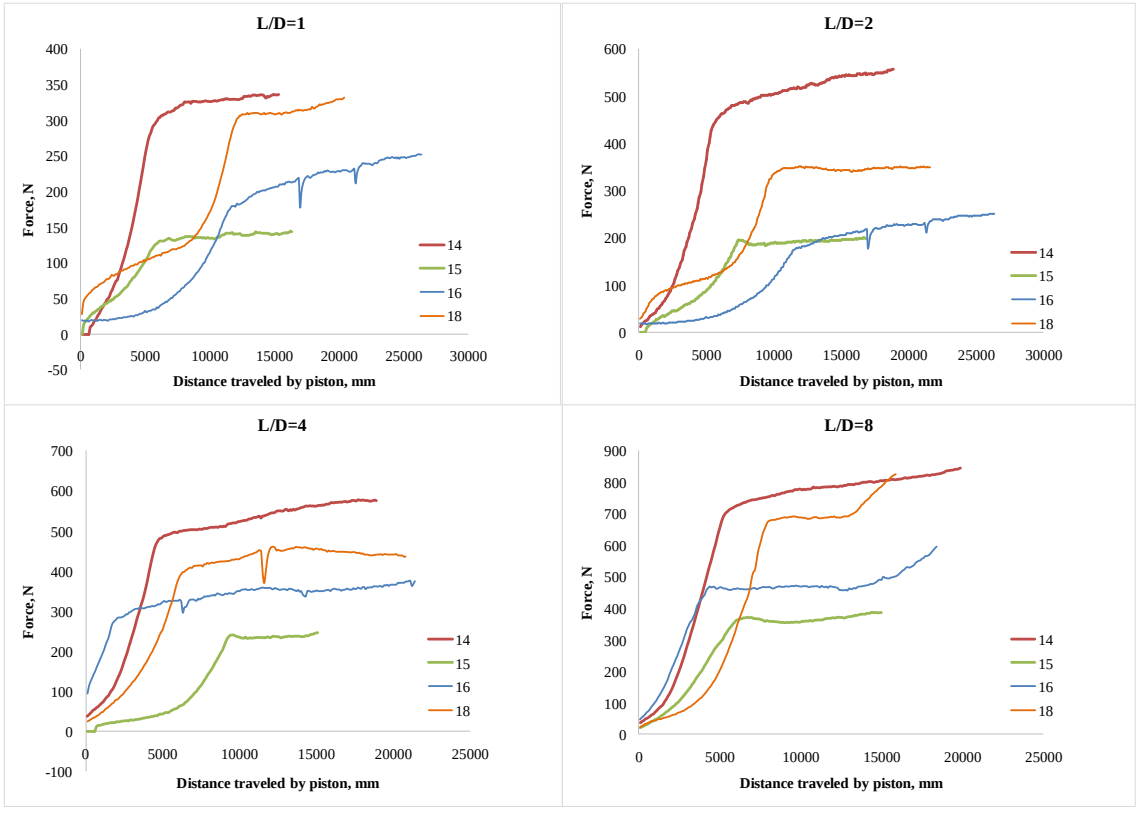

Figure 6.16. Extrusion forces of batches 14, 15, 16 and 18 at velocity 0.0002m/s.

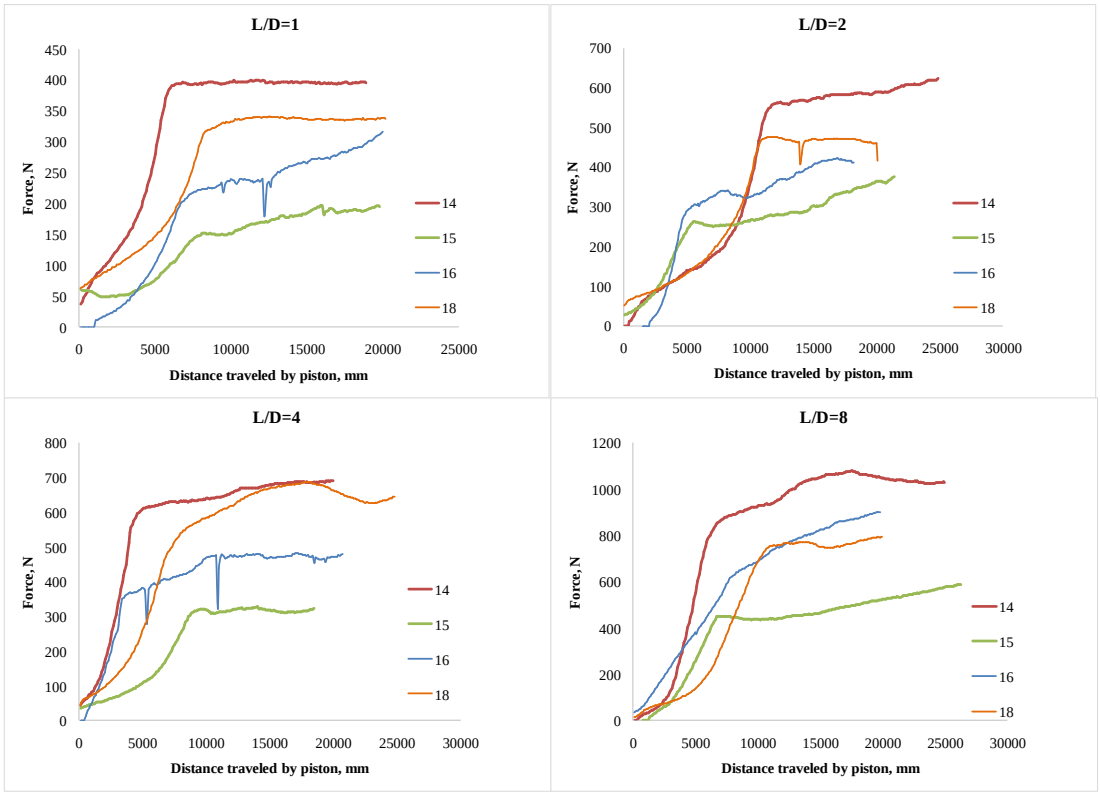

Figure 6.17. Extrusion forces of batches 14, 15, 16 and 18 at velocity 0.0011m/s.

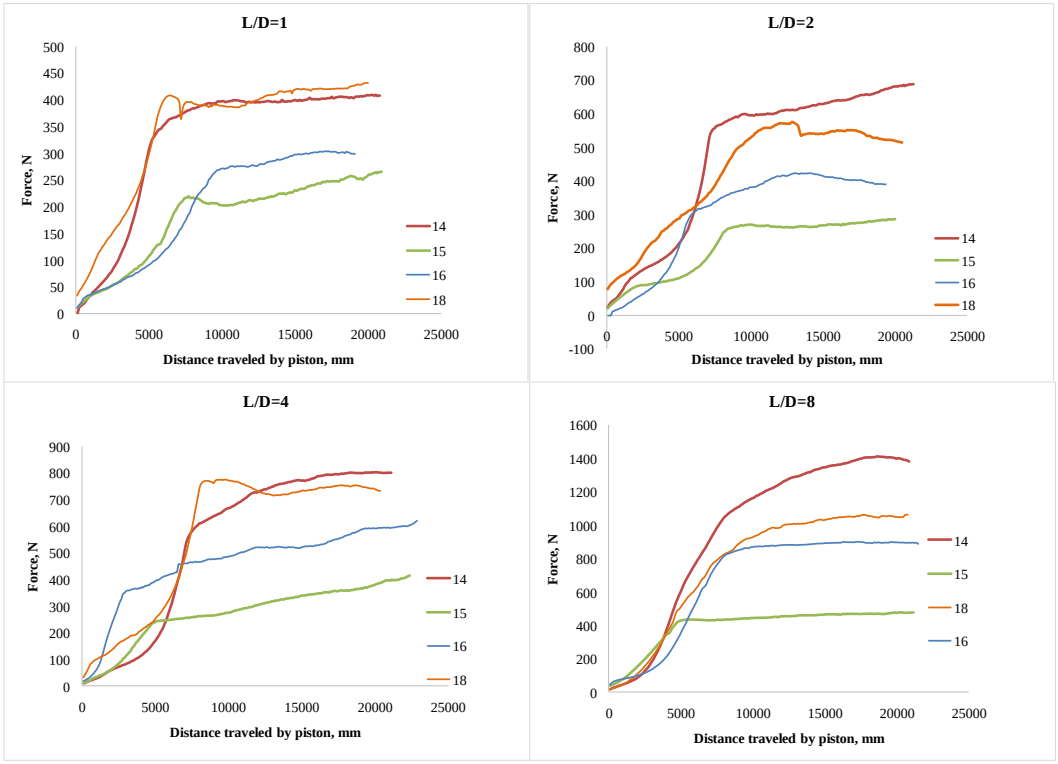

Figure 6.18. Extrusion forces of batches 14, 15, 16 and 18 at velocity 0.0021 m/s.

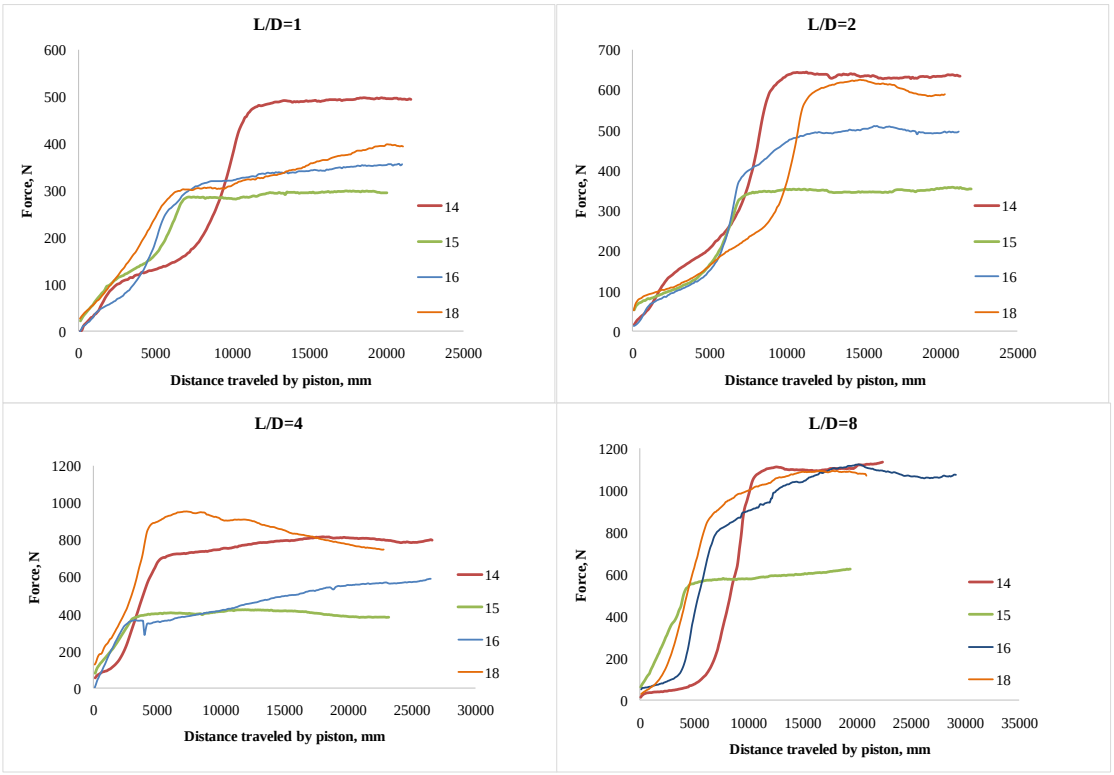

Figure 6.19. Extrusion forces of batches 14, 15, 16 and 18 at velocity 0.0053m/s.

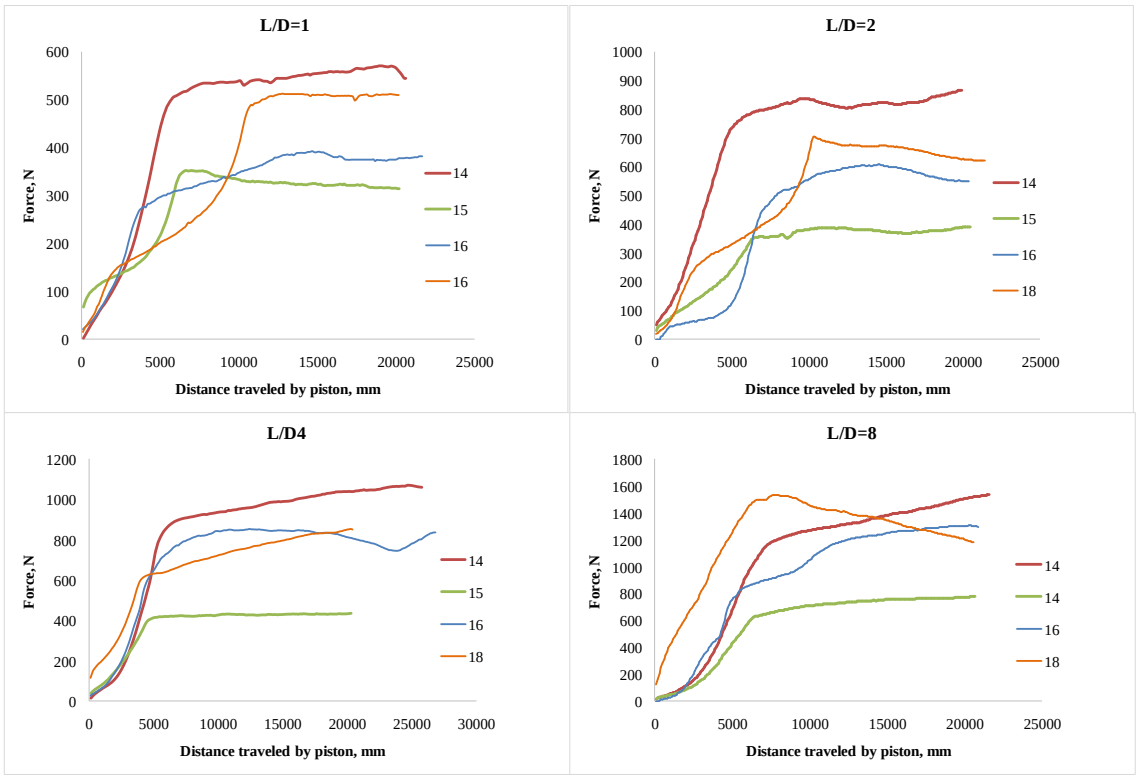

Figure 6.20. Extrusion forces of batches 14, 15, 16 and 18 at velocity 0.0106m/s.

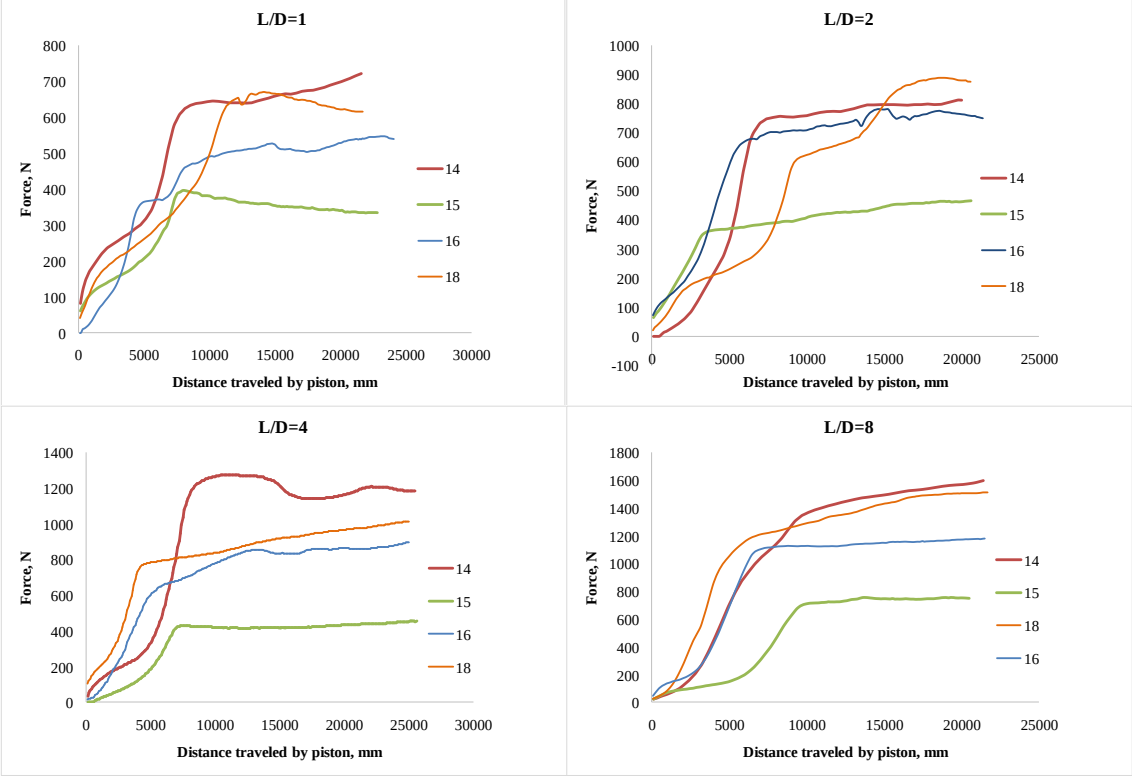

Figure 6.21. Extrusion forces of batches 14, 15, 16 and 18 at velocity 0.0213m/s.

Figure 6.22 shows P versus L/D curves of batch 14. Equation 4.5 was solved by extrapolatingP – L/D curves to zero L/D, giving P_1. After determination of P_1 values, P_1 versusV graph was drawn and intercept of this curve is equal to $2\sigma_0 \ln(D/D_0)$ value. σ_0 was determined from solution of "intercept=$2\sigma_0 \ln(D/D_0)$" equation. Figure 6.23. shows the P_1-V curve of batch 14.

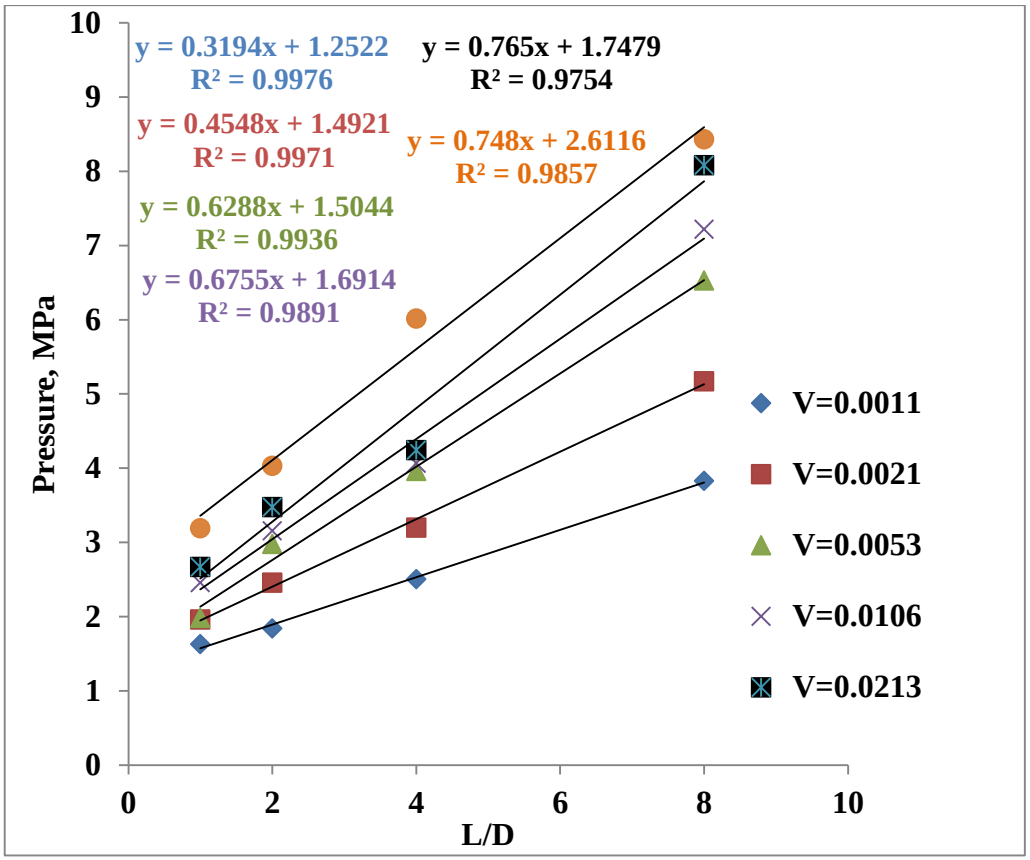

Figure 6.22. P vs. L/D plots of Batch 14.

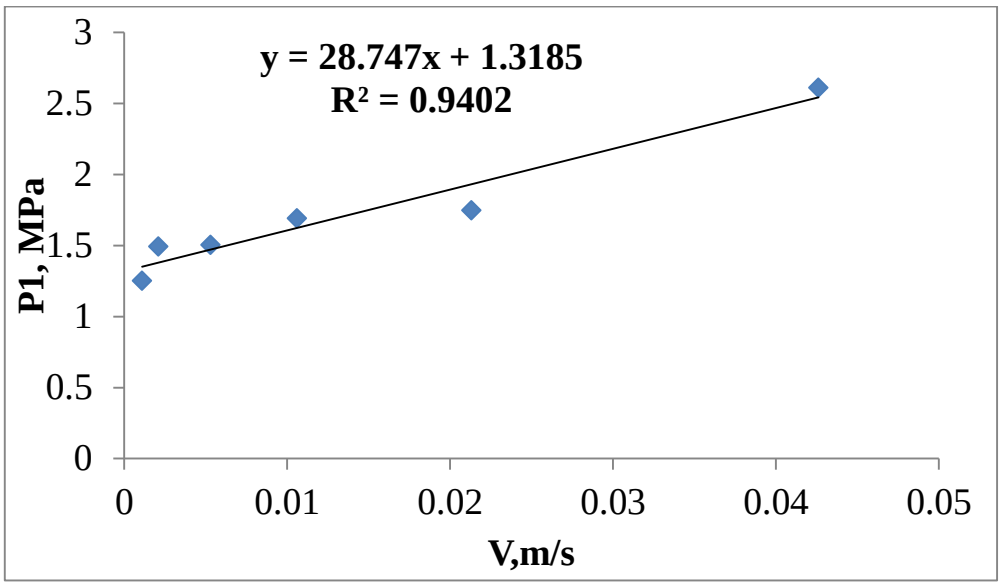

Figure 6.23. P_1 vs.V plot of Batch 14.

After determinaton of σ_0, lnV vs $\ln[P_1/2\ln(D_0/D)]-\sigma_0$ graph was drawn, intercept of this curve is equal to $\ln\alpha_1$ and slop is equal to m. Figure 6.24. shows lnV vs $\ln[P_1/2\ln(D_0/D)]-\sigma_0$curve of batch 14.

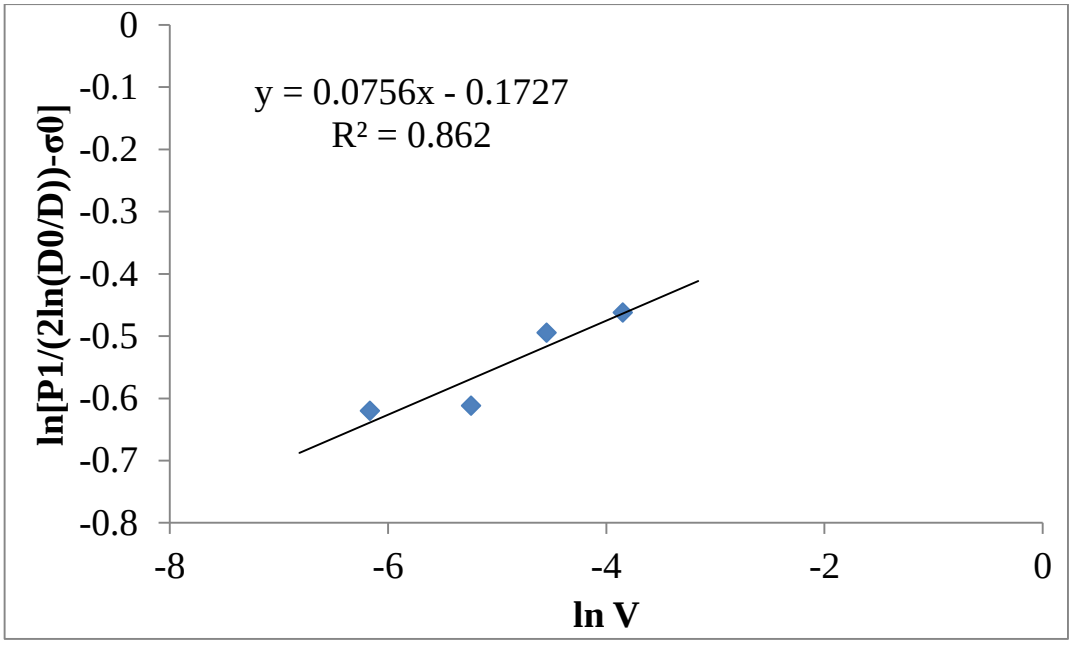

Figure 6.24 lnV vs $\ln[P_1/2\ln(D_0/D)]-\sigma_0$ plot of batch 14.

P_2 was determined by substracting P from P_1. For determination of τ_0, P_2 vs L/D graph was drawn. Slope of the lowest velocity curve was assumed to be equal to $4\tau_0$. Figure 6.25 shows P_2 vs L/D curves for batch 14.

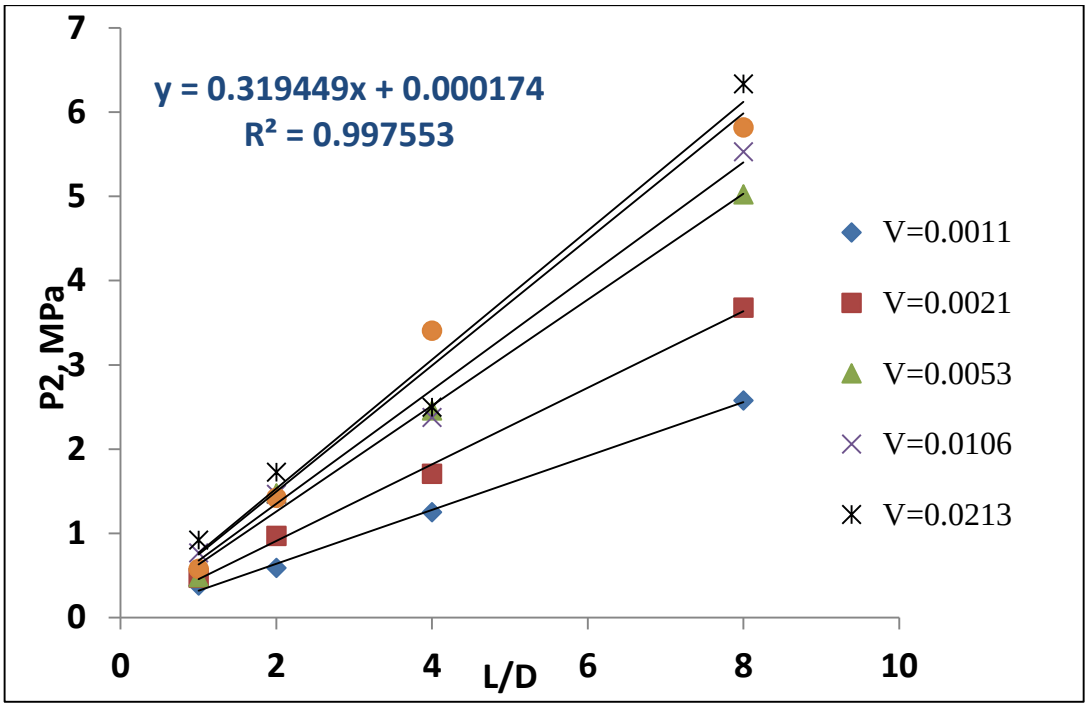

Figure 6.25. P_2 vs L/D plots of Batch 14.

ln[P_2/4L/D]- τ_0 vs lnV graph was drawn for the determination of both n and β_1. Average of the determined slope values of the curves should be equal to n and average of intercept values of curves is equal the lnβ_1. Figure 6.26shows ln[P_2/4L/D]- τ_0 vs lnV plots of Batch 15.

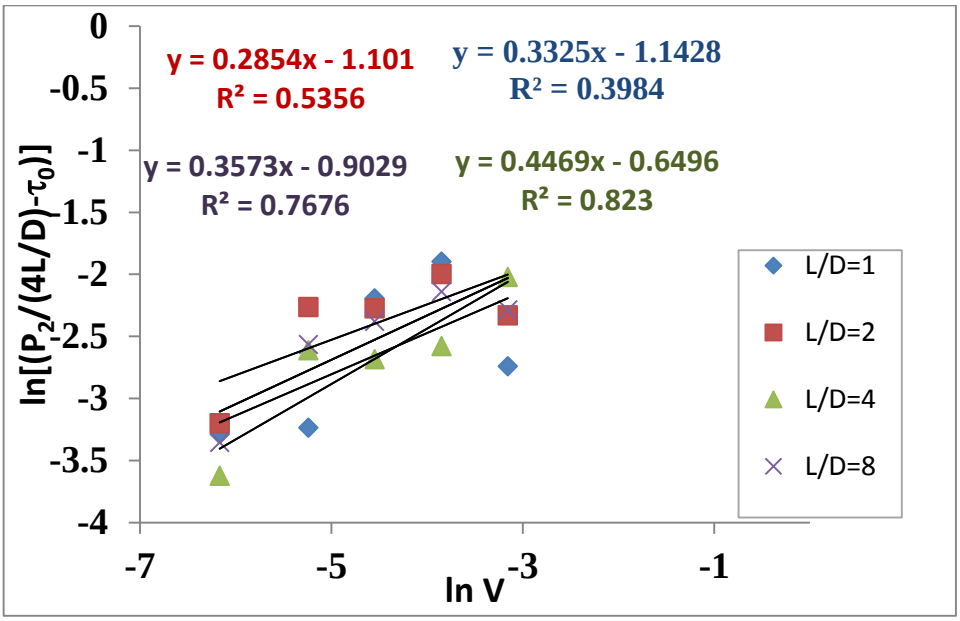

Figure 6.26. ln[P_2/4L/D]- τ_0 vs lnV plots of Batch 14.

6 parameters of Benbow and Bridgwater equation for batchs 14, 15, 16 and 18 were determined by following same algorithm.A similar algorithm was used for the determination of Benbow and Bridgwater's four parameter model. σ_0 and τ_0, P_2, P_1 values were equal to the six parameter model because the same total extrusion pressure P values were used in both models.

The α parameter of the four parameter model was determined by plotting $[P_1/2\ln(D_0/D)]- \sigma_0$ vs V curve. Intercept of this curve is equal to α. Figure 6.27 shows $[P_1/2\ln(D_0/D)]- \sigma_0$ vs V plot for batch 14.

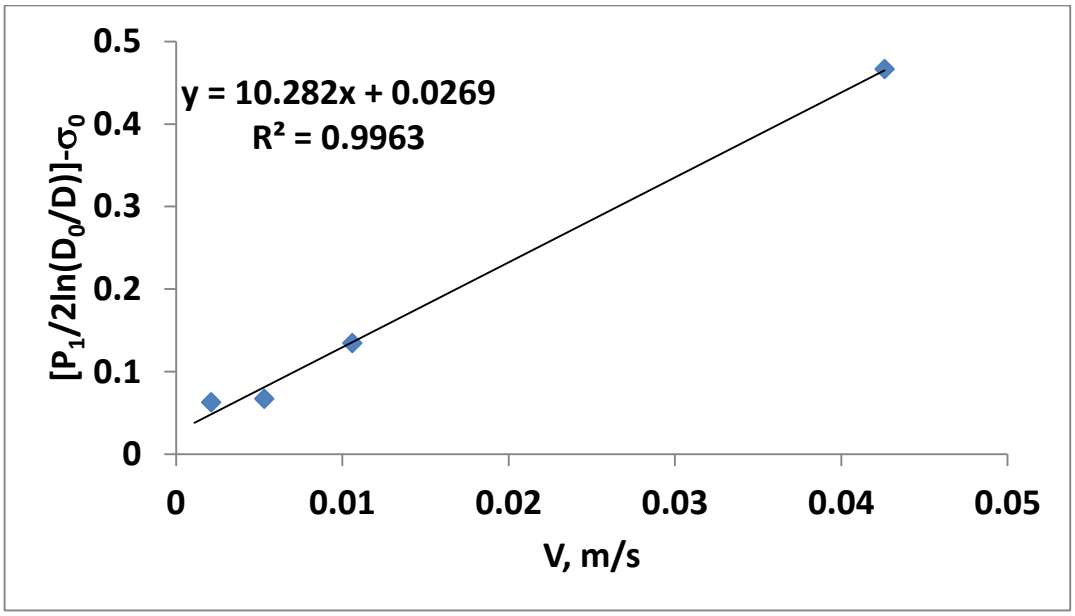

Figure 6.27. $[P_1/2\ln(D_0/D)]- \sigma_0$ vs V plot of batch 14.

β value of the four parameter model was determined by plotting $\{[P_2/4L/D]- \tau_0\}$vs V. Slope of the lowest velocity plot is equal to the β value. Figure 6.28 shows the $\{[P_2/4L/D]- \tau_0\}$ vs V plot of batch 14.

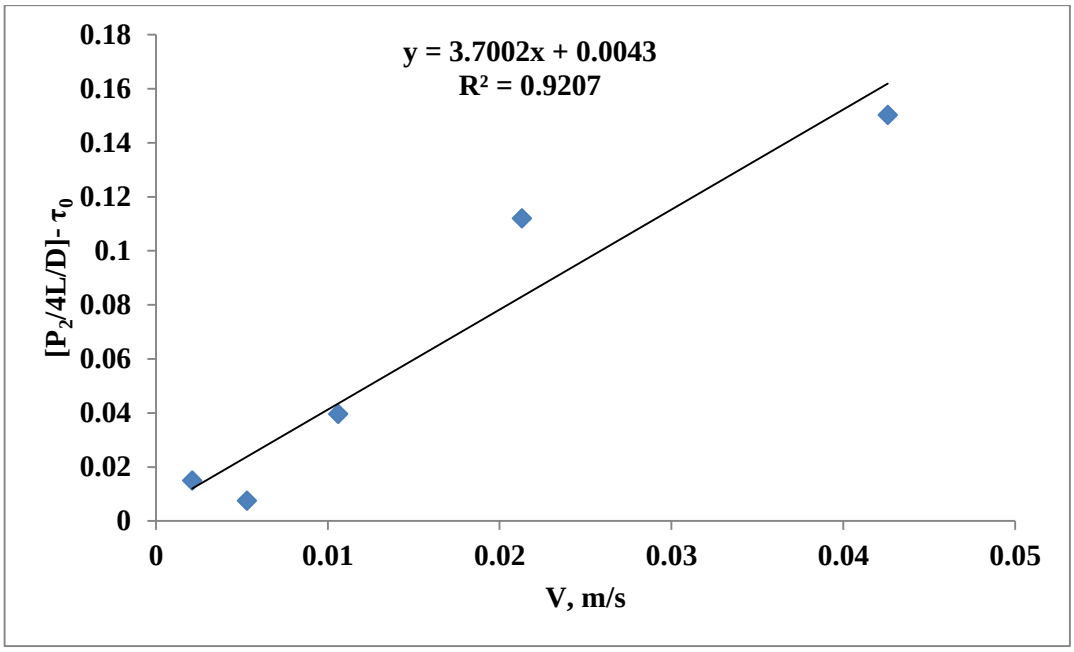

Figure 6.28. $[P_2/4L/D]- \tau_0$ vs V plotof batch 14.

4 parameters of Benbow and Bridgwater equation for batches 14, 15,16 and 18 were determined by following thesame algorithm.

P value was recalculated by using equation 4.5 with the six parameters given in Table 6.2. The P values were also calculated for the four parameter model (where m and n values are equal to unity) similarly by using equation 4.2 and the results are tabulated in Table 6.3. The comparisonof experimental, 6 and 4 parameter models are given in Figures 6.29 to 6.32. Some of the researchers claimed the use of β and α values (four parameter model) satisfactorily explainsthe rheologyof the paste. The results of this thesis work indicated that the 6-parameter model better represents the experimentaldata. In this study m values for batch 15 varied in the 0.07-0.31 range and the paste shows pseudoplastic behaviour according to Das et al. (2002). Characteristic velocity factor in the die entry, α_1, was increased by using organic binder methocel A4M (batch 16) instead of using methocel F4M (Batch 14). Besides that, α_1 valuewas decreased with increasing amount of inorganic binder boehmite (Batch 16). the characteristic velocity factor in the die land, β1, values varied in the range of 0,07 and 0,39. Initial wall stress, τ_0, was found to be less than 1/10 times than initial yield stress, σ_0. Table 6.2 shows that σ_0 value was increased by using methocel A4M (Batch 16) instead of using methocel F4M (Batch 14) and again value of σ_0 was decreased with increasing amount of

inorganic binder boehmite (Batch 16). It can be said that, use of organic binder methocel A4M (Batch 15) and use of high amount of water effects positively dispersion of ceramic particles. These four pastes (14, 15, 16, 18) extruded in the piston extruder and lowest extrusion pressure was obtained for paste 15.

Table 6.2. Results of six parameter model.

Batch No	σ_0 (MPa)	τ_0 (MPa)	*m*	*n*	β_1 (MPa$(sm^{-1})^n$)	α_1 (MPa$(sm^{-1})^n$)	%Moisture
14	0.47	0.08	0.07	0.35	0.39	0.84	15.33
15	0.23	0.03	0.31	0.24	0.09	1.99	16.8
16	0.33	0.04	0.09	0.16	0.07	0.71	14.72
18	0.54	0.07	0.09	0.41	0.36	1.17	15.73

Table 6.3. Results of four parameter model.

Batch No	σ_0 (MPa)	τ_0 (MPa)	β (MPa(sm^{-1}))	α (MPa(sm^{-1}))
14	0.47	0.08	3.7	10.28
15	0.22	0.04	1.37	10.48
16	0.38	0.03	4.97	9.75
18	0.54	0.07	3.03	11.08

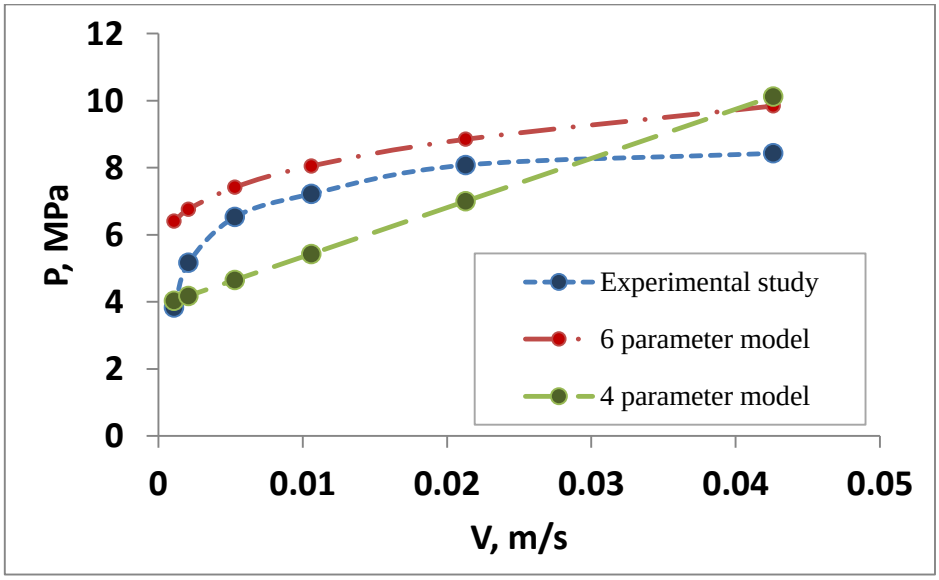

Figure 6.29. The comparison of experimental, 6 and 4 parameter models of batch 14.

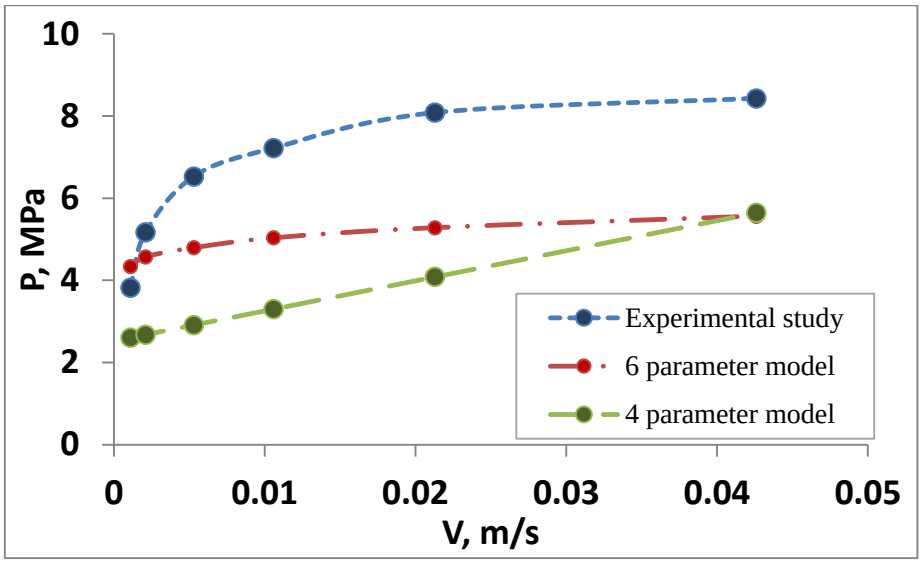

Figure 6.30. The comparison of experimental, 6 and 4 parameter models of batch 15.

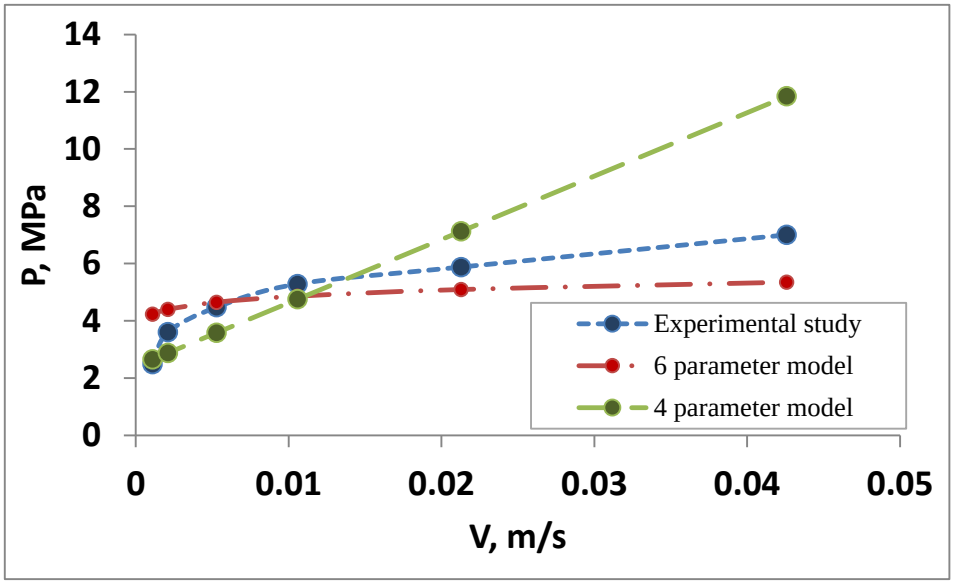

Figure 6.31. The comparison of experimental, 6 and 4 parameter modelsof batch 16.

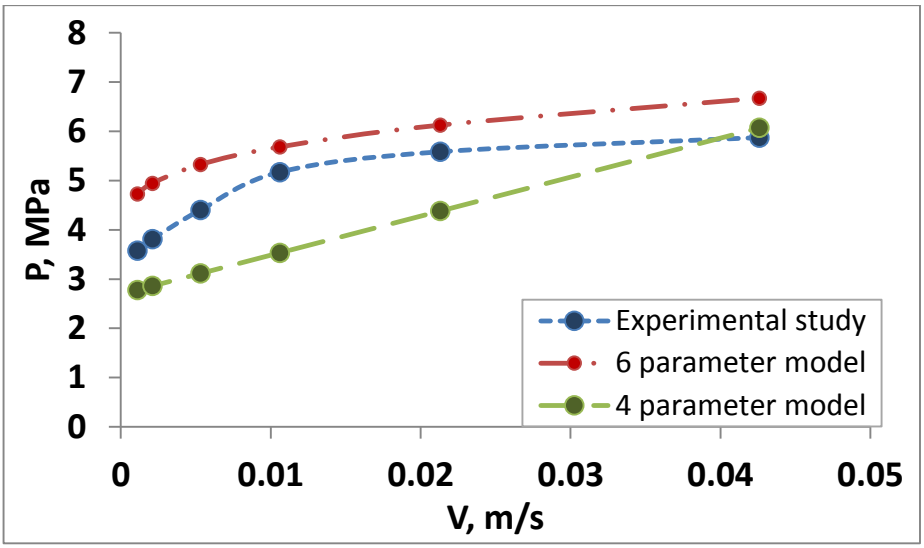

Figure 6.32. The comparison of experimental, 6 and 4 parameter models of batch 18.

Benbow and Bridgwater six parameter model β, τ_0 and n values were further used for viscosity estimations. These three parameters were used to calculate the wall shear stress (τ_w) by using equation 4.7. Apparent shear rate ($\dot{\gamma}_a$) values were estimated by using equation 3.7 for six different velocites. After calculating both wall shear stress (τ_w) and shear rate ($\dot{\gamma}_a$),apparent viscosity was calculated by using equation 3.6. Table 6.3 shows the apparent viscosity values of batches 14, 15, 16 and 18. The variation of apparent viscosity with shear rate and the wall shear stress with shear rate are presented in Figure 6.33 and 6.34 respectively. The apparent viscosity - shear rate plots (Figure 6.33) of prepared pastes indicated that apparent viscosity decreases with increasing shear rate which follows a shear thining (or pseudoplastic) behaviour. It can also be seen from Figure 6.28 that batches 15 and 16 have lower apparent viscosity values than the other two batches at the same apparent shear rate values. This may be due to the lower initial wall shear stress values (τ_0) compared to batches 14 (τ_0=0.08) and 18 (τ_0= 0.07). The shear stress - shear rate plots given in Figure 34 of the prepared pastes have shown that wall shear stress has a specific value (yield stress) at about zero shear rate and increased with shear rate which follows a shear thining (pseudoplastic) behaviour.

Table 6.4. Apperant viscosity values of batches 14, 15, 16 and 18

$\dot{\gamma}$ (s^{-1})	Viscosity, (Pa.s)			
	Batch 14	Batch 15	Batch 16	Batch 18
0.71	143276.28	59748.02	82632.47	115776.02
5.6	22333.07	9016.35	11803.70	17631.26
14.13	10069.13	3933.24	4971.78	7924.57
28.26	5639.80	2130.47	2611.48	4450.67
56.8	3193.49	1157.24	1369.94	2540.34
113.6	1841.79	635.55	724.01	1485.12

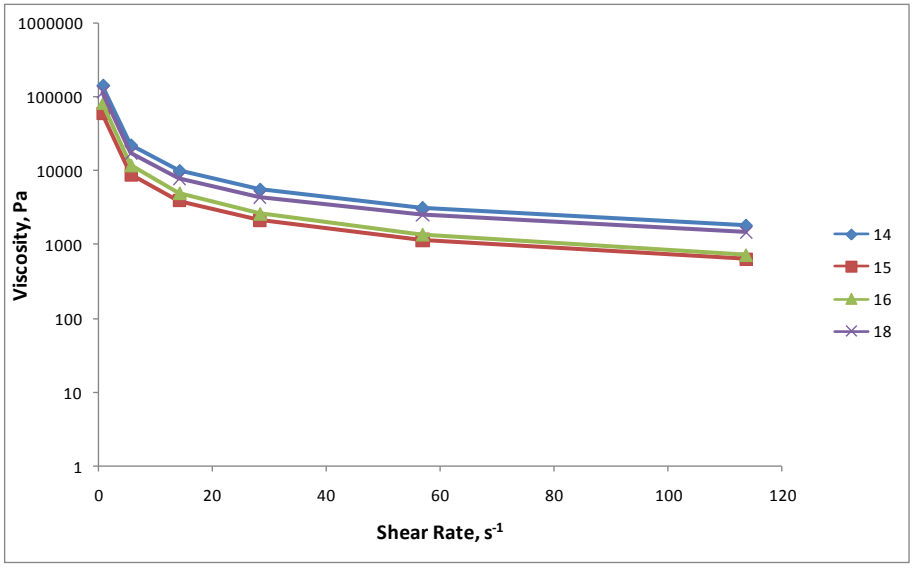

Figure 6.33. Viscosity versus shear rate plots of batches 14, 15, 16 and 18

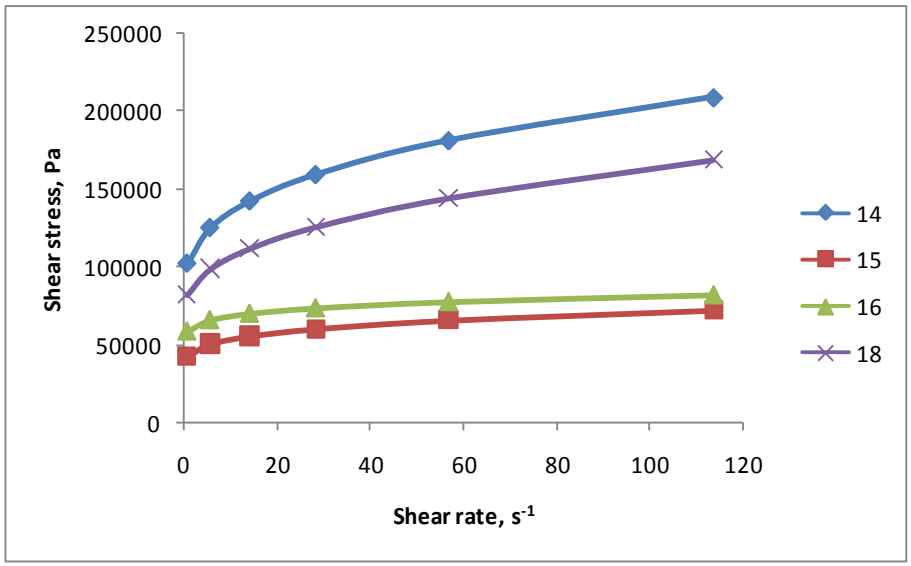

Figure 6.34. Shear stress versus shear rate plots of batches 14, 15, 16 and 18

6.4. Characterization of Tubular Alumina Ceramic Supports

Archimedesdensity analysis,mechanical strength test results and volumetric compositions of batches are given Table 6.5.The porosity of the tubes were found to be approximately between in the 45-50% range. These results indicated that open porosity increases with increasing polymer content and decreases with increasing boehmite content in the heat treated tubes. Higher open porosity was obtained with A4M compared to F4M polymeric binder (Batches14 and 15 comprison). The mechanical strength of heat treated tubes were increased by increasing boehmite content. Batch 16 was prepared with higher boehmite addition than other pastes and had the highest mechanical strength. It can be seen from Table 6.5 that tubes prepared by using methocel A4M had the lowest mechanical strength (8 bars).

Table 6.5. Archimedesdensity analysis and mechanical strength test results for different batches.

Batch No	% Volume						
	Alumina	Water+Glycerol	Boehmite	Polymer		Porosity	Mechanical Strength (bar)
5	46.1	45.75	1.9	6.25	F4M	49.61	25
8	51.08	44	-	4.92	F4M	45.29	30
14	51.36	42	1.87	4.77	F4M	45.55	37
15	46.17	47.73	1.68	4.42	A4M	49.02	8
16	51.18	41.73	5.06	2.03	F4M	40.18	55
17	51.35	41.8	3.38	3.47	F4M	40.68	45
18	50.7	43.08	-	6.22	F4M	45.02	28

SEM pictures of the heat treated tubes are given in Figures 6.35-6.40. Images were taken from fracture and inner top surfaces at different magnifications. It was observed that microstructure of the prepared tubes consistedof small grains. Small particles below 0.5 μm are α-alumina which were expected to be transformed from boehmite at after the heat treatment. The SEM pictures of the fracture surfacesindicated that the partial dissolution of the binder polymers was achieved in the pastes causing the formation of large pores (approximately 10-20 μm) in the tube microstructure. The SEM pictures of the tube inner top surfaces indicated that the shear zone on the die walls during extrusion prevented the formation of large pores. A higher level of packing of particles were determined at the inner top surfaces of the tubes. It was observed from the SEM pictures the increase in the boehmite content reduced the formation of large pores in the tubes. The tubes prepared by using A4M polymeric binder had a relatively higher large pore concentration as can be seen in Figure 6.37. No apparent cracks were detected on the membrane surfaces during SEM analysis.

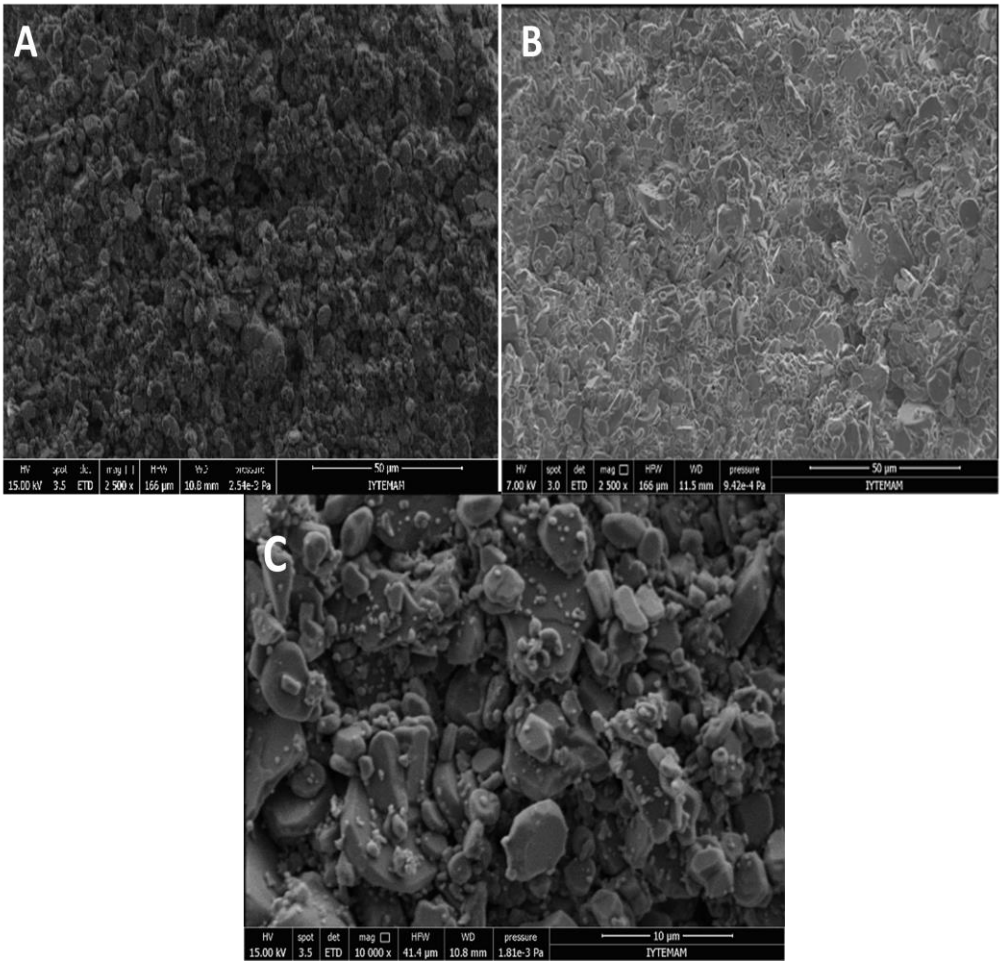

Figure 6.35. SEM images of Batch 5; A. Fracture surface at 2500 X,B. Tube inner Surface 2500 X, C Fracture surface at higher magnification at 10 kX.

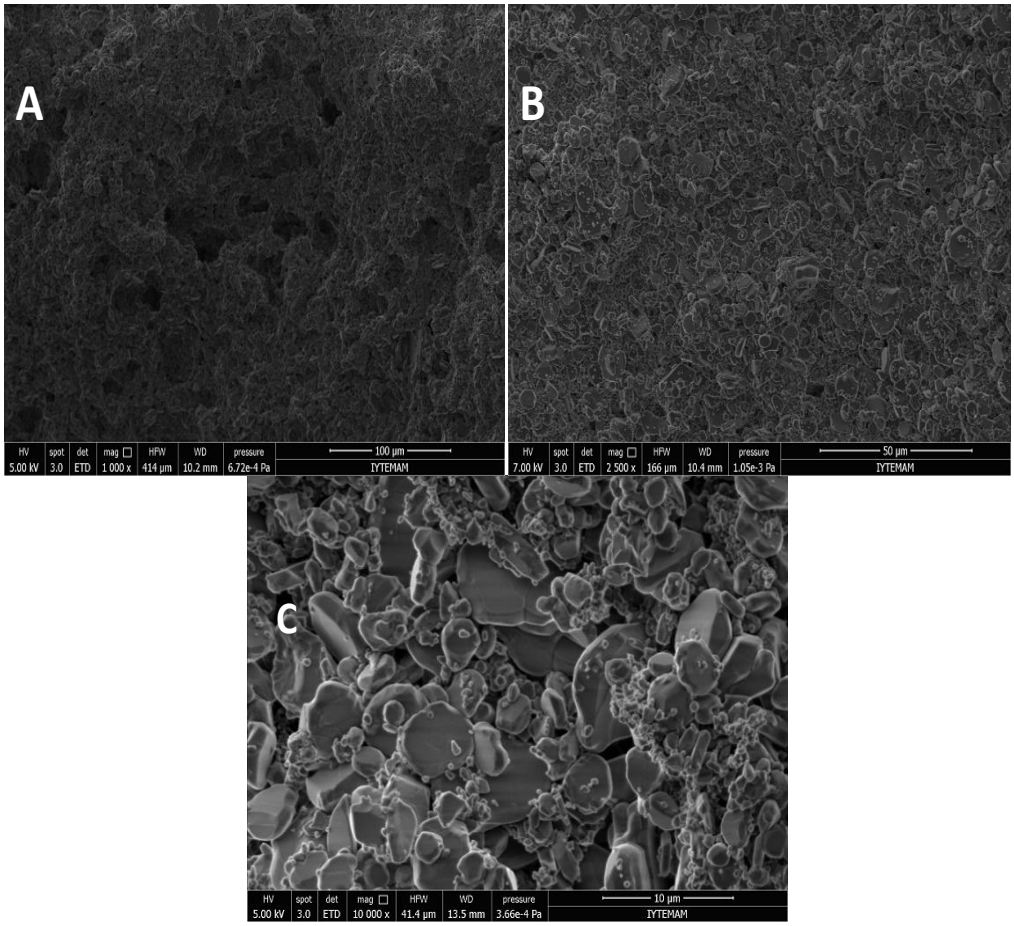

Figure 6.36. SEM images of Batch 8; A. Fracture surface at 2000 X,B. Tube inner Surface 2500 X, C Fracture surface at higher magnification at 10 kX.

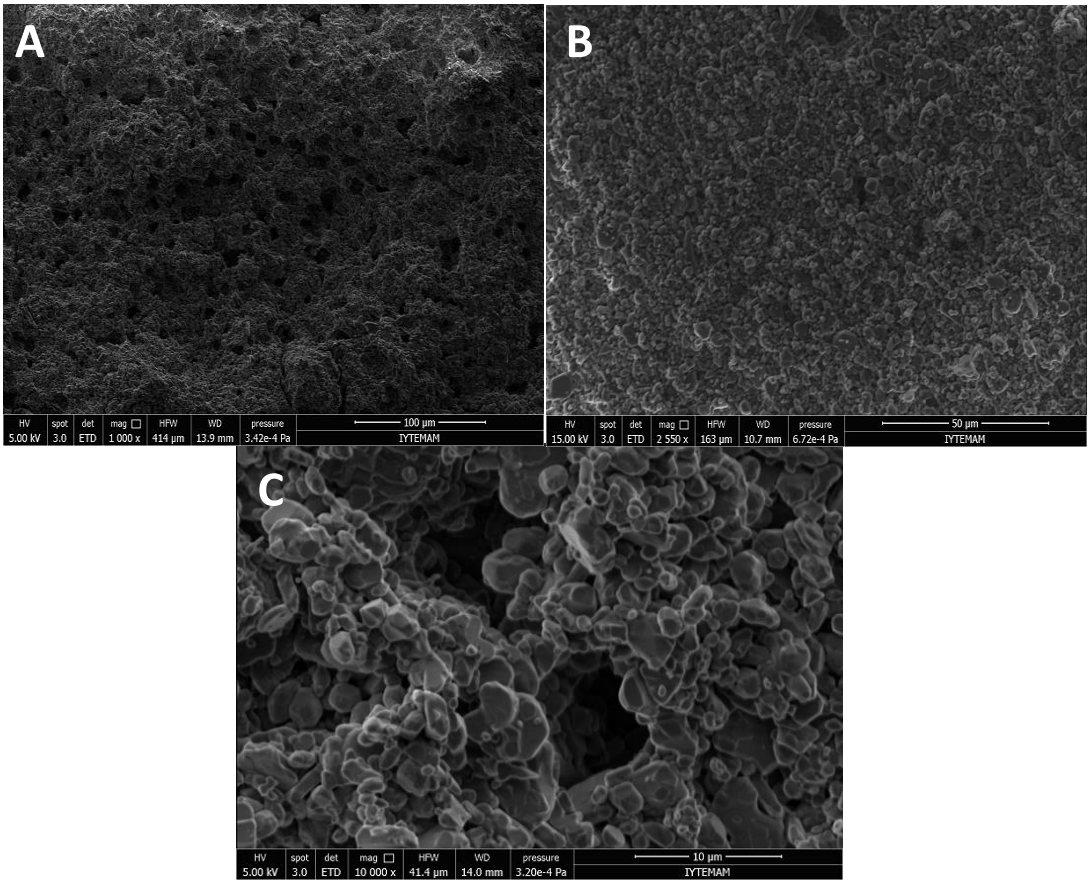

Figure 6.37. SEM images of Batch 15; A. Fracture surface at 2500 X,B. Tube inner Surface 2500 X, C Fracture surface at higher magnification at 10 kX.

.

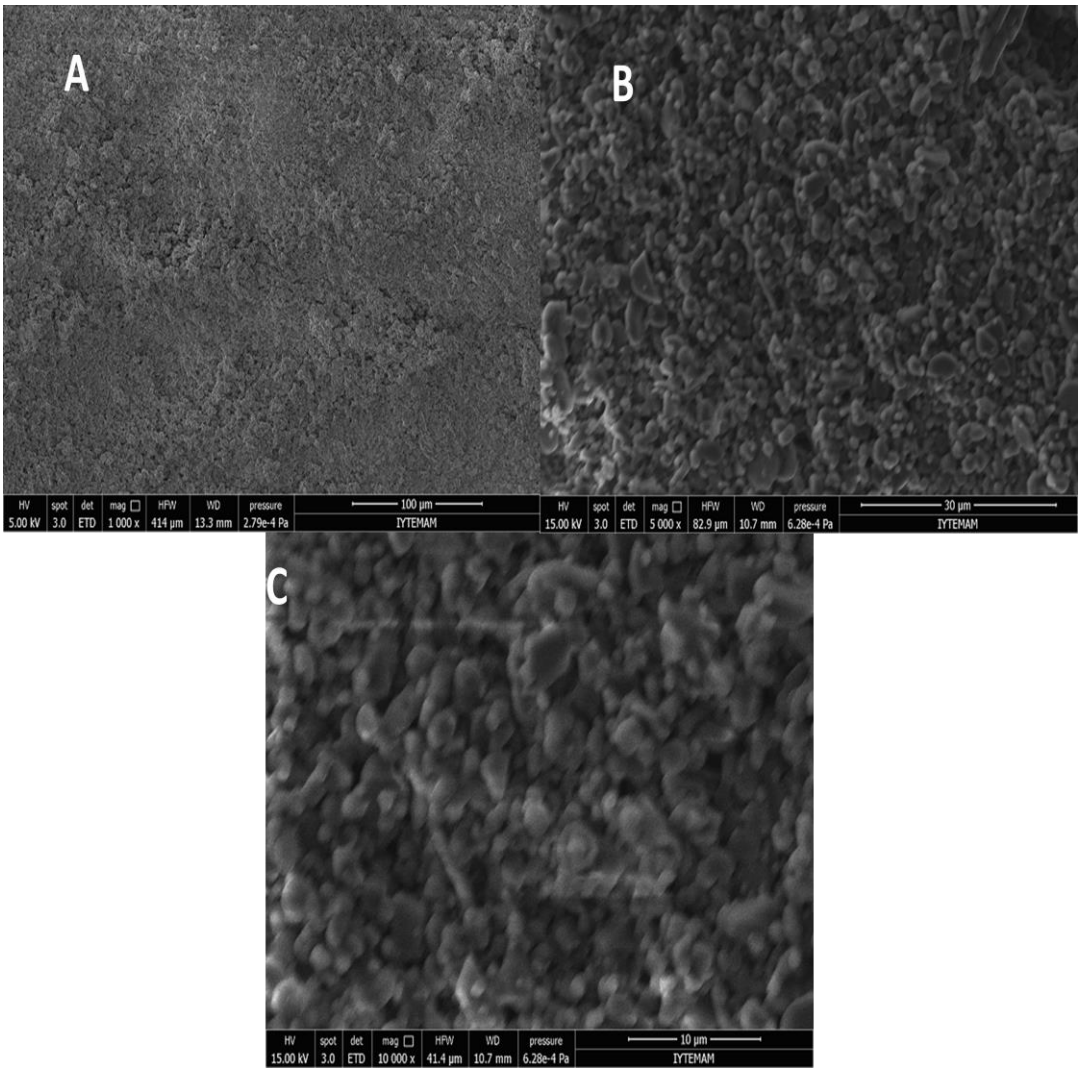

Figure 6.38. SEM image of Batch 16; A. Fracture surface at 1000 X,B. Tube inner Surface5000 X, C. Fracture surface at higher magnification at 10 kX.

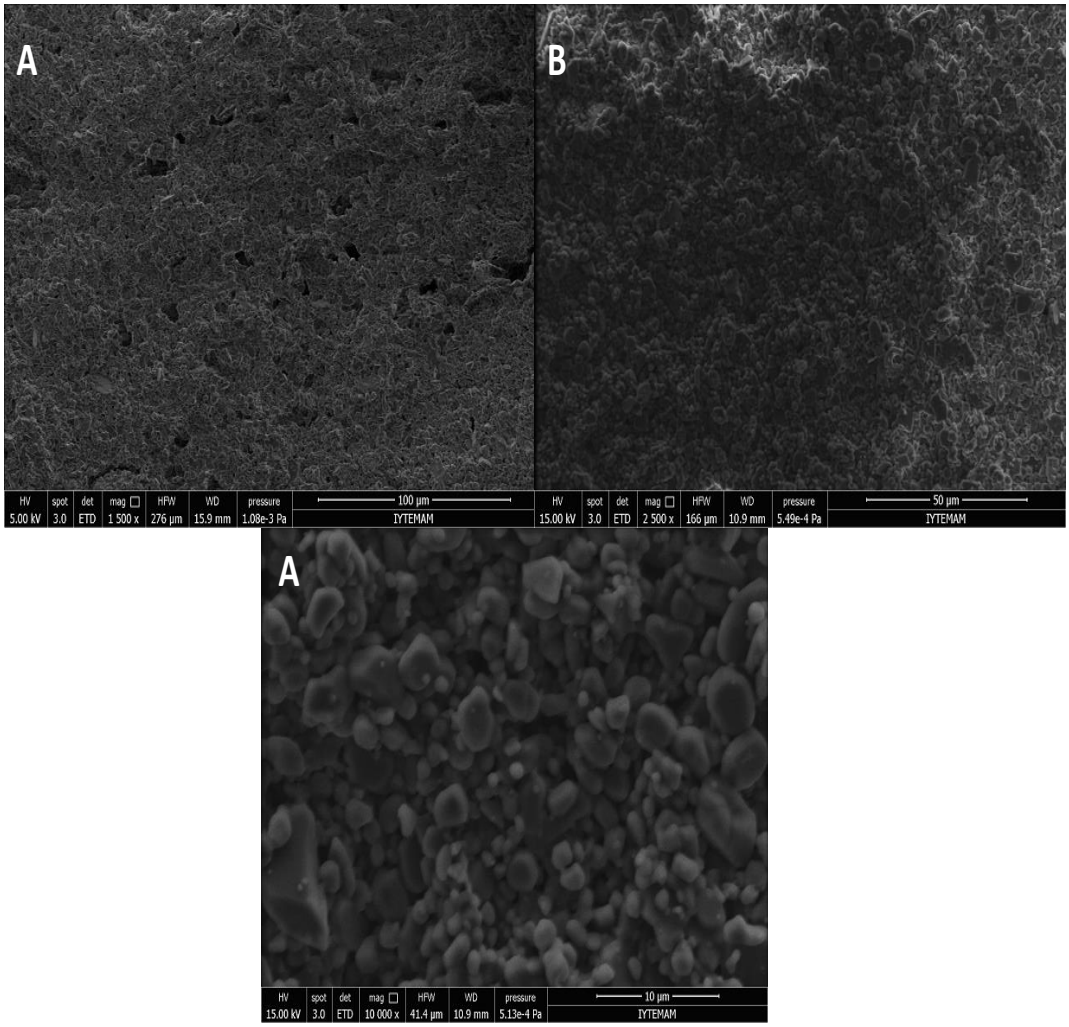

Figure 6.39. SEM image of Batch 17; A. Fracture surface at 1500 X,B. Tube inner Surface5000 X, C. Fracture surface at higher magnification at 10 kX.

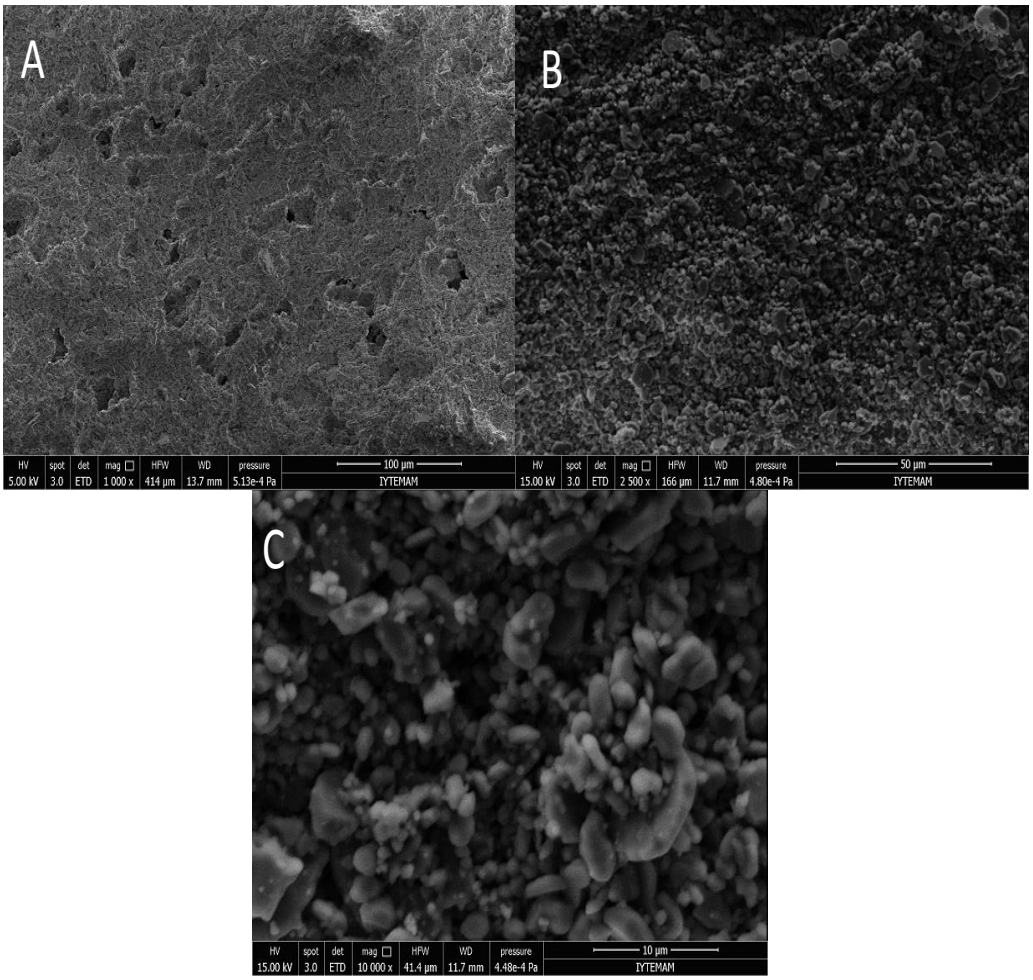

Figure 6.40. SEM image of Batch 18; A. Fracture surface at 1000 X,B. Tube inner Surface 2500 X, C Fracture surface at higher magnification at 10 kX.

Figures 6.41-42 and 43 shows both Cumulative Pore Area versus Pore size (a) and Log Differential Intrusion vs Pore size graphics (b). Analyzed samples compositions were given in Table 5.6. Pore size was determined approximately 1 µm for batch 14,batch 12 and batch 15showed a pore diameter between 1 and 2.5 µm. The increase in the pore size was indicated the use of different polymeric binders and this results showed parallelism with Archimedesdensity analysis. Figures 6.36 (a), 6.37 (a), 6.38 (a) shows the cumulative pore area. Batch 14 and 12 had relatively narrow pore size than batch 15, the reason of that Batch 15 was prepared with different polymeric binder (A4M) than other batches.

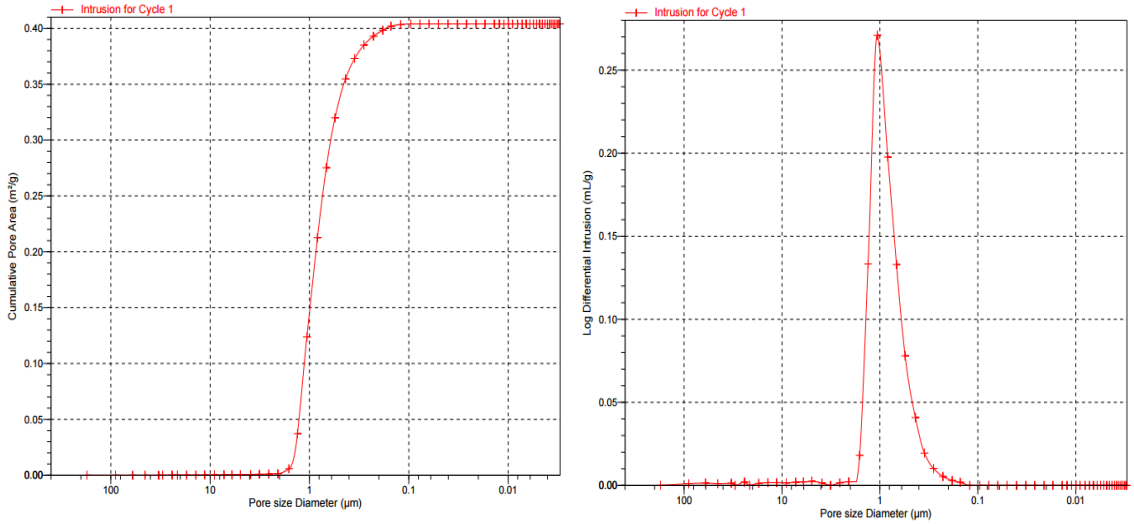

a b

Figure 6.41. Mercury porosimetry plots of Batch 12 a. Cumulative Pore Area versus Pore size and b. Log Differential Intrusion vs Pore size

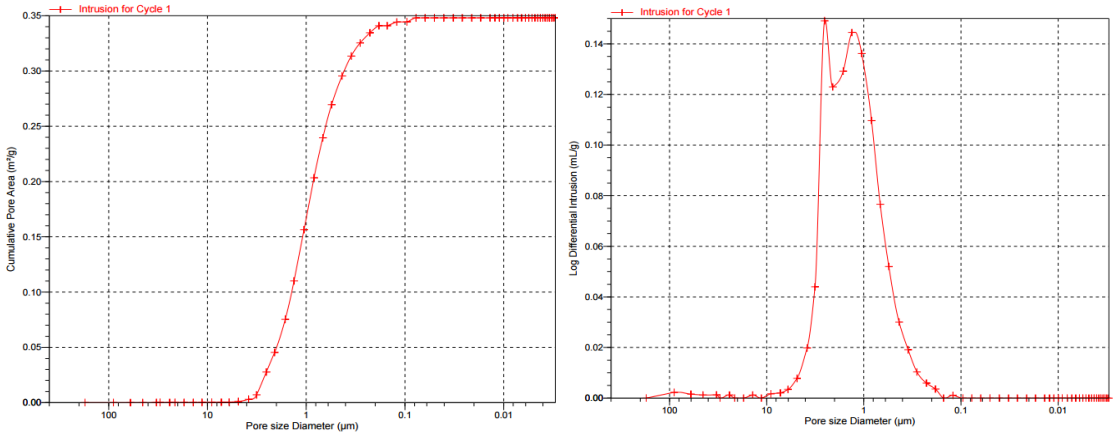

a b

Figure 6.42. Mercury porosimetry plots of Batch 14 a. Cumulative Pore Area versus Pore size and b. Log Differential Intrusion vs Pore size

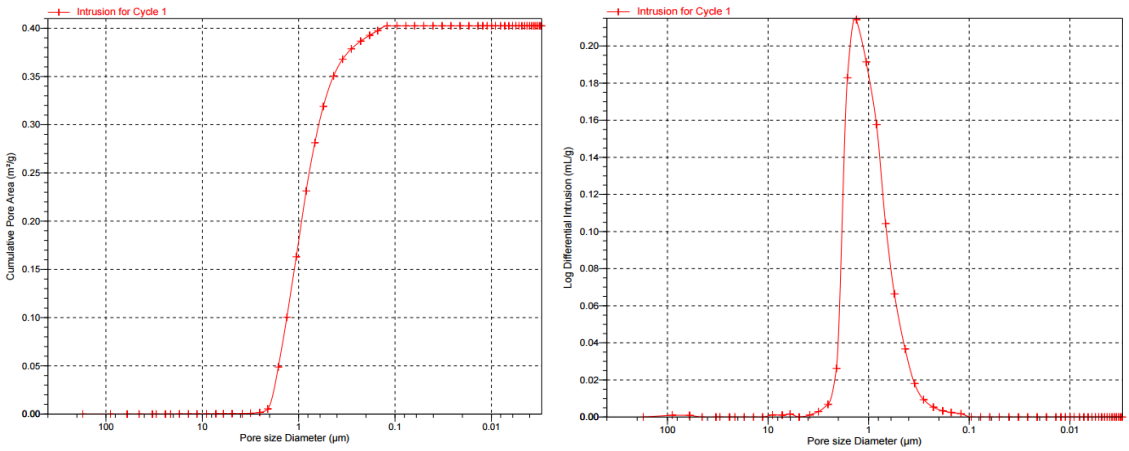

a b

Figure 6.43. Mercury porosimetry plots of Batch 15 a. Cumulative Pore Area versus Pore size and b. Log Differential Intrusion vs Pore size.

CHAPTER 7

CONCLUSIONS

Alumina powders with different particle sizes (0.5, 1.3, 4.0 and 5.2μm) with the addition of different organic (Methocel A4M and F4M) and inorganic (Boehmite) binders were used for paste preparation. Rheological characteristics of these pastes were investigated with Benbow and Bridgwater model for the prediction of extrusion behaviour.The water and binder type/content (polymeric and inorganic) of the pastes were found to be important and effective parameters during extrusion of ceramic pastes. The six parameter model was concluded to better represent the experimental data. The viscosities of the paste batches were also determined by using the model parameters σ_o, β_1, and exponent n. The pastes were determined to have a shear thinning behaviour.

The results of this work proved that the use of Benbow and Birdgwater model may accurately predictthe alumina paste extrusion pressure. The binder amount and type is an important key factor for achieving desired plasticity. The most suitable amount of binder content (by volume) was found to be 6% for alumina paste extrusion. Rheological parameters had shown that using both organic and inorganic binders in the paste decreased the extrusion pressure. Pastes prepared with methocel A4M had shown pseudoplastic behaviour according to Benbow and Bridgwater model however pore size (1.0-2.5 μm) of heat treated tubes were determined to be larger than tubes prepared by using Methocel F4M (1μm) as an organic binder. Porosity decreased (from %49 to %40) and mechanical strength increased (from 25 bar to 55 bars) with increasing amounts of boehmite in the paste content.

In future studies, tubes with smaller pore sizes may be extrudedby using finer alumina powders for use in various applications. The effects of the utilization of various other binders on the rheological behaviour of alumina pastes can be further investigated for improving the extrudedceramic membrane tube characteristics.

REFERENCES

Abdelhamid, H. and Bouzerara, F. 2011. “Fabrication of Tubular Membrane Supports from Low Price Raw Materials, Using Both Centrifugal Casting and/or Extrusion Methods”, Expanding Issues in Desalination, In Tech, 2011

Adams, M. J., Briscoe, B. J. and Sinha, S. K. 1995. “Interfacial and bulk rheological characterisations of paste materials in extrusion flow”. In 27th International SAMPE Technical Conference

Akbarnezhad, Sh., Mousavi, S. M., Sarhaddi, R. 2010. “Sol-gel synthesis of alumina-titania ceramic membrane: Preparation and characterization.”, Indian Journal of Science and Technology, 3 (10):1048

Alford, N. M., Brichall, J.D., and Kendal, K. 1987. “High-strength ceramics through colloidal control to remove defects”, Nature 330 (5): 51-53

Ananthakumar S., Menon, A.R.R., Prabhakaran, K., Warrier, K.G.K. 2001. “Rheology and packing characteristics of alumina extrusion using boehmite gel as a binder”, Ceramics International, (27), 231-237.

Anderson, M. A., Gieselmann, M. J. and Xu, Q., (1988), ” Titania and alumina ceramic membranes”. Journal of Membrane Science, 39 (3): 243–258

Azzolını A., Sglavo V.M., Downs J. A. 2014. “Novel method for the identification of the maximum solid loading suitable for optimal extrusion of ceramic pastes”, Journal of Advanced Ceramics, 3(1): 7–16

Barlow F. D., Elshabini A. “Ceramic Interconnect Technology Handbook”, CRC Press, 2007.

Bayer, R. and M. Lang, (2012),”High-strength and Corrosion-resistant Alumina Tubes through Extrusion- Part 1.” Process Engineering ceramic forum international cfi/Ber. 89:5.

Benbow, J. And Bridgwater, J. 1993, “Paste Flow and Extrusion”, Oxford series on advanced manufacturing .

Bengisu, M. 2001. ”Engineering Ceramic”,Sipringer-Verlag Berlin Heidelberg

Boch, P., Nièpce, J. C. ”Ceramic Materials: Processes, Properties, and Applications”, ISTE Ltd. UK and USA, 2007.

Buonomenna, M.G., Golemme, G. “Advanced Materials for Membrane Preparation”, Bentham Science Publishers, Bentham e-Books, 2012.

Carter, C. B., Norton, M. G. " Ceramic Materials: Science and Engineering", Springer Science & business Media, 2013.

Das, R.N. , Madhusoodana, C.D., Okada, K. 2002, "Rheological studies on cordierite honeycomb extrusion", Journal of the European Ceramic Society 22:2893–2900.

de Jong, K. P. "Synthesis of Solid Catalysts", Wiley-VCH Verlag GmBH & Co., 2009.

Erdem, I. 2002. "Preparation of Ultrafiltration / Microfiltration Ceramic Composite Membranes for Biotechnology Applications", Thesis, İzmir Institute of Technology

Guire, M. R., Michael, Z. Hu, Gogotsi, Y. and Lu, S. W. 2004,"Ceramic Nanomaterials and Nanotechnology II", The American Ceramic Society, 148:182

Handle, F. "Extrusion in Ceramics", Springer-Verlag Berlin Heidelberg, 2007.

Horrobin, D. J., Nedderman, R. M. 1998. "Die entry pressure drops in paste extrusion", Chemical Engineering Science, 53, (18): 3215-3225.

Horrobin, D. J., Nedderman, R. M. 1998. " Die entry pressure drops in paste extrusion", Chemical Engineering Science, 53:3215-3225.

Khan, A. U., Briscoe, B. J., Luckman P.F. 2001. "Evalation of slip in cappilary extrusion of cermic pastes", Journal of the European Ceramic Society, 21: 483-491.

Kingsbury, B.F. 2010. " A morphological study of ceramic hollow fibre membranes: A prespective on multifunctional catalytic membrane reactors", Thesis, Imperial Collage London

Kong L. B.,Y. Z. Huang,W. X. Que,T. S. Zhang,S. Li,J. Zhang,Z. L. Dong,D. Y. Tang, (2015)"Transparent Ceramics", Springer International Publishing, 978-3-319-18956-7.

Kumar, C. S., Hareesh, U. S., Pai, B. C., Damodaran. A.D., Warrie, K. 1997. "Aqueous Extrusion of Alumina-Zirconia (12mol% Ceria) Composite using Boehmite as Extrusion Aid", Ceramics International 24 , 583±587.

Larbot, A., Julbe, A., Guizard, C., Cot, L. 1989. "Silica membranes by the sol-gel process." Journal of Membrane Science, 44 (2–3): 289–303

Leo, S., Tallon, C., Stone, N., Franks, G. V. 2014. "Near-Net-Shaping Methods for Ceramic Elements of (Body) Armor Systems", The American Ceramic Society, 97 (10):3013–3033.

Li, K. “Ceramic Membranes for Separation and Reaction”, John Wiley & Sons Ltd, 2007.

Liu, F.-J., Chou, K.-S. 2000. “Determining critical ceramic powder volume concentration from viscosity measurements.” Ceramics International 26: 159-164.

Li, Y.Y., Bridgwater, J., 2000. “Prediction of extrusion pressure using an artificial neural network” Powder Technology 108: 65–73.

Martin, P. J., Wilson, D. I., Challis, K., 2001. “Extrusion of Paste Through Non-Axisymmetric Systems”, 6th World Congress of Chemical Engineering.

Miller, M., Haber, R.A, 1991. “The use of montmorillonite as extrusion aids for alumina” Ceramic Engineering Science Proceedings, 12:13–48.

Mooney, M. 1931. “Explicit formulas for slip and fluidity”, J. Rheology, 30: 210–222

Moosemiller, M. D., Hill, C. G., Anderson, M. A. 1989. “Physicochemical properties of supported gamma-Al2O3 and TiO2 ceramic membranes.” Separation Science and Technology, 24 (9–10): 641–657.

Nagaoka, T., Duran, C., Isobe, T., Hotta, Y., Watari K. 2007, “Hydraulic Alumina Binder for Extrusion of Alumina Ceramics”, The American Ceramic Society, 90 (12): 3998–4001.

Ochoa, I., Hatzikiriakos S. G. 2005. “Paste extrusion of polytetrafluoroethylene (PTFE): Surface tension and viscosity effects” , Powder Technology 153:108 – 118

Ribeiro, M.J., Blackburn S., Ferreira J.M. and Labrincha J.A. 2006. “Extrusion of alumina and cordierite-based tubes containing Al-rich anodising sludge”, Journal of the European Ceramic Society 26:817–823.

Richerson, D. W., “Modern Ceramic Engineering: Properties, Processing, and Use in Design” CRC Press, 2005.

Sharmin, K., Schoegl, I. 2014. “Two-step debinding and co-extrusion of ceramic-filled PEBA and EVA blends”, Ceramics International, 40: 14871–14879

Terpstra, R.A, Pex A. C., de Vries, A.” Ceramic Processing “, Chapman & Hall, 1995.

APPENDIX

BENBOW AND BIRIDGWATER MODEL 4 AND 6 PARAMETER PLOTS

Plots of 6 Parameter Model Batch 15

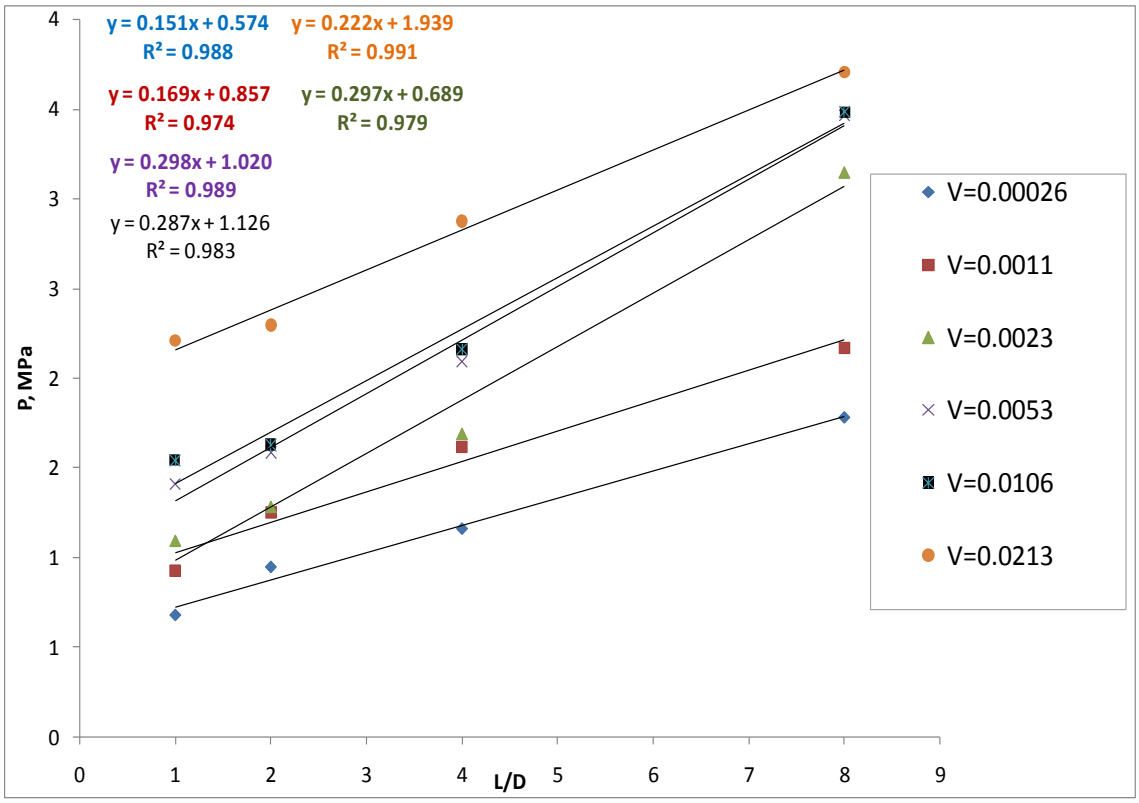

Figure A.1.. P vs. L/D curves of batch 15.

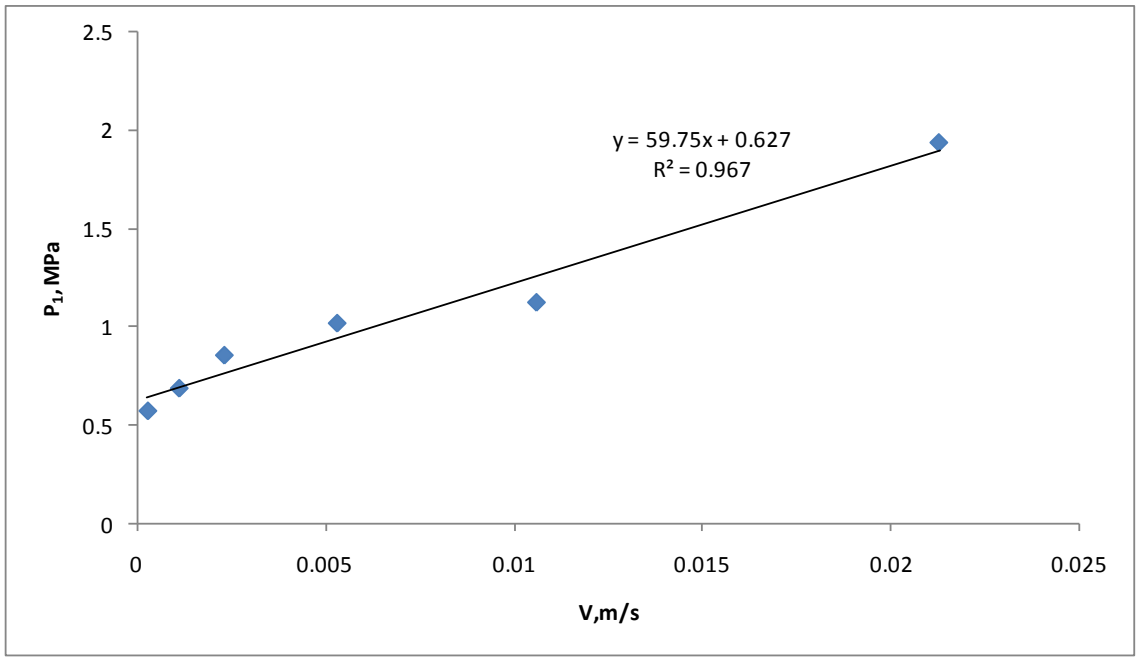

Figure A.2. P_1 vs.V curve of batch 15.

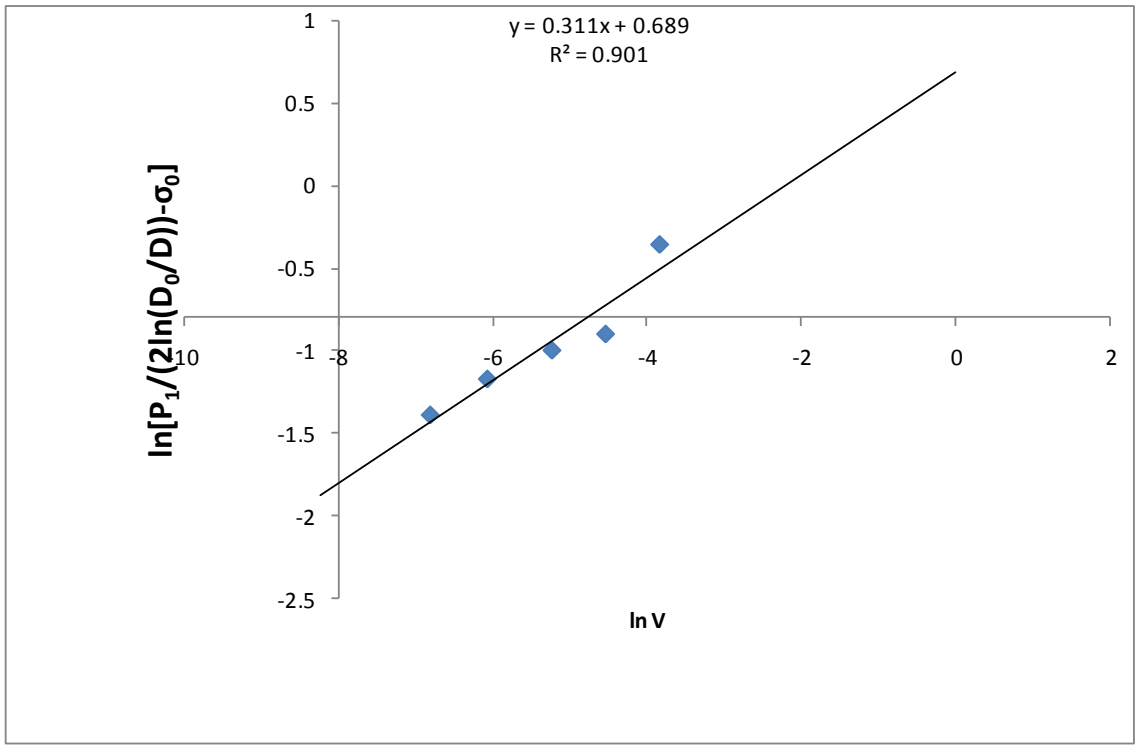

Figure A.3. lnV vs $\ln[P_1/2\ln(D_0/D)]$- σ_0 curve of batch 15.

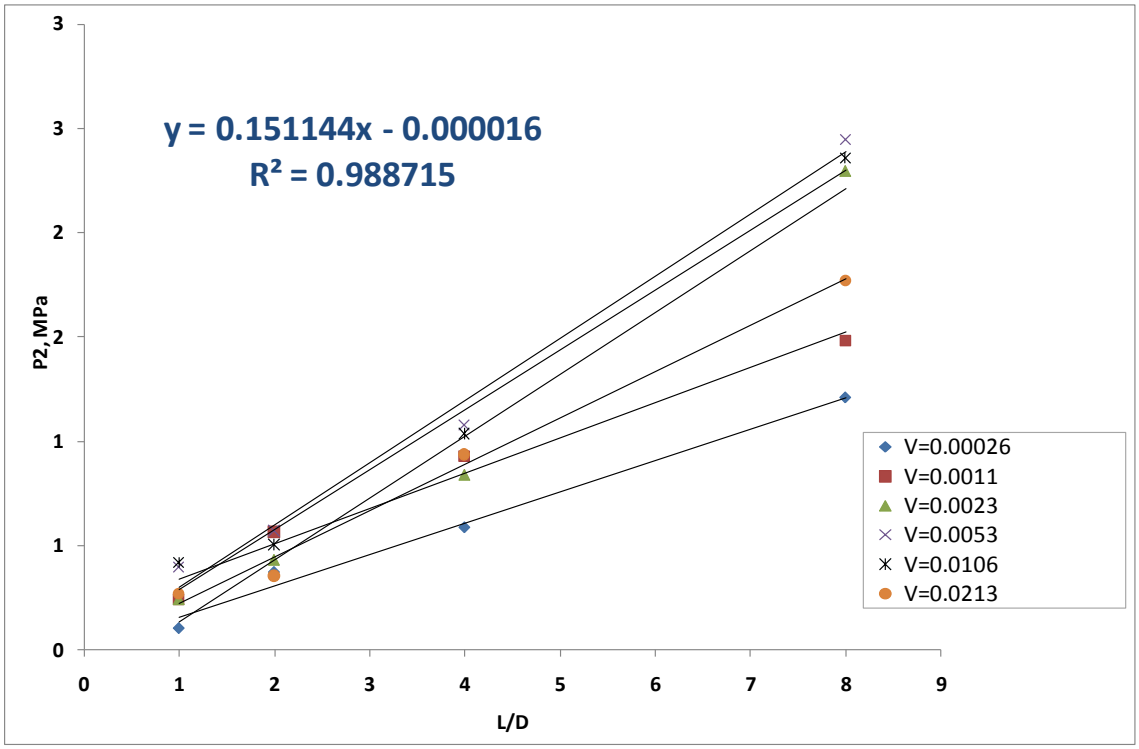

Figure A.4. P_2 vs L/D curves of batch 15.

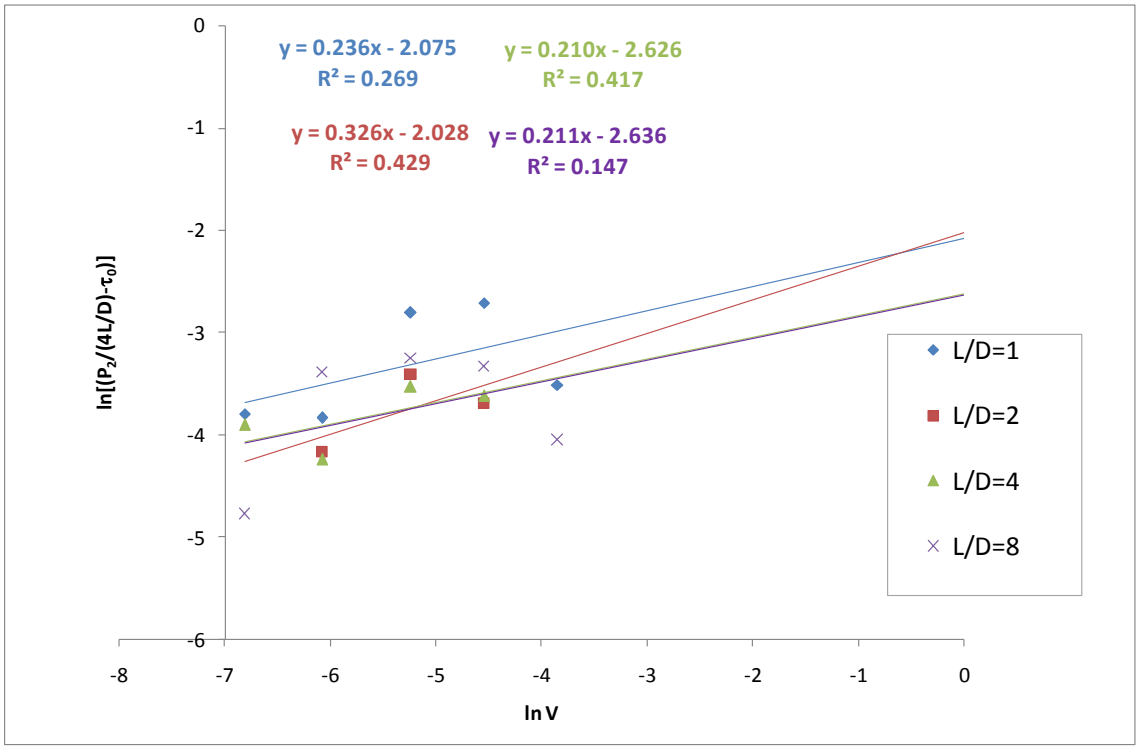

Figure A.5.ln[P_2/4L/D]- τ_0 vs lnV curves of batch 15.

Plots of 4 Parameter Model Batch 15

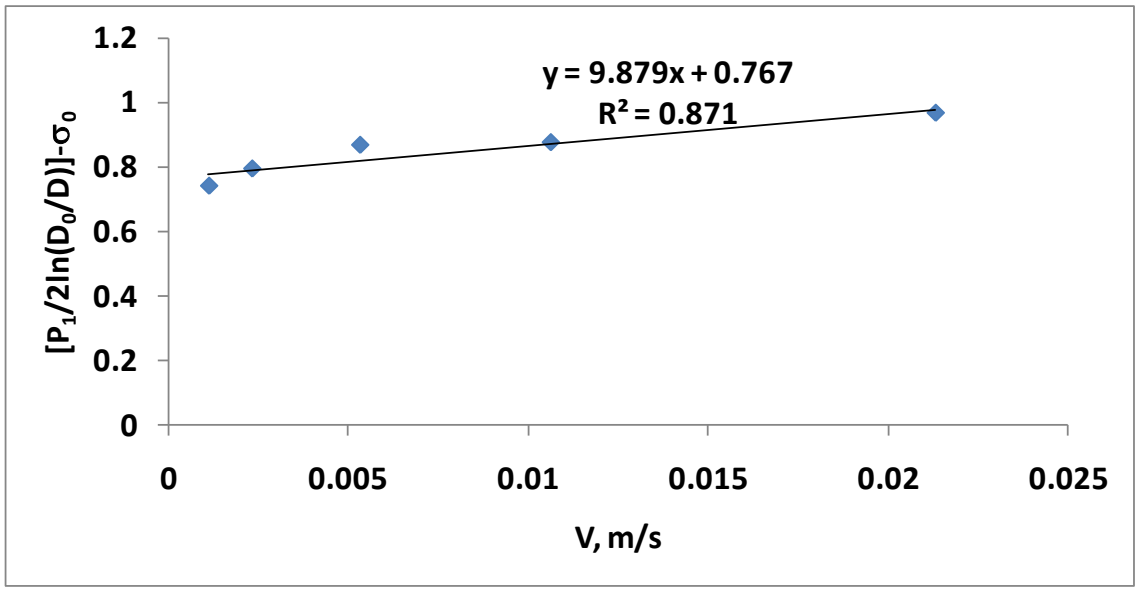

Figure A.6. $[P_1/2\ln(D_0/D)]- \sigma_0$ vs V curve of batch 15.

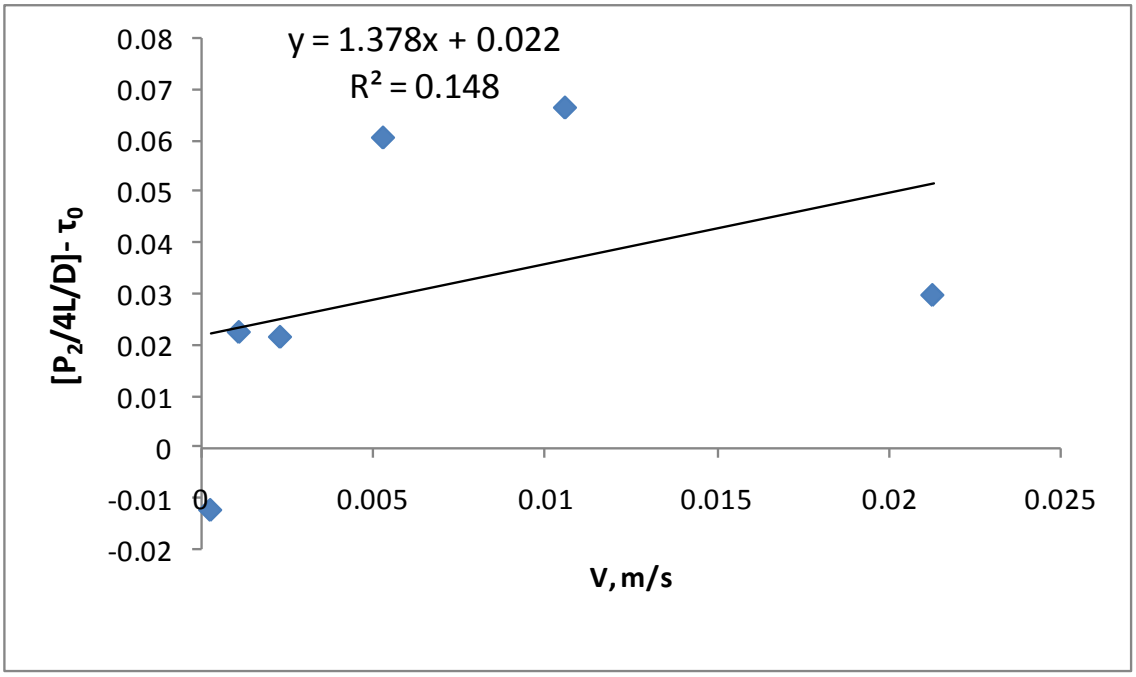

Figure A.7. $[P_2/4L/D]- \tau_0$ vs V curve of batch 15.

Plots of 6 Parameter Model Batch 16

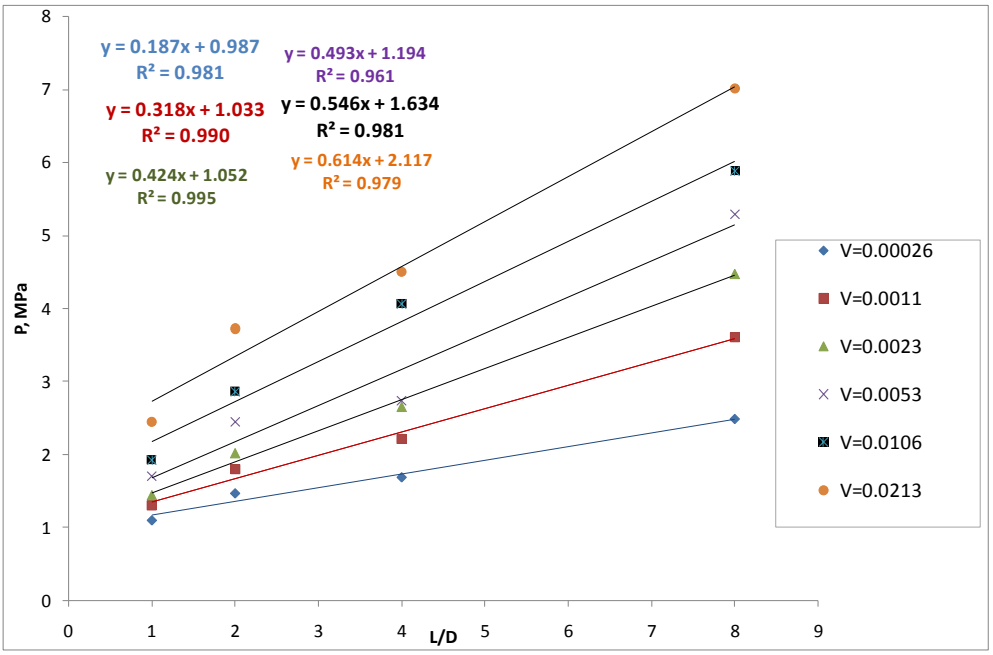

Figure A.8. P vs. L/D curves of batch 16.

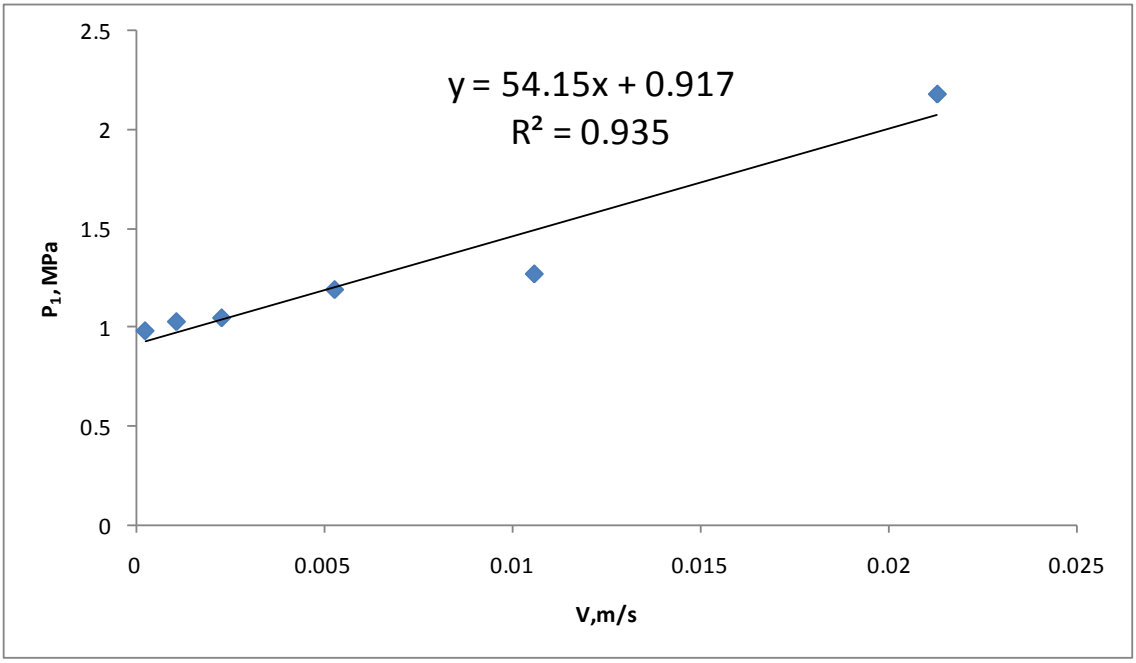

Figure A.9. P_1 vs.V curve of batch 16.

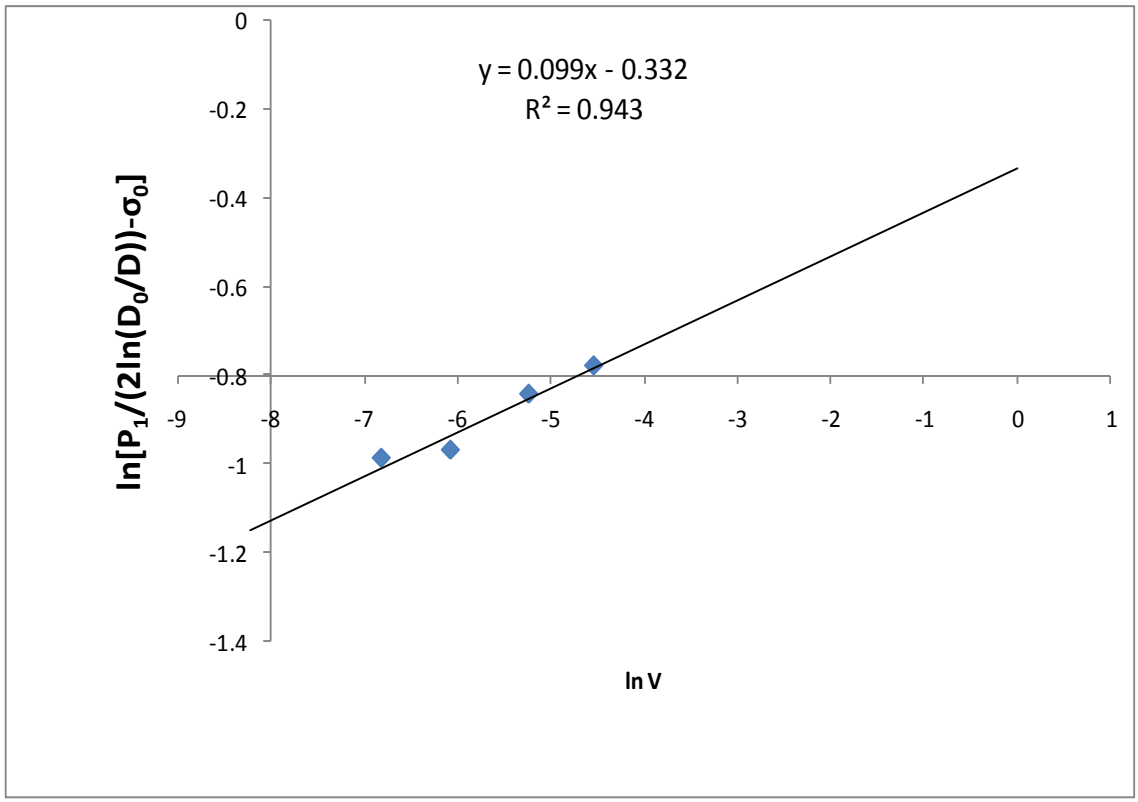

Figure A.10.lnV vs $\ln[P_1/2\ln(D_0/D)]-\sigma_0$curve of batch 16.

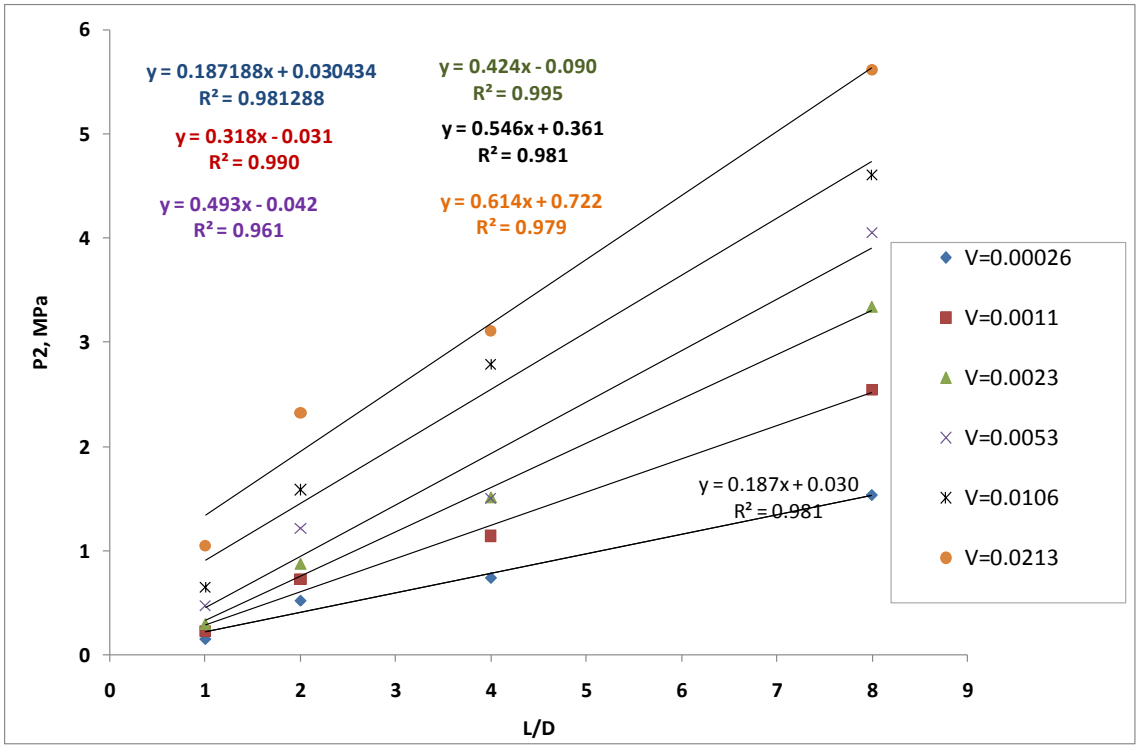

Figure A.11. P_2 vs L/D curves of batch 16

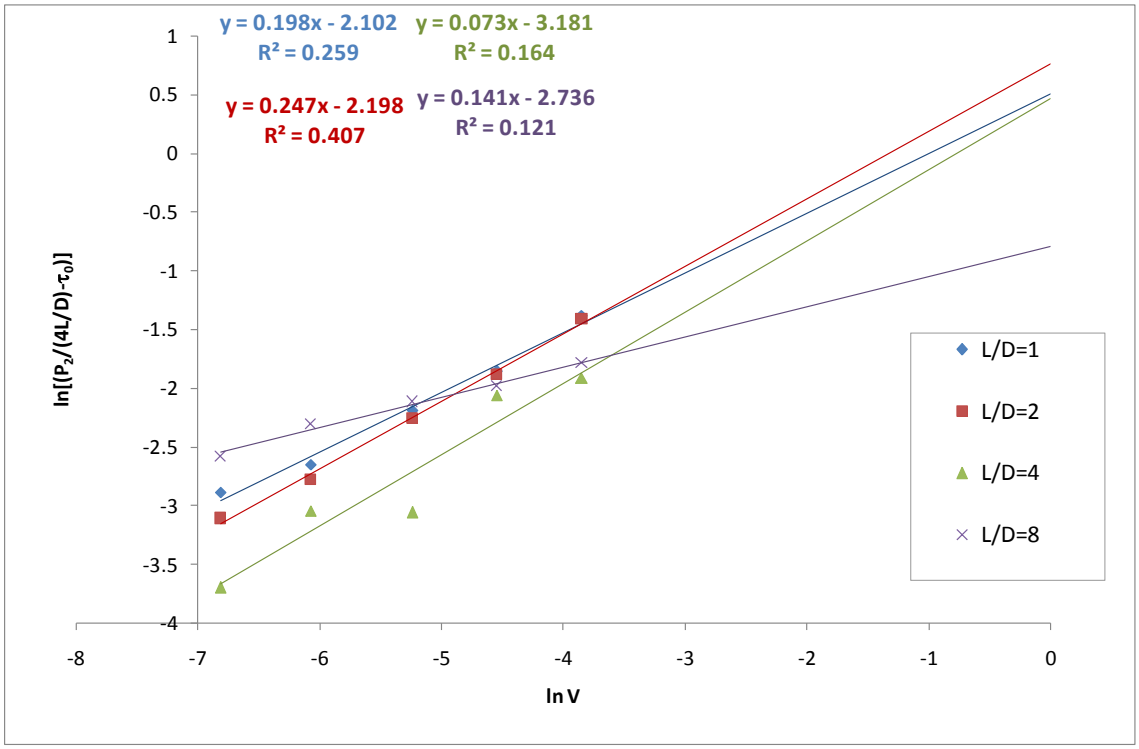

Figure A.12.ln[P_2/4L/D]- τ_0 vs lnV curves of batch 16.

Plots of 4 Parameter Model Batch 16

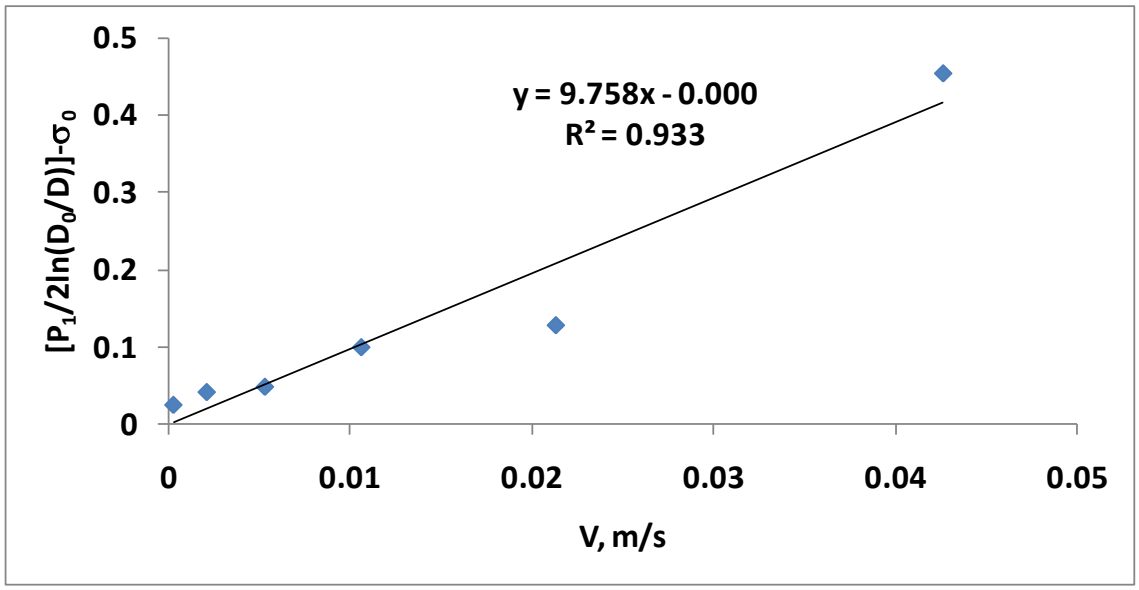

Figure A.13. [P_1/2ln(D_0/D)]- σ_0 vs V curve of batch 16.

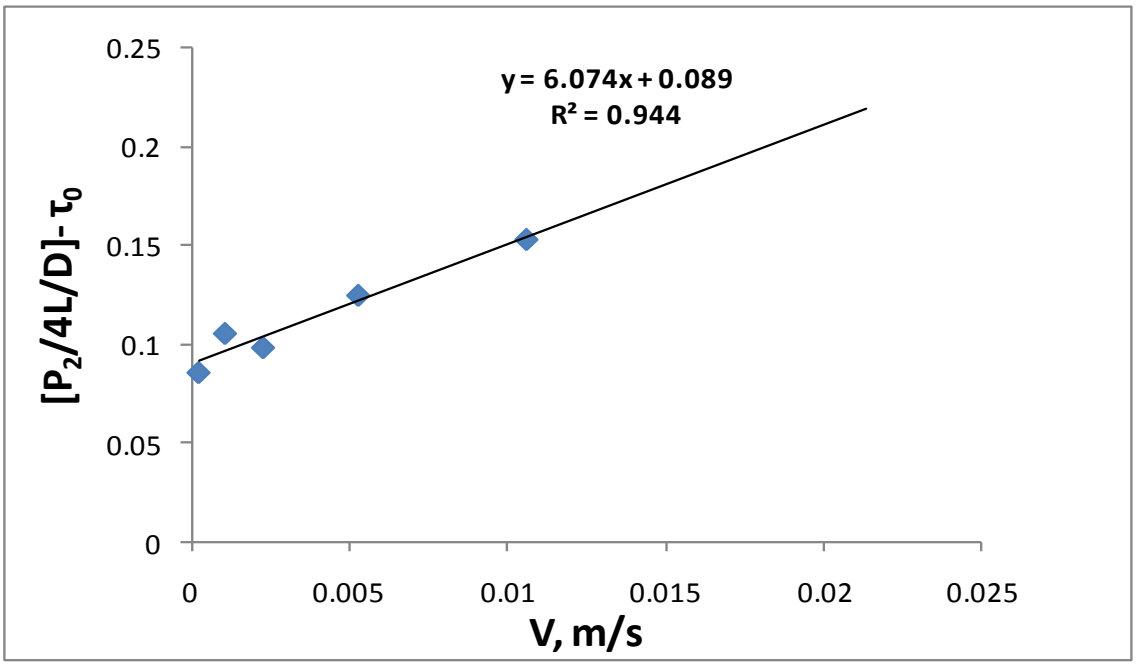

Figure A.14. [P_2/4L/D]- τ_0 vs V curve of batch 16.

Plots of 6 Parameter Model Batch 18

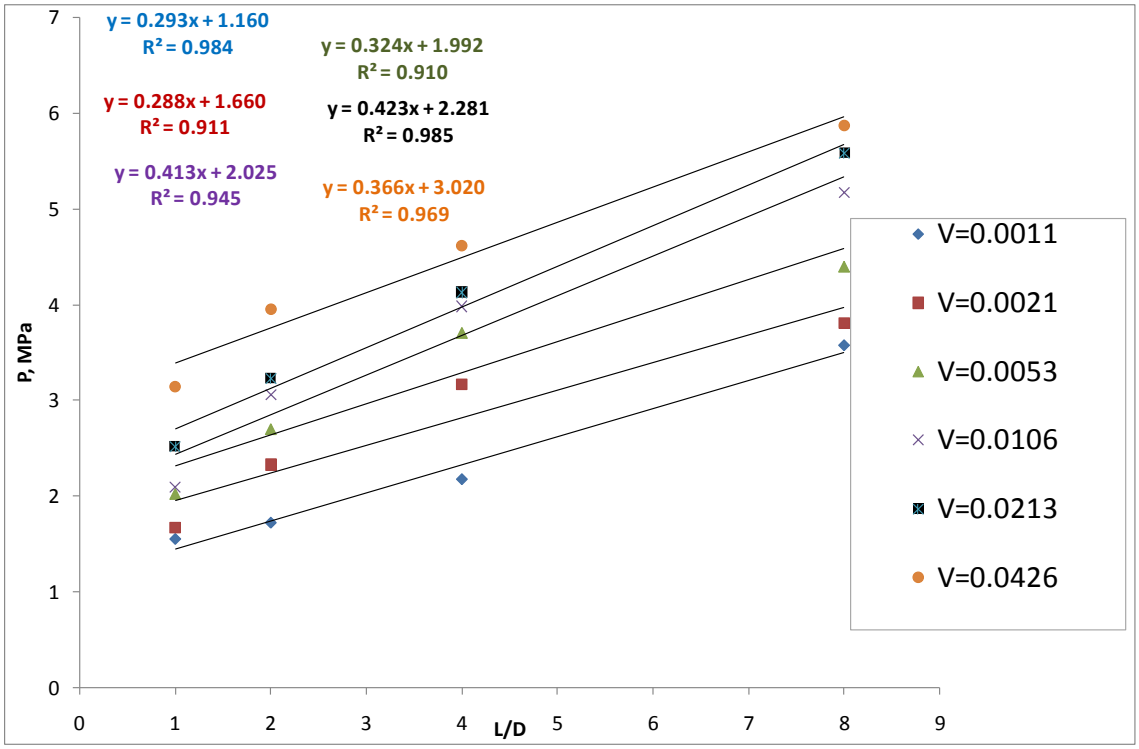

Figure A.15. P vs. L/D curves of batch 18.

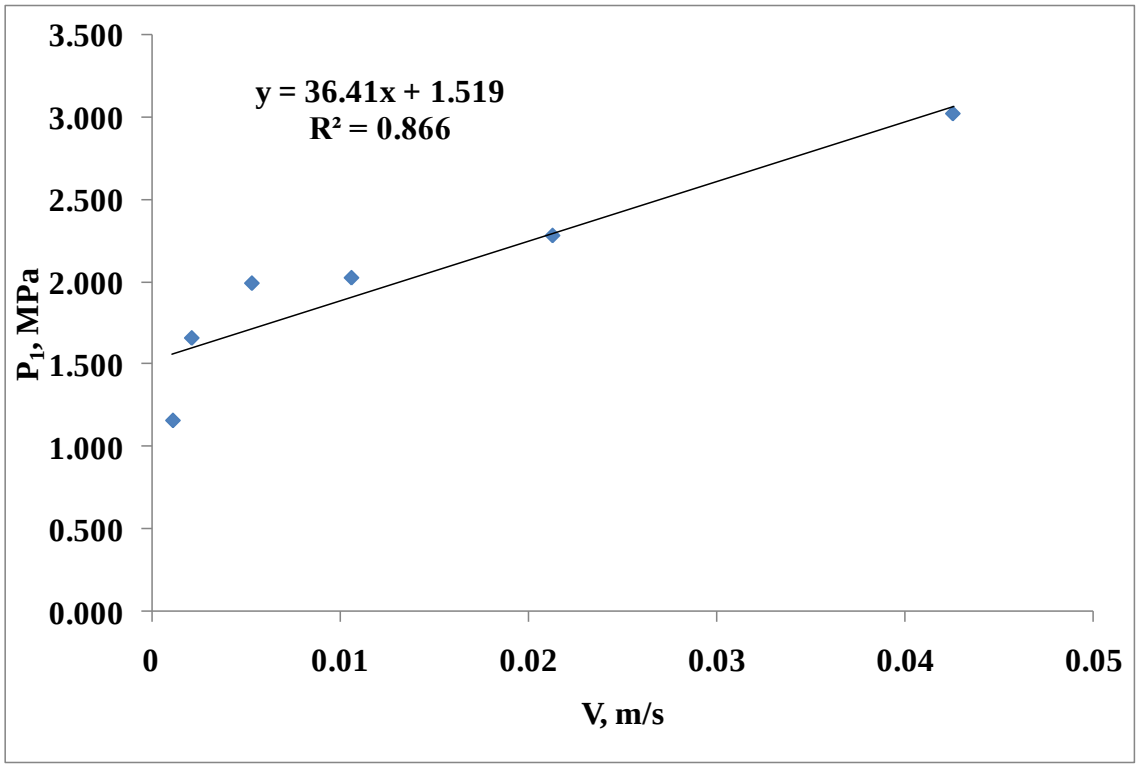

Figure A.16. P_1 vs.V curve of batch 18.

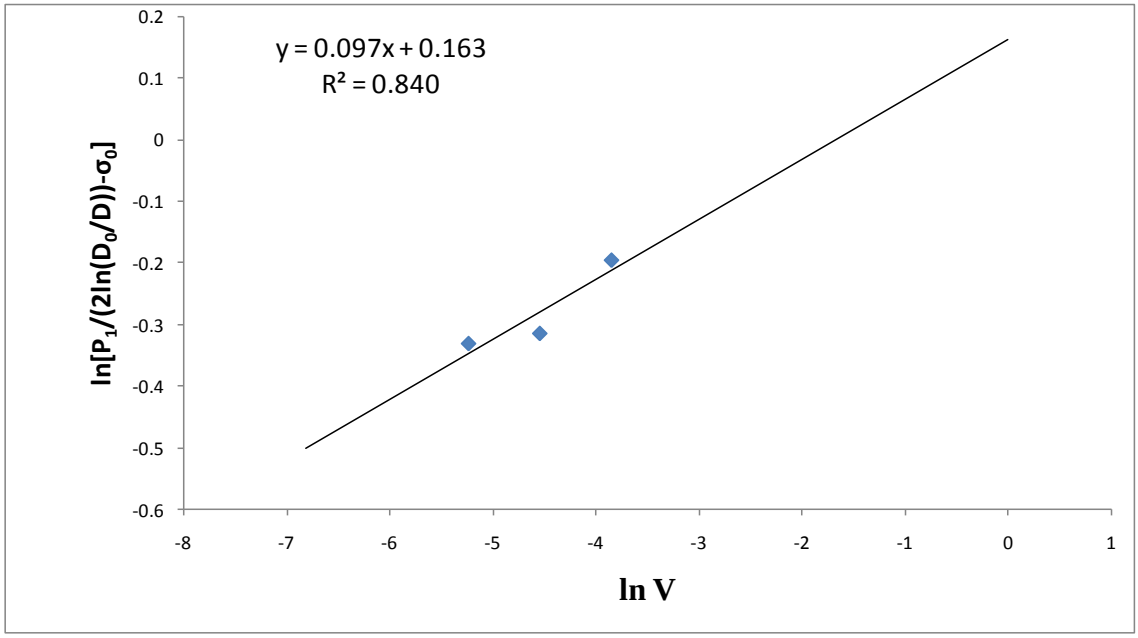

Figure A.17. lnV vs $\ln[P_1/2\ln(D_0/D)]- \sigma_0$ curve of batch 18.

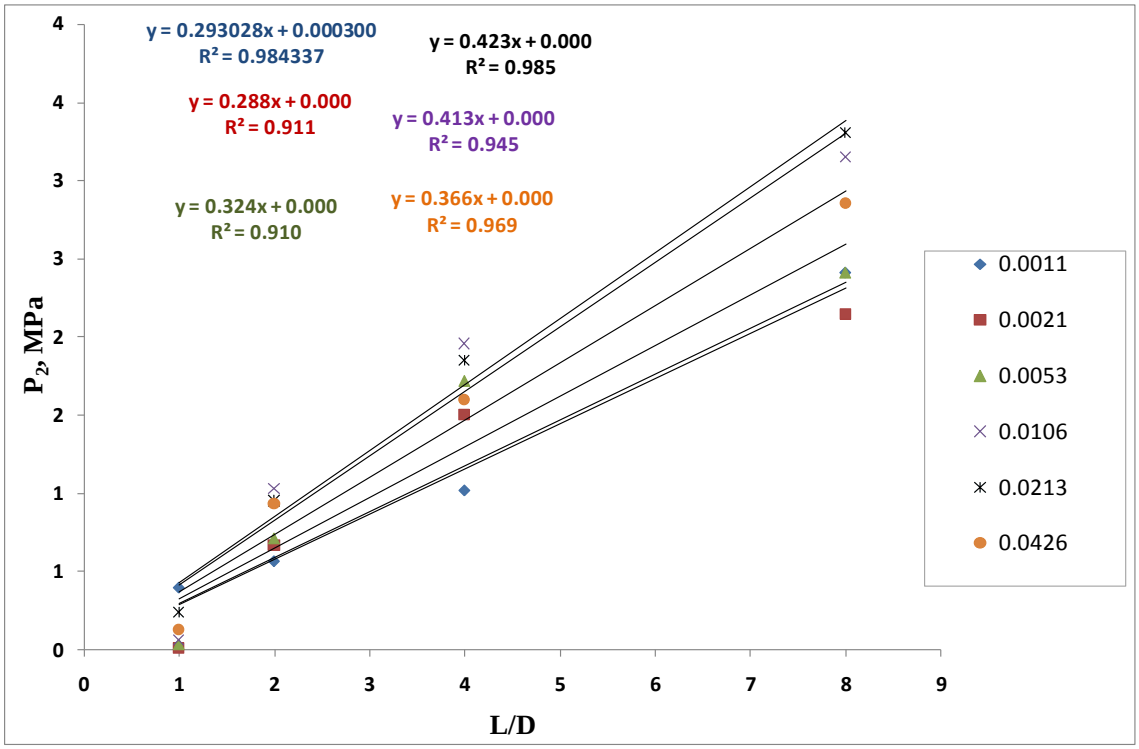

Figure A.18. P_2 vs L/D curves of batch 18.

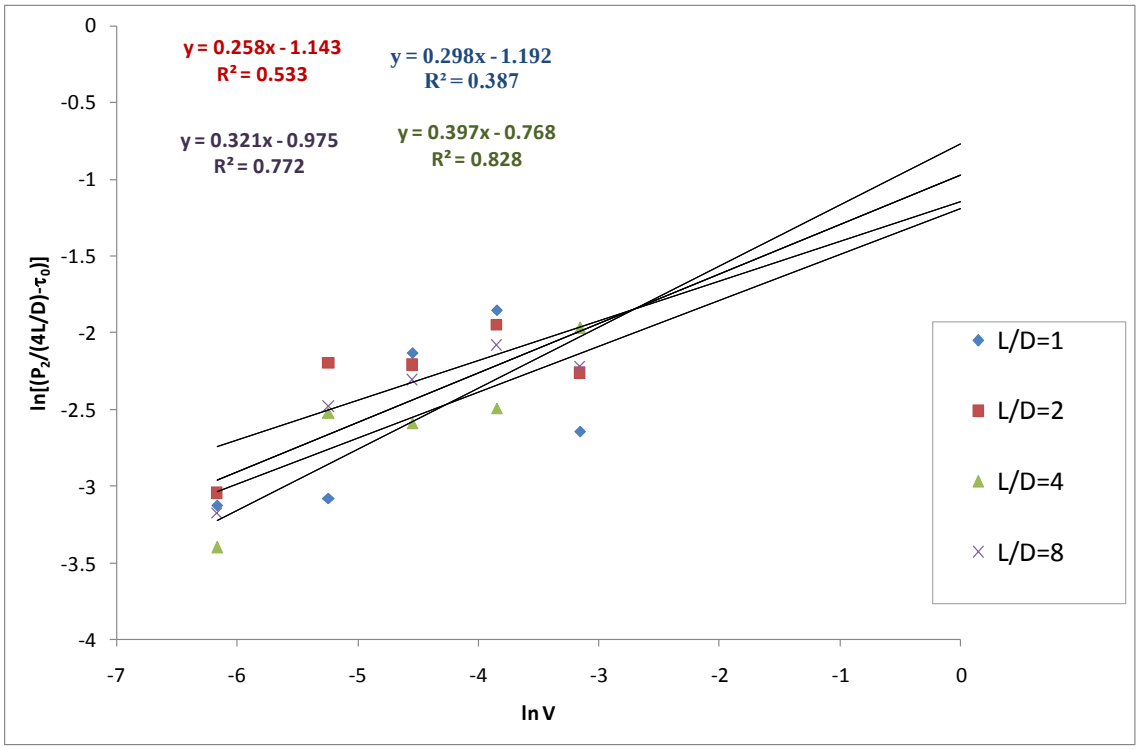

Figure A.19.ln[P_2/4L/D]- τ_0 vs lnV curves of batch 18.

Plots of 4 Parameter Model Batch 18

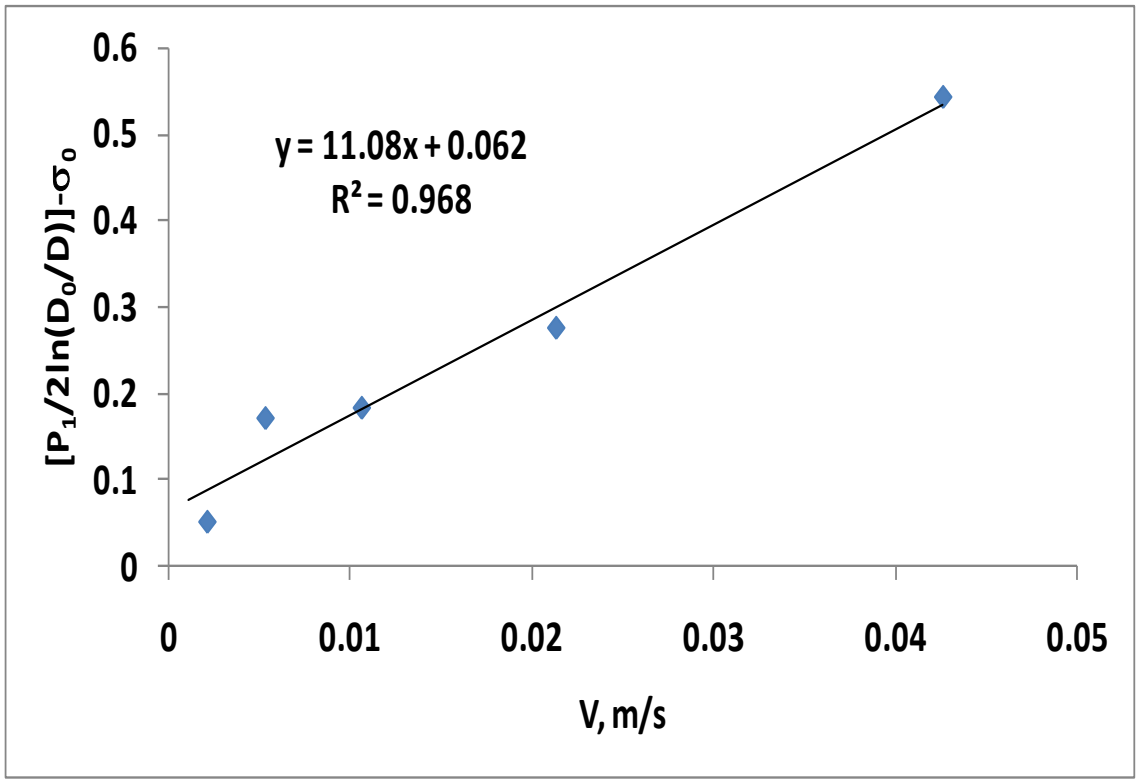

Figure A.20. $[P_1/2\ln(D_0/D)]- \sigma_0$ vs V curve of batch 18.

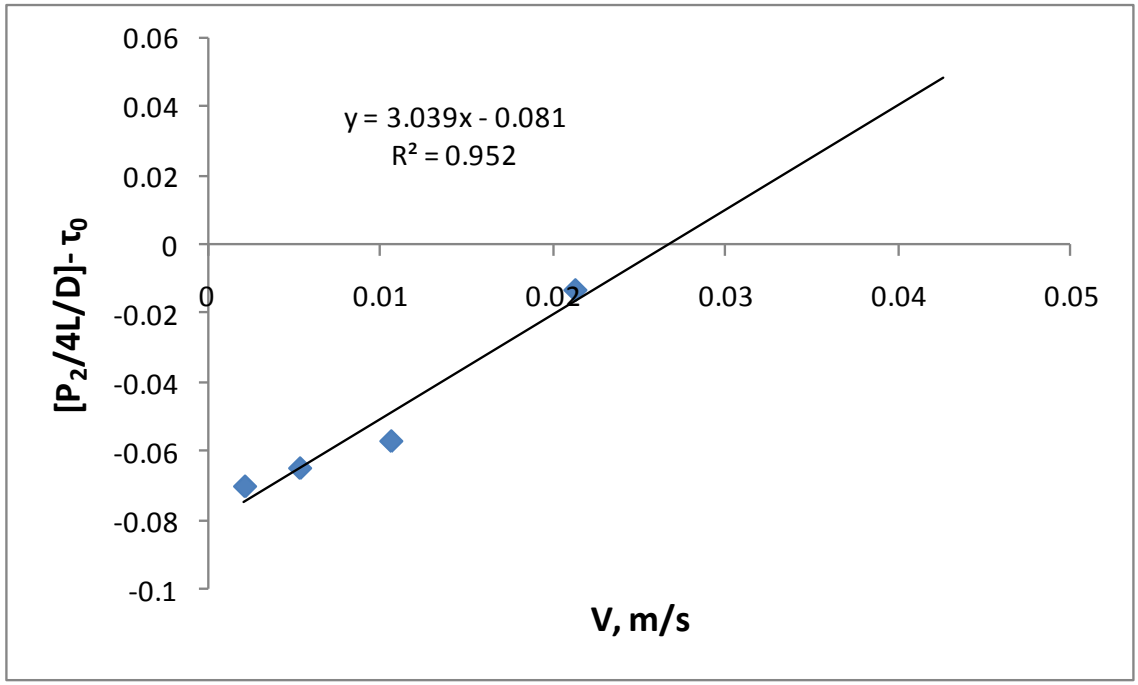

Figure A.21. $[P_2/4L/D]- \tau_0$ vs V curve of batch 18.